Investigating the Role of 4E-BPs in the Polyomavirus (PyV) Middle-T Oncogene Mouse Model for Mammary Tumorigenesis

Sophie Hélène Guénin

Department of Biochemistry

McGill University

Montreal, Canada

A thesis submitted to McGill University in partial fulfillment of the requirement of the degree of

Master of Science

Submitted April 2019

Abstract

As of 2018, the 5-year survival rate for metastatic breast cancer was 27%. Among breast cancers, the metastatic luminal B molecular subtype has proven to be difficult to treat given its relative insensitivity to endocrine therapy and chemotherapy. Thus, the lack of efficacious treatment in conjunction with the unique heterogenic make up of luminal B breast cancers make it a challenge for scientists and clinicians.

The PI3K/AKT/mTOR signaling pathway is hyperactivated in most breast cancers, especially in the luminal B molecular subtype. Herein, we employed the MMTV-PyV-MT mouse model, a metastatic breast cancer model mimicking hyperactive PI3K signaling and the luminal B molecular subtype of breast cancer, to investigate the role of 4E-BPs which are the major effectors of the PI3K/AKT/mTOR pathway in mammary tumorigenesis. 4E-BPs are negative regulators of mRNA translation and have been ascribed tumor-suppressive properties. However, in patient samples, 4E-BPs are frequently overexpressed. Thus, this study seeks to elucidate the role of 4E-BPs in each stage of the mammary tumorigenesis process from normal tissue to metastasis.

To this end, transgenic MMTV-PyV-MT 4E-BP1/4E-BP2 null mice were generated and monitored for tumor development. Notwithstanding that 4E-BP1/2 loss did not appear to alter tumor onset, it did lead to an increase in the primary tumor volume at experimental endpoint. Strikingly, loss of 4E-BPs led to an unexpected and dramatic decrease in lung metastasis at endpoint. Decrease in lung metastasis in 4E-BP1/2 null mice was correlated with a reduction in eIF4E protein levels in primary tumors. Re-expression of 4E-BP1 in primary cells isolated from 4E-BP1/2 null tumors

resulted in restitution of eIF4E levels, thus suggesting that the regulation of 4E-BP and eIF4E levels in the MMTV-PyV-MT model, is coordinated.

This work draws attention to the importance of maintaining a stoichiometric ratio of eIF4E and 4E-BPs in a cancer cell in order to conserve its metastatic potential.

Abrégé

En 2018, le taux de survie pour le cancer du sein avec métastases était de 27%. Parmi les cancers du sein, le sous-type moléculaire “luminal B” s’est révélé difficile à traiter à cause de sa résistance aux thérapies endocrinienne et à la chimiothérapie. Ainsi, le manque d’efficacité du traitement en conjonction avec la composition hétérogène des cancers du sein du type “luminal B” en font un défi pour les scientifiques et les cliniciens.

La voie de signalisation PI3K/AKT/mTOR est hyperactivée dans la plupart des cancers du sein, spécialement dans le cas du sous-type moléculaire “luminal B”. Compte-tenu de cette information, le modèle de souris MMTV-PyV MT est un modèle de cancer du sein avec métastase qui mimique la signalisation hyperactivée PI3K et qui a été choisi pour étudier le rôle de 4E-BPs dans la tumorigenèse mammaire. Les 4E-BPs ont été bien établis comme régulateurs négatifs de la translation de mARN. Pourtant, dans les échantillons de patients, on a aussi observé que les 4E-BPs sont surexprimés. Cette étude cherche à élucider le rôle des 4E-BPs dans chaque étape du processus de tumorigenèse mammaire des tissus normaux jusqu’aux métastases.

Dans ce but, des souris transgéniques MMTV-PyV-MT/4E-BP1/2 null ont été élevées/produites afin de développer des tumeurs. Les taux de 4E-BPs n'ont pas semblé avoir d'effet sur la vitesse d'apparition des tumeurs. La perte de 4E-BPs a pourtant conduit à une augmentation du volume des tumeurs au point final de l'expérimentation. De plus, une diminution inattendue des métastases pulmonaires au point final de l'expérimentation a été remarquée. La diminution des métastases pulmonaires était aussi corrélée avec une diminution des niveaux de protéine eIF4E dans les tumeurs primaires. Les lignées primaires de cellules ont été développées à partir de tumeurs de souris MMTV-PyV-MT/4E-BP1/2 null et étudiées in vitro. La réintroduction de 4E-BP1 dans ces cellules a montrée une augmentation des niveaux de eIF4E, suggérant ainsi que la régulation des niveaux de 4E-BP et eIF4E sont liés dans le modèle MMTV-PyV-MT.

Cette recherche démontre l'importance de maintenir un ratio stœchiométrique de eIF4E et 4E-BP dans une cellule cancéreuse pour qu'elle se métastases.

Table of Contents

ABSTRACT ..... **I**

ABRÉGÉ ..... **III**

TABLE OF CONTENTS ..... **V**

ACKNOWLEDGEMENTS ..... **VII**

CONTRIBUTIONS TO ORIGINAL KNOWLEDGE ..... **VIII**

LIST OF FIGURES AND TABLES ..... **IX**

LIST OF ABBREVIATIONS ..... **XI**

CHAPTER ONE: REVIEW OF LITERATURE **1**

1.1 Breast Cancer 1
1.2 Breast Cancer Subtypes 2
1.3 Standard of Care Therapies for Breast Cancer 4
1.3.1 Targeting of Insulin Signaling 6
1.4 Translation in Cancer 8
1.4.1 Translation Initiation 9
1.4.2 eIF4E 11
1.4.3 4E-BP1 and 4E-BP2 15
1.4.4 Coregulation of 4E-BPs and eIF4E 17
1.5 mTOR 19
1.5.1 Therapies Targeting mTOR in Cancer 22
1.6 PI3K/AKT/mTOR Signaling Pathway in Breast Cancer 23
1.6.1 ShcA Adaptor Protein 28
1.7 MMTV-PyV-MT Mouse Model of Breast Cancer 31
1.8 Metastasis 34
1.9 Rationale/Objectives 36

CHAPTER TWO: METHODS **38**

CHAPTER THREE: RESULTS **44**

3.1 PyV-MT Cells Exhibit Low Responsiveness to Mitogenic Stimulation 44
3.2 PyV-MT/ShcA2F Cells Most Responsive to mTOR inhibition 46
3.3 4E-BPs Mediate the Effects of ShcA on Breast Cancer Tumor Onset in PyV-MT Model 48
3.4 The Loss of 4E-BP1 and 4E-BP2 Accelerates Primary Tumor Growth but Dramatically Decreases Lung Metastasis in PyV-MT/4E-BP1/2 null Mice 50

3.5 Decreased Metastasis Phenotype in PyV-MT/4E-BP1/2 null Mice Correlated to Decreased eIF4E Levels in Primary Tumor 53
3.6 4E-BP1 Status, not PI3K Signaling, modulates eIF4E levels 56
3.7 Dissecting the Mechanisms of 4E-BP-loss Induced eIF4E Downregulation 59
3.8 Correlative Decrease of eIF4E Levels in 4E-BP1/2 null Contexts Is Not Conserved Across Model Systems 63

CHAPTER FOUR: DISCUSSION 65

4.1 Two Potent Oncogenic "Hits" 67
4.2 eIF4E/4E-BP Equilibrium 69
4.3 Other Potential Factors 70
4.4 Limitations 71
4.5 Conclusion 72

LITERATURE CITED 73

Acknowledgements

A big thank you to my supervisors, Dr. Josie Ursini-Siegel and Dr. Ivan Topisirovic, whom have given me this great opportunity to pursue a graduate degree in their labs. I am extremely grateful for their guidance, help, and support throughout this process. I would also like to thank both for their belief in me and this project.

I would like to thank the lab members from both the Ursini-Siegel and Topisirovic labs: Angie, Jackie, Rachel, Stephanie, Eduardo, Kyle, Predrag, Young, Valerie, Laura, Oro, David, Kris, Hayley, Matthew and Shannon. Without their advice, support, and help, this degree would not have been possible. A special thanks also to Marie-José and Elena for their insights on mouse experiments and questions during lab meetings.

In addition, thank you to my committee members: Dr. Jose Teodoro and Dr. Phillippe Roux. Thank you to McGill University Department of Biochemistry for accepting me into their program.

Thank you to my parents for supporting me in every way possible. Thank you to my brother for always making me laugh. Thank you to my best friend, Rasha, for showing me the meaning of true friendship through the best of times and the worst of times. Finalement, merci à mon Hadrien, pour ton amour.

Contribution to Original Knowledge

The following thesis, titled: "Investigating the Role of 4E-BPs in Polyomavirus (PyV) Middle-T Oncogene Mouse Model for Mammary Tumorigenesis", is written in the mono-graph based format and is composed of four chapters.

1. Chapter One - Review of Literature
2. Chapter Two -Methods
3. Chapter Three- Results
4. Chapter Four -Discussion

The contributions of the authors who participated in this project are described below.

The 4E-BP1/2 CRISPR/Cas9 knock-out cell line (NMuMG-NeuNT2197 Clone 17) were generated by Dr. Laura Hulea. The wild-type MT cell line used for *in vitro* experiments was generated by Dr. Josie-Ursini-Siegel. Valerie Sabourin performed immunohistochemistry for eIF4E on breast tumor tissue samples. The transgenic tumor curves for the MT wild-type mice were generated by Ryuhijn Ahn, Stephanie Totten, Valerie Sabourin, and Young Im. The MT/Shc3F heterozygous mouse tumor curve was generated by Young Kyuen Im. The 4E-BP1/2 null mice were a gift from the lab of Dr. Nahum Sonenberg at McGill University. MT/4E-BP1/2 null and MT/Shc3F heterozygous/4E-BP1/2 null mice were in part generated by Young Im. Predrag Jovanovic has helped with the continuation and thought process behind this project.

Dr. Josie Ursini-Siegel helped with analysis of transgenic mouse data. Dr. Ivan Topisirovic and Dr. Josie Ursini-Siegel conceptualized and supervised the project and helped with thesis revisions.

List of Figures and Tables

Figures

Figure 1. Cancer Today (GLOBOCAN 2018)……..….1

Figure 2. Overview of 5' Cap-Dependent Translation Initiation……10

Figure 3. The mTOR Complexes……20

Figure 4. Receptor Tyrosine Kinase Signaling Through PI3K/AKT and RAS/ERK Pathways……28

Figure 5. ShcA Structure and Mutations…….30

Figure 6. Transgenic PyV-MT Mouse Model Recapitulates Human Breast Cancer…….…..33

Figure 7. PI3K/AKT/mTOR Pathway Downstream of PyV-MT……..…..34

Figure 8. Metastatic Cascade…….….36

Figure 9. PyV-MT Cells Unresponsive to Mitogenic Stimulation…….….45

Figure 10. ShcA2F Mutant Sensitive to Torin1 Treatment in PyV-MT Cell Lines…….47

Figure 11. Loss of 4E-BP1/2 Rescues PyV-MT/Shc3F Heterozygous Phenotype…….…49

Figure 12. Loss of 4E-BP1/2 Does Not Change Tumor Onset, Tumor Burden, Nor Tumor Bearing Glands……...51

Figure 13. Loss of 4E-BP1/2 Impairs Metastasis……52

Figure 14. Loss of 4E-BPs *in vivo* Leads to Reduced Total eIF4E Protein Levels in Tumors…..54

Figure 15. Protein Levels of Translation Initiation Machinery are Unchanged in PyV-MT/4E-BP1/2 null Tumors…….55

Figure 16. 4E-BP Status in the cell Does Not Affect PI3K/AKT/mTOR Signaling……..57

Figure 17. 4E-BP1 Re-expression Increases eIF4E Levels……58

Figure 18. eIF4E mRNA Levels are Unchanged by Loss of 4E-BP1/2……..60

Figure 19. Loss of 4E-BP1/2 Leads to Decreased eIF4E Protein Stability…….61

Figure 20. eIF4E Stability is Rescued by Blocking Proteasome in PyV-MT/4E-BP1/2 null *in vitro*……...…….62

Figure 21. Decreased eIF4E protein levels does not appear in NT2197 cells……..….64

Figure 22. Working Model…….……68

Tables

Table 1. List of Potential Targeted Therapies Focused on IGF and PI3K Signaling for Luminal B Breast Cancer ……...…8

Abbreviations

GLOBOCAN International Agency for Research on Cancer Report on Global Cancer Statistics
HR Hormone Receptor
ER Estrogen Receptor
PR Progesterone Receptor
HER Human Epithelial Growth Factor Receptor
cDNA complementary deoxyribonucleic acid
mRNA messenger ribonucleic acid
HER2+ HER2 amplified
IHC Immunohistochemistry
EGFR Epidermal Growth Factor Receptor
RTK Receptor Tyrosine Kinase
MAPK Mitogen-Activated Protein Kinase
ERK Extracellular-Signal-Regulated Kinase
PI3K Phosphoinositide 3-kinase
TNBC Triple Negative Breast Cancer
CL Claudin-Low
CDK Cyclin Dependent Kinase
PARP Poly ADP Ribose Polymerase
IGF Insulin Growth Factor
IGF-1R Insulin Growth Factor 1 Receptor
eIF eukaryotic initiation factor
TC Ternary complex
$tRNA_i^{Met}$ Initiator Methionyl tRNA
43S PIC 43S Pre-Initiation Complex
eIF4F Eukaryotic Initiation Factor 4F
eIF4E Eukaryotic Initiation Factor 4E
eIF4A Eukaryotic Initiation Factor 4A
PABP Poly A Binding Protein
UTR Untranslated Region
IRES Internal Ribosome Entry Site
4E-BP eIF4E Binding Protein
4E-BM eIF4E Binding Motif
VEGF Vascular Endothelial Growth Factor
MMP Metalloproteinase
MMTV-PyV MT Mammary Tumor Virus- Polyomavirus Middle-T Antigen
Mnk MAP Kinase Integrating Kinase
MEK MAPK/ERK Kinase
PTEN Phosphatase and Tensin Homolog
PD-L1 Programmed Death Ligand 1
RocA Rocaglamide A
EGF Epidermal Growth factor
mTOR Mechanistic Target of Rapamycin
Raptor Regulatory-Associated Protein of mTOR
mLST8 mTOR Associated Protein, LST8 homolog

TOS TOR signaling
PRAS40 Proline rich AKT substrate of 40 kDa
DEPTOR DEP domain containing mTOR Interacting Protein
Rictor Rapamycin Insensitive Component of mTOR
S6K p70S6 Kinase
TOP 5' Terminal Oligopyrimidine
LARP1 La Related Protein 1
CAGE Cap Analysis of Gene Expression
TSC Tuberous Sclerosis Complex
asTORi Active Site mTOR Inhibitors
PI Phosphatidylinositol
GPCR G-protein coupled receptors
CS Cowden Syndrome
Shc Src homology and Collagen
PTB Phospho-Tyrosine Binding
CH1 Collagen Homology 1
MIN Mammary Intraepithelial Neoplasia
PLC-γ1 Phospholipase C -γ1
EMT Epithelial-Mesenchymal Transition
TME Tumor Microenvironment
ECM Extracellular Matrix
FBS Fetal Bovine Serum
MEGS Mammary Epithelial Growth Supplement
H&E Hematoxylin and Eosin
CHX Cycloheximide
ROS Reactive Oxygen Species

Chapter One: Review of Literature

1.1 Breast Cancer

The 2018 International Agency for Research on Cancer Report on Global Cancer Statistics (GLOBOCAN) estimates cancer incidence and mortality across 20 world regions. For both sexes, the GLOBOCAN 2018 report indicates that lung cancer and breast cancer remain the two most commonly diagnosed cancer accounting each for about 11.6% of the total cancer incidence worldwide [1]. Breast cancer was identified as the cause of 6.6% of cancer deaths worldwide in both sexes [1]. In 2018, the report predicts that there will be 2.1 million newly diagnosed female breast cancer cases, thereby positioning it as the leading cause of cancer-associated deaths in over 100 countries [1].

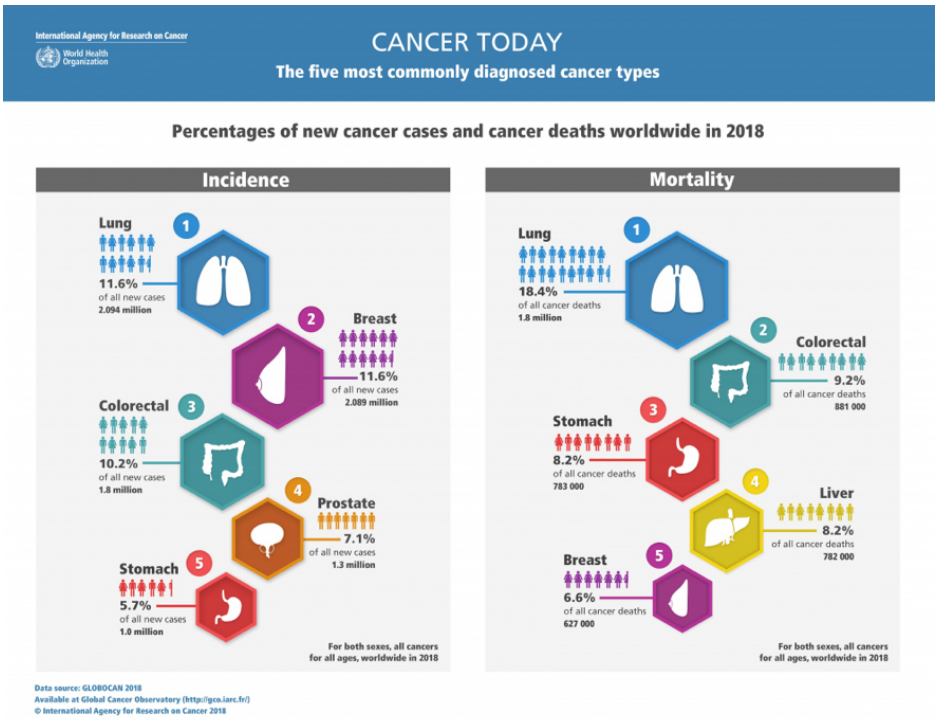

Figure 1. Cancer Today (GLOBOCAN 2018) Breast cancer is ranked second in terms of number of new cases and 5th in cancer mortality rate. Figure adapted from World Health Organization GLOBOCAN 2018

1.2 Breast Cancer Subtypes

Breast cancers are heterogenous tumors with varying gene expression signatures, histology, immunopathology, prognosis, and treatment responses [2, 3]. Thus, understanding the differences and similarities between different breast cancers is essential to developing more efficient treatments. Breast cancer can be categorized by histologic grade, expression of steroid and growth factor receptors, estrogen-inducible genes, protooncogenes, mutations in p53, and lymph node metastasis [4]. Immunohistochemically, breast tumors are categorized by the presence or absence of hormone receptors (HR) such as estrogen receptor (ER), progesterone receptor (PR), or by amplification of human epithelial growth factor receptor 2 (HER2), which can help to select appropriate treatment [5, 6].

Using complementary deoxyribonucleic acid (cDNA) microarrays, Perou and colleagues, using cDNA microarrays, classified patient breast tumors based on steady-state messenger ribonucleic acid (mRNA) levels or gene expression signatures [3-5] These studies among others have established at least 5 breast cancer tumor molecular subtypes: (i) luminal subtype A, (ii) luminal subtype B, (iii) HER2+, (iv) basal-like, and (v) normal breast-like [3].

Luminal A is the most common subtype of breast cancer with the best early-stage prognosis and low rates of relapse [7, 8]. This subtype is characterized as ER positive, HER2 negative, and with low rate of proliferation measured by Ki67 immunohistochemistry (IHC) staining [9]. The luminal B subtype makes up 10-20% of all breast cancers and has worse prognosis than luminal A. Luminal B tumors can be ER+ and/or PR+, HER2 amplification negative, high Ki67, or ER+ and/or PR+, HER2+ (7,9,10). Unlike other subtypes of breast cancer, only 10% of luminal B breast cancers

were HER2-enriched by IHC staining [10]. In general, luminal B breast cancer exhibit overexpression of ER, ER-regulated, proliferation-related, and cell cycle genes. In the clinic, luminal B breast cancer patients show poorer disease-free survival rates, increased risk of early relapse, and predisposition to relapse in bone and pleura compared to the luminal A breast cancer subtype [11]. Luminal B breast cancers show relative insensitivity to anti-hormone therapy compared to luminal A subtypes and relative insensitivity to chemotherapy compared to basal-like and HER2-enriched subtypes[11]. Luminal/ER+ breast cancers seem to be among the most heterogenous showing significant variation in gene expression, mutation spectrum, copy number variations, and patient outcomes [12]. Thus, the unique heterogenic make-up of the luminal B subtype has made it challenge for clinical management.

HER2-enriched breast cancers are identified by the amplification and overexpression of the HER2 gene. Within the HER2 subtype, breast tumors are highly proliferative, and are generally ER-, and PR- [3]. HER2 is part of the HER family of proteins which are transmembrane growth factor receptors that function to activate intracellular signaling in response to extracellular stimuli [13]. The HER family of proteins, also known as the ErbB-2 protein family, includes EGFR, HER2, HER3 and HER4 [13]. Compared to other HER family members, HER2 has the strongest catalytic kinase activity and HER2-containing heterodimers have the strongest signaling output downstream [13]. HER2 receptor tyrosine kinases undergo dimerization and transphosphorylation of their intracellular domains, which serve as docking sites for signaling molecules downstream of this receptor tyrosine kinase (RTK) [13]. In particular, activation of the HER2 RTK leads to activation of MAPK/ERK and PI3K signaling, which promotes aggressive tumor growth and proliferation [13].

Lastly, the basal-like subtype of breast cancer expresses genes present in normal breast myoepithelial cells such as cytokeratin CK5 and CK17, P-cadherin, CD44, and EGFR (epidermal growth factor receptor). In general, basal-like tumors are ER, PR, and HER2 amplification negative [8, 9]. These basal-like tumors include triple negative breast cancer (TNBC) which is negative for ER, PR, and HER2 amplification. The majority of TNBC (95%) are classified histologically as invasive mammary carcinoma and associated with poor prognosis [14]. Within the basal subtype, Herchkowitz et al. (2007) discovered another molecular subtype of breast cancer with low claudin levels and termed it 'claudin-low' (CL) breast cancer subtype [15]. The claudin-low subtype is characterized by low expression of genes involved in tight junctions and cell-cell adhesions such as *claudins 3,4,7,* occludin, and E-cadherin [15]. Human CL tumors also showed decreased expression of luminal epithelial genes and increased expression of endothelial cell markers [15]. CL tumors have been reported to account for 7-14% of TNBCs and generally lack ER, PR, and HER2 amplification [16].

1.3 Standard of Care Therapies for Breast Cancer

For non-metastatic breast cancer, the goals of therapy are eradication of the primary tumor and regional lymph nodes and prevention of metastatic recurrence. These non-metastatic breast tumors are removed by surgical resection, removal of axillary lymph nodes, and potential postoperative radiation [17]. HR positive tumors are determined by more than 1% of tumor cells staining positive for ER or PR, and in these cases anti-hormone agents are the first choice therapy [17]. These agents include tamoxifen, letrozole, anastrozole, or exemestane [17]. Tamoxifen is a selective estrogen receptor modulator that competitively inhibits binding of estrogen to ER [18]. Other therapies (letrozole, anastrozole, and exemestane) are categorized as aromatase inhibitors that decrease

circulating estrogen levels by inhibiting the enzyme which converts androgens to estrogens [17]. Aromatase inhibitors are generally only effective in post-menopausal women or women with medical ovarian suppression or oophorectomy [17]. In a meta-analysis study conducted by the early breast cancer trialists' collaborative group (EBCTCG), the 10-year breast cancer recurrence rate for tamoxifen was 22.7% versus 19.1% for aromatase inhibitors [19]. In HR positive breast cancer patients an anti-hormone therapy regimen is frequently combined with cytotoxic chemotherapy [17]. These standard chemotherapeutic agents include docetaxel, cyclophosphamide, adriamycin, and paclitaxel[19]. Docetaxel and paclitaxel disrupt mitosis by inhibiting microtubule function [19]. Cyclophosphamide and adriamycin, which are alkylating agent and anthracycline antibiotic, respectively, are DNA damaging agents [19].

In cases of HER2 amplified breast cancer subtypes, the standard of care is HER2 targeted therapies such as trastuzumab. Trastuzumab is a monoclonal antibody that targets the extracellular domain of HER2. It is most effective when given for 1-year to patients in conjunction with paclitaxel treatment for 12 weeks [20]. This targeted therapy has dramatically improved treatment of HER2 overexpressing breast cancers [21, 22].

Breast cancer deaths are mostly attributed to the metastatic progression of the disease [23].Of approximately 41,000 annual deaths from breast cancer virtually all were due to metastatic disease [23]. Current treatments for metastatic disease are not cures nor do they afford a promising five-year survival rate [17]. Thus, it is important to understand who is at risk, how subtypes metastasize, and eventually how to better treat metastatic disease.

Voduc et al. in 2010 contributed a study that sought to identify metastatic risk of breast tumor subtype [8]. The group found that the median duration of survival with distant metastasis were 2.2 years for luminal A, 1.1 years for luminal B, 0.7 years for HER2 enriched, and 0.5 years for basal-like. For all subtypes except basal, the bone was the most common site of metastasis [8]. Luminal A, luminal/HER2, and HER2+-enriched breast tumors saw significantly higher metastases in the brain, liver and lung compared to basal-like tumors that exhibit higher rate of metastasis to brain and lung with low rate of metastasis to liver and bone [7]. Interestingly, the molecular profiles of breast cancer subtypes appear to be preserved at metastatic sites [24].

For metastatic disease, the goals of care are symptom palliation and life prolongation [17]. Approved metastatic breast cancer drugs such as abemaciclib, palbociclib, and riociclib are administered to inhibit cell cycle progression through blocking of CDK4/6 in HR+/HER- cancers [17]. Poly ADP Ribose Polymerase (PARP) inhibitors, that interfere with DNA damage repair, have been approved for HER2- breast cancers in patients with germline mutations in BRCA [17]. Lastly, HER2+ metastatic breast cancers are treated with Trastuzumb-emtansine which consists of the HER2 monoclonal antibody conjugated with cytotoxic microtubule inhibitory agent, DM1, to ensure precise delivery of chemotherapy[17]. However, despite available treatments, median progression-free survival rate of 24.8 months[17].

1.3.1 Targeting Insulin Signaling

Insulin signaling has been recognized as a major signaling pathway that is activated in cancer [25]. Insulin and insulin-like growth factors (IGF) regulate organismal physiology by affecting blood glucose levels and cellular mitogenesis [25]. Low or reduced insulin levels have been linked to

anti-cancer effects *in vivo* [26]. In humans, insulin and IGF1 bind insulin receptor (IR)- IGF1 receptor (IGF1R) family to transduce signals in most tissues [25]. The IGF1R has been shown to be expressed in cancer cell lines, but more specifically in tumors with luminal B profiles [27-29]. In a 2012 study, Kennecke's group (2010) analyzed 2,871 female breast tumors by IHC to identify IGF1R as a potential prognostic marker [29]. Interestingly, 53.8% of ER+ and 50% of HER2- breast tumors were IGF1R positive, while luminal B breast tumors had the highest IGF1R expression (57% of tumors) of all the subtypes [29]. Thus, inhibition of IGR1R signaling has been an attractive target for luminal B cancers.

Alternatively, there have been efforts to target downstream of IGF1R, including kinase inhibitors that inhibit PI3K signaling. The PI3K pathway is a key pathway for carcinogenesis and is hyperactivated in the vast majority of breast cancer [30]. Further, high PI3K signaling activity has been associated with luminal B breast cancers [31]. Many pharmaceutical companies have focused on these two signaling pathways in their drug development efforts; however few of these drugs have come to fruition in the clinic [11]. (Table 1)

Agent	Pathway	Supplier	Class	Targeted Population
BMS-754807	IGF	Bristol Myers Squibb	IGF-1R-IR TKI	ER-positive locally advanced/metastatic breast cancer,
Cixutumumab	IGF	ImClone	IGF-1R mAb	Locally advanced/metastatic breast cancer progressed on one or two chemotherapy lines

Dalotuzumab	IGF	Merck	IGF-1R mAb	ER-positive locally advanced/. metastatic breast cancer, progressed on at least one line of endocrine therapy
XL-147	PI3K	Exelixis	PI3K inhibitor	ER-positive metastatic breast cancer refractory to nonsteroidal aromatase inhibitors
XL-765	PI3K	Exelixis	PI3K/mTOR inhibitor	ER-positive metastatic breast refractory to nonsteroidal aromatase inhibitors
MK-2206	PI3K	Merck	AKT inhibitor	ER-positive metastatic breast cancer progressed on endocrine therapy

Table 1. List of Potential Targeted Therapies focused on IGF and PI3K signaling for Luminal B Breast Cancer [11]

1.4 Translation in Cancer

Dysregulated mRNA translation is a common feature of cancer cells [32]. Under normal conditions, mRNA translation is a tightly regulated process involving tRNAs, ribosomes, auxiliary factors, and mRNA [32]. However, the dysregulation of mRNA translation is common in cancer and can lead to aberrant proliferation, cell survival, angiogenesis, and altered immune response and metabolism [32]. mRNA translation or protein synthesis is the most energy-consuming process in the cell; thereby, it must be tightly regulated to avoid wasted energy expenditure [33].

1.4.1 Translation Initiation

Translation initiation is thought to be the most regulated and rate-limiting step of translation [32]. This step requires assembly of a functional 40S subunit with its associated eukaryotic translation initiation factors (eIFs): eIF1, eIF1A, eIF5, and eIF3 [32, 34]. Next, the 40S subunit associates with the ternary complex (TC) which consists of eIF2 (including α-, β-, γ- subunits), initiator methionyl tRNA ($tRNA_i^{Met}$) and GTP. This signifies the assembly of the 43S pre-initiation complex (43S PIC). The 43S PIC then associates with the eIF4F complex at the 5' mRNA cap [32, 35]. The eIF4F complex is a heterotrimeric complex consisting of: (1) eIF4E, the mRNA 5'-cap binding subunit, (2) eIF4G, a large scaffolding protein, and (3) eIF4A, the DEAD box RNA helicase [32, 36-40]. eIF4F recruits ribosomes to the mRNA via the eIF4E-mRNA cap and eIF4G-eIF3 interaction [37]. The final result is the assembly of the 48S initiation complex. Simultaneously, eIF4G interacts with Poly-A Binding Protein (PABP) that associates with the mRNA 3' poly(A) tail, which is thought to result in mRNA circularization and stabilization of mRNA on the 48S complex [41]. Once the initiation codon is recognized by the 43S PIC, the 60S ribosomal subunit joins followed by the release of the eIFs [37]. The eIF4A helicase facilitates scanning of the 43S pre-initiation complex towards the initiation codon by unwinding the secondary structure in the 5' untranslated region (UTR) [32]. It is also important to note that mRNA can also be translated independent of the 5' cap. These mRNA employ an internal ribosome entry site (IRES) within their 5' UTR; thus, recruiting ribosomes and initiating translation independent of the 5' cap structure [42, 43]. (Figure 2)

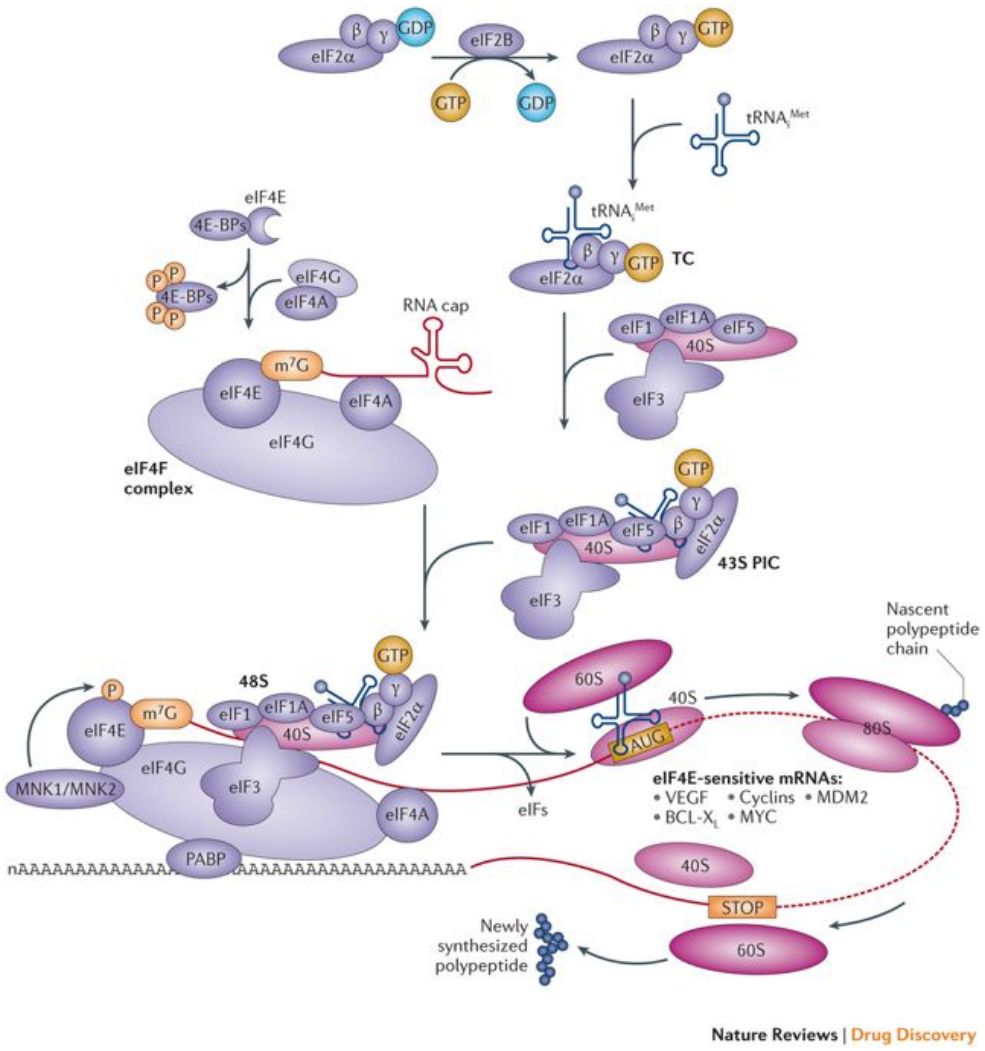

Figure 2. Overview of 5' Cap-Dependent Translation Initiation[32]
Translation initiation is the most tightly regulated step of mRNA translation. The rate-limiting steps of translation initiation are assembly of the 43S PIC and association of 43S PIC with mRNA through the eIF4F complex. To assemble the 43S PIC, the ternary complex must first form. The ternary complex consists of eIF2 (including α, β, and γ subunits), $tRNA_i^{Met}$ and GTP. The ternary complex associates with the 40S ribosome with associated initiation factors: eIF1, eIF1A, eIF3, and eIF5. This forms the 43S PIC. Through eIF3 binding to eIF4G, the 43S PIC associates with eIF4F on the 5' cap. eIF4G also interacts with PABP to stabilize mRNA on the initiation complex. The eIF4A helicase helps to resolve the 5' UTR structure in order to scan for initiation codon. Once the initiation codon is recognized, the eIFs are released from the 43S PIC and the 60S ribosomal subunit joins. Elongation begins and translation of eIF4E-sensitive mRNAs. Adapted from Bhat et al. (2015) [32]

1.4.2 eIF4E

The eIF4F complex assembly is a tightly regulated and rate-limiting step in mRNA translation. The eIF4E protein is thought to be the least abundant translation initiation factor whereby changes in its availability and/or activity have profound qualitative and quantitative effects on the translatome [44]. The eIF4E family of proteins consists of eIF4E1, eIF4E2, and eIF4E3. Both eIF4E1 and eIF4E2 recognize the 5' cap using the negative π electron clouds from their aromatic residues to interact with the positively charged 5' cap [45]. eIF4E1 for instance binds to the 5'm^7 GpppN (N is any nucleotide and m is a methyl group) cap through π-π stacking interactions between the guanine base and the indole side chains of Trp56 (human) and Trp102 (human) residues of eIF4E1 [46, 47]. In contrast, eIF4E3 does not recognize the 5' cap due to a cysteine residue in the place of aromatic Trp56 residue that appears in the other eIF4E family members [45].

In addition to binding the cap, eIF4E binds to 4E-BPs (eIF4E-binding proteins) and eIF4G through the region on its dorsal surface centered around Trp73 (murine) residue [48]. This Trp73 residue is part of the canonical eIF4E-binding motif (4E-BM) with the consensus sequence $YX_4L\phi$ (where Y is Tyr, X is any amino acid, L is Leu, and ϕ is any hydrophobic residue [49]. However, there is also evidence to show that eIF4G auxiliary sequences bind to the lateral surface of eIF4E [49]. Thus, eIF4G and 4E-BPs bind to eIF4E on both its dorsal and lateral surface through canonical and non-canonical motifs [49].

eIF4E can be regulated transcriptionally or post-translationally through phosphorylation events or through the binding of negative regulators such as 4E-BPs [50]. EIF4E1 gene has two functional

MYC-binding sites in its promoter region. Studies showing correlation between MYC and eIF4E mRNA levels during cell cycle reinforce the idea that eIF4E is transcriptionally regulated by MYC [51, 52]. eIF4E is also regulated at the level of mRNA stability or through ubiquitination at the Lys159 residue [53, 54]. Surprisingly, ubiquitinated eIF4E was reported to reduce its phosphorylation and eIF4G binding, but not its cap-binding activity [54]. eIF4E ubiquitination appears to be mediated by Chip ubiquitin E3 ligase [54].

eIF4E overexpression has been shown to induce cellular transformation, tumorigenesis, invasion, and metastasis by selectively upregulating the translation of mRNAs encoding growth-promoting proteins such as cyclin D1, c-myc, HIF-1α, and ornithine decarboxylase (ODC) [32]. In 1990, Lazaris-Karatzas et al. made the seminal discovery that eIF4E1 (henceforth referred to as eIF4E) was capable to induce malignant transformation of NIH-3T3 cells and rat primary embryo fibroblasts in collaboration with oncogenes such as adenovirus E1A or c-myc [55, 56]. Interestingly, only a modest (about 2.5-fold) excess of eIF4E was sufficient to cause transformation in cell culture [57]. Thus, eIF4E has come to be regarded as a proto-oncogene [58]. eIF4E protein levels are also elevated in breast, head and neck, and prostate cancers [59]. The eIF4E upregulation in breast cancer is especially apparent as normal breast tissue typically has lower eIF4E levels relative to other tissues [60]. Overexpression of eIF4E in breast carcinoma has even been proposed to be a valuable prognostic marker [61]. In tumors, high eIF4E levels correspond to an enhanced translation of a subset of pro-tumorigenic mRNAs such as those encoding c-myc, vascular endothelial growth factor (VEGF), cyclin D1, and matrix metalloproteinase 9 (MMP-9) [62]. These mRNAs, referred to as “eIF4E-sensitive”, are characterized by 5’ UTR features including long, G+C rich, highly structured, 5’ UTRs [63].

Downregulation of eIF4E expression has been shown to reduce xenograft tumor growth [64]. Specifically, eIF4E promotes breast cancer progression in mice and be associated with poor prognosis, specifically in luminal B cancer [65, 66]. Notably, Nasr et. al (2013) demonstrated that in a mouse mammary tumor virus- polyomavirus middle-T antigen (MMTV-PyV-MT) breast cancer model on a C57Bl/6 background, with constitutively activated mTOR activity, there was an increase in pulmonary metastasis with no difference in primary tumor initiation or burden [65]. This phenotype was disrupted by decreasing eIF4E levels, which led to increased apoptosis [65]. eIF4E-overexpression driven by the ubiquitous β-actin promoter in transgenic mice increases tumorigenesis [67]. Thus, this further supports the role of eIF4E as an oncogene *in vivo* [67]. Reducing eIF4E levels, through use of eIF4E heterozygous mice, has been reported to decrease cellular transformation and reduced tumorigenesis [68]. This decrease in transformation was demonstrated to be due to a reduction specific mRNAs related to reactive oxygen species tolerance, suggesting that eIF4E may also contribute to cell survival in tumorigenesis [68].

eIF4E is also phosphorylated on its Ser209 residue by MAP Kinase Integrating Kinases (MNK1/2) which are downstream of both the MAPK/ERK and p38 MAP Kinase signaling pathways [69, 70]. Phosphorylation of eIF4E does not seem to be required for transformation, translation, or development of mice [71]. However, when phosphorylated, eIF4E has enhanced ability to transform cells and facilitate transport of a subset of mRNAs [72]. In addition, $eIF4E^{Ser209Ala}$ mutation abrogates tumor development in a PTEN-null mouse model of prostate cancer whereas mouse embryonic fibroblasts (MEFs) isolated from $eIF4E^{Ser209Ala}$ knock-in mice are resistant to neoplastic transformation [73]. Inhibition of eIF4E phosphorylation by MNK1/2 inhibitor, cercosporamide, was also shown to impair xenograft growth in mice [74]. eIF4E phosphorylation

also enhances metastatic properties such as colony formation and anchorage independent growth *in vitro* through promoting the translation of a subset of mRNAs involved in EMT/invasion and metastasis such as MMP3 and SNAIL [75]. Finally, $eIF4E^{S209A}$ mice expressing the PyV-MT transgene were found to be resistant to mammary tumor development and metastasis [75]. Collectively, this evidence suggests that the phosphorylation of eIF4E increases its oncogenic potential.

The pro-oncogenic properties of eIF4E in many common cancers has made it an attractive target for drug development. Anti-sense eIF4E nucleotides (eIF4E ASO) inhibited tumor growth in mice without toxicity [64, 76]. eIF4E ASO has gone to phase II trials for colorectal cancer patients and has been shown to stabilize 47% patients with progressing disease [76]. Another effort led by Gerhard Wagner discovered a compound, 4E-GI-1, which disrupts the eIF4E-eIF4G interaction resulting in inhibition of cap-dependent translation and *in vitro* cancer cell growth [77]. SBI-0640756, another eIF4G targeting compound, was reported by Feng et al. (2015) to significantly disrupt eIF4F complex formation *in vitro* and *in vivo* independently of mTOR and 4E-BPs [78]. However, the mechanism of SBI-0640756 remains unknown.

Lastly, eIF4A inhibitors have also seen preclinical success in cell and mouse models by targeting the translation initiation step in cancer cells. Among these eIF4A inhibitors include: hippuristanol, pateamine A and silvestrol [32]. Pateamine A increases the ATPase and RNA binding activity of eIF4A and thereby prevents ribosome-recruitment during the translation initiation phase [79, 80]. Pateamine A is an irreversible inhibitor of protein synthesis and thus shows high toxicity *in vivo* [80, 81] . Of the eIF4A inhibitors, silvestrol appears to be most potent *in vivo* [82] . The use of

silversterol has been shown to inhibit eIF4F and block programmed death-ligand 1 (PD-L1) in cancer cells [83]. Blocking immune inhibitory checkpoints PD-L1 and its receptor PD-1 can help prevent immune evasion of cancer cells [83]. This positions eIF4A inhibitors as a potential component of immunotherapy. More recently, rocaglamide A (RocA) was discovered as an eIF4A inhibitor that traps eIF4A on polypurine RNA selectively, bypassing the ATP requirement for RNA binding. eIF4A-RocA complexes block ribosome scanning and repress mRNA translation [84].

1.4.3 4E-BP1 and 4E-BP2

eIF4E availability is also regulated by 4E-BPs. 4E-BPs are small (15-20 kDa) translational repressors that interfere with eIF4F complex assembly [85]. 4E-BPs inhibit cap-dependent translation by binding to eIF4E; thereby preventing the association of eIF4E with eIF4G [50, 86]. 4E-BPs engage two orthogonal surfaces on eIF4E, giving it its canonical name: the elbow loop. The 4E-BP elbow loop interacts with eIF4E primarily through π-π stacking and van der Waal interactions of hydrophobic surfaces [87].

In mammalian cells, there are 3 4E-BP paralogs: 4E-BP1, 4E-BP2, and 4E-BP3 [50, 88]. 4E-BP1 is ubiquitously expressed and the most abundant out of all 3 4E-BPs in most of the tissues. 4E-BP2 is predominantly expressed in the brain, where it appears to play an important role in synaptic plasticity and memory [86]. Lastly, 4E-BP3 seems to be enriched in the skeletal muscle and heart and, unlike 4E-BP1 and 4E-BP2, lacks a regulatory motif of four amino acids (RAIP motif) in its N-terminus [88]. The RAIP (arginine, alanine, isoleucine, proline) motif is required for efficient phosphorylation of 4E-BP1 by mechanistic target of rapamycin 1 (mTORC1) [89]. Disruption of

RAIP motifs by mutagenesis diminishes 4E-BP1 and 2 phosphorylation which suppresses eIF4F complex assembly and cap-dependent translation in insulin stimulated cells [89, 90].

Activated mTORC1 phosphorylates 4E-BP1 and 4E-BP2 first on its Thr37 and Thr46 residues and then on its Ser65 and Thr70 residues [91]. Phosphorylation of 4E-BPs results in their dissociation from eIF4E, which subsequently allows for eIF4F complex assembly and cap-dependent translation [50, 92]. 4E-BPs have been extensively studied both *in vitro* and *in vivo* models. Loss of 4E-BP1 and 4E-BP2 (4E-BP1/2 null) in mice has been reported to lead to increased sensitivity to diet-induced obesity and insulin resistance [93]. In cancer, loss of 4E-BP1/2 leads to senescence in a wild-type p53 context and accelerated tumorigenesis upon p53 loss [94]. Further, loss of 4E-BP1/2 in a PTEN null prostate cancer mouse model leads to increased tumorigenesis and tumor invasiveness as well as increased cell death within hypoxic tumor regions [95]. Thus, 4E-BPs appear to play a tumor suppressive role in certain cancer contexts and modulate glucose and lipid metabolism.

Although pre-clinical studies generally reported tumor-suppressive properties of 4E-BPs, 4E-BP1 overexpression has been observed across a variety of human cancers such as brain, prostate, colorectal and breast [96]. Braunstein et al. (2007) reported that 4E-BP1 was highly overexpressed specifically in advanced breast cancers [97]. Alternatively, 4E-BP1 expression was also reported to be inversely correlated with tumor progression in gastrointestinal cancers, wherein earlier stages of cancer had higher 4E-BP1 levels than later stages [98] Notably, in human tumors hyperphosphorylation commonly accompanies the increase in 4E-BP1 levels, whereby high phospho-4E-BP1 levels correlate with poor prognosis [99].

The apparent counterintuitive increase in 4E-BP1 levels can be explained by discussing the alternative ways that 4E-BPs can function. For instance, under normal growth conditions, cells use cap-dependent translation; however, under hypoxic conditions, 4E-BPs may help in promoting cap-independent (IRES-mediated) mechanisms of translation initiation. This, in turn, is thought to promote translation of mRNAs that stimulate angiogenesis (VEGF-A), hypoxia responses (transcription factor HIF-1α), and inhibition of apoptosis (Bcl2); thereby, promoting tumor survival [97].

1.4.4 Coregulation of 4E-BPs and eIF4E

eIF4F levels are largely determined by the eIF4E/4EBP ratio and mTOR activity [100]. Recently emerging evidence suggests that the eIF4E/4EBP ratio may be actively regulated. For instance, Yanagiya et al. (2012) report that knockdown of eIF4E resulted only in minor decrease in cap-dependent translation, which is explained by degradation of the excess unphosphorylated 4E-BPs in eIF4E depleted cells [101]. This E3 ubiquitin ligase, KLHL25-CUL3 complex mediated mechanism may thus be employed to adjust eIF4E/4E-BP ratio in the cell [101]. Importantly, it appears that in cell culture and mouse xenograft models the eIF4E/4E-BP ratio is a better predictive marker for response to mTOR inhibitors than individual eIF4E or 4E-BP levels [100]. Under conditions where the eIF4E/4E-BP ratio is elevated, the effects of mTOR, HER2, and BRAF inhibitors are attenuated [100, 102]. In turn, depletion of eIF4E and the corresponding reduction in eIF4E/4E-BP1 ratio enhanced anti-neoplastic efficacy of mTOR inhibitors [100]. Thus, the eIF4E/4E-BP ratio was a better predictive marker for response to mTOR inhibitors than individual eIF4E or 4E-BP levels [100].

Studies on patient tumor samples have indicated that characterizing levels of 4E-BPs in respect to eIF4E has greater prognostic power than measurement of individual protein levels [99]. In the analysis of 424 breast tumors, 4E-BPs and eIF4E were shown to be positively correlated [99]. While analyses show that high eIF4E expression in tumors leads to poor patient prognosis, the level of eIF4E is also highly correlated to levels of 4E-BPs [99]. Using Spearman's ρ correlation, eIF4E was reported to have high correlation figures of 0.31, 0.34, and 0.21 when compared to 4E-BP1, 4E-BP2, and p-4E-BP1, respectively [99]. 4E-BP1 and p-4E-BP1 were identified to be positively correlated with a correlation figure of (ρ=0.36) [99]. This is likely due to high levels of total 4E-BP1 being in its phosphorylated state to allow for cap-dependent mRNA translation through eIF4E [99]. Still, the positive correlation between eIF4E and 4E-BPs, whom have seemingly opposing functions, may point to important modulating influences of 4E-BPs on eIF4E [99].

As such, important modulating influences that regulate 4E-BPs and eIF4E ratios warrants discussion. In both esophageal and gastrointestinal cancers, eIF4E and 4E-BP levels do not seem to be positively correlated [98, 103]. While eIF4E levels increase with tumor stage in these cancers, 4E-BPs appear to decrease [98]. Due to this discrepancy, it has been proposed to utilize the ratio of 4E-BPs to eIF4E [103]. In normal adjacent esophageal tissue, the ratio of 4E-BP/eIF4E ranges from 0.08 to 0.15 [103]. In comparison, esophageal tumor tissue has higher 4E-BP/eIF4E ratios ranging from 0.28-0.54 [103]. In gastrointestinal cancers, the increasing 4E-BP/eIF4E ratio seemed to be positively correlated with metastatic potential [98]. In patients without distant metastasis, the relative difference between 4E-BP1 elevation and eIF4E elevation is much greater than that of patients with distant metastases [98]. The latter findings suggest that tumors that

maintain an equilibrium between 4E-BP1 and eIF4E have greater tumorigenic and metastatic potential compared to normal tissue.

1.5 mTOR

mTOR is a serine/threonine protein kinase that belongs to the PI3K-related kinase family [104]. mTOR is the central orchestrator for cell growth and metabolism. It integrates environmental inputs such as amino acids levels, glucose, oxygen, insulin, and growth factors such as EGF to signals that respond and regulate cellular processes such as protein synthesis, proliferation, cell growth, autophagy, and metabolism [104]. mTOR was discovered as the target of rapamycin. Rapamycin (known as sirolimus in the clinic) is a macrolide produced by *Streptomyces Hygroscopicus* bacteria[104]. *S. Hygroscopicus* were found in a set of soil samples collected in Rapa Nui (Easter Island), an island in the South Pacific. These bacteria were isolated and found to have significant antifungal, immunosuppressive, and anti-proliferative properties [105-107]. TOR was later identified as target of rapamycin isolated in both yeast and mammals [108-112]. Chung et al. in 1992 reported that rapamycin interacts with immunophilin/peptidyl-prolyl-isomerase FKBP12 to inhibit mTORC1 [113].

mTOR interacts with several proteins to form two distinct complexes named mTOR complex 1 (mTORC1) and mTOR complex 2 (mTORC2). These two mTOR complexes differ in sensitivity to rapamycin, composition, upstream regulation and downstream effects. mTORC1 consists of three main components: mTOR kinase, Raptor (regulatory- associated protein of mTOR), and mLST8 (mTOR associated protein, LST8 homolog) [104]. Raptor recruits substrates to mTORC1 through binding to TOR signaling (TOS) motifs on mTORC1 substrates [104]. In addition to

mTORC1 core components, the complex also includes two negative regulators PRAS40 (proline rich AKT substrate of 40kDa) and DEPTOR (DEP domain containing mTOR interacting protein) [104]. Rapamycin-FKBP12 inhibits mTORC1 through binding to the FRB domain of mTOR thereby restricting the catalytic cleft and obstructing substrate binding to active site [113]. Rapamycin sensitivity is one of the defining features setting it apart from mTORC2 [104]. mTORC2 is less sensitive to rapamycin relative to mTORC1; however, prolonged rapamycin treatment abrogates mTORC2 signaling at least in certain cell types [104]. While mTORC2 contains both mTOR and mLST8, mTORC2 comprises of Rictor (rapamycin insensitive component of mTOR) regulatory protein instead of Raptor [104]. mTORC1 is the most studied of the two mTOR complexes and plays a central role in metabolic activity in response to environmental cues [104]. While mTORC2 plays a role in cytoskeletal organization and cell survival via phosphorylating AGC kinases (e.g. PKC and AKT), its role in lipid and glucose metabolism has also been suggested [104, 114]. (Figure 3)

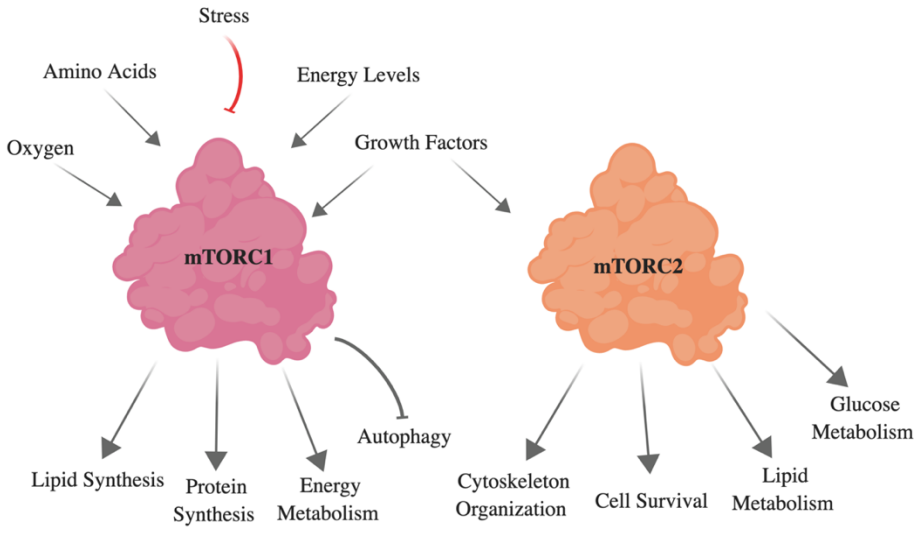

Figure 3. The mTOR Complexes
mTOR, a serine/threonine kinase, exists in two complexes: mTORC1 and mTORC2. mTORC1 senses amino acid levels, oxygen levels, energy levels, and the presence of growth factors. Dependent on environmental conditions, mTORC1 may increase certain protein synthesis, energy

metabolism, or lipid synthesis programs. mTORC1 can also block autophagy and be blocked by stressful conditions. In contrast, mTORC1 responds mostly to growth factors. In response to these growth factors, mTORC2 functions to modulate cytoskeleton organization, cell survival, lipid metabolism, and glucose metabolism [104].

A primary function of mTORC1 is to promote protein synthesis. This is achieved through the mTORC1-dependent phosphorylation of p70S6 Kinase 1 and 2 (S6K1 and 2) and eIF4E binding proteins (4E-BP1, 2, 3 in mammals). mTORC1 phosphorylates S6K1 on its hydrophobic motif site, Thr389 which allows for subsequent phosphorylation and activation by PDK1 on Thr229. S6K2 is phosphorylated by mTORC1 on its Thr388 residue and subsequently on its Thr228 residue by PDK1. At the same time, mTORC1 phosphorylates 4E-BPs at multiple sites (e.g. Thr70, Ser65, Thr37/46 in human proteins) [91]. Phosphorylation inactivates the 4E-BPs which leads to their dissociation from eIF4E and consequent eIF4F complex assembly [92, 115].

Akin to eIF4E, mTORC1 also selectively stimulates translation of a subset of mRNAs. For example, while the translation of mRNAs encoding house-keeping proteins such as actin and tubulin is only marginally affected by changes in mTOR activity, translation of a subset of mRNA containing 5'-terminal oligopyrimidine tracts (TOPs), which encode components of the translation machinery such as ribosomal proteins, elongation factors, and PABP are exceptionally sensitive to changes in mTORC1 activity [116]. The 5' TOP sequence consists of a C nucleotide at the 1+ position of the mRNA followed by a stretch of 4-14 pyrimidines [116]. Stimulation of 5' TOP mRNA translation was initially thought to occur through mTOR-dependent phosphorylation of 4E-BPs [117, 118]; however, this has been challenged as it was found that 4E-BPs do not mediate the effects of mTOR on TOP mRNA translation in response to physiological stimuli [119]. More

recently it has been reported that, La related protein 1 (LARP1), acts as a major effector of mTORC1 on TOP mRNA translation [120-123].

Transcription start profiling by cap analysis of gene expression (CAGE) revealed that non-TOP mRNAs are also regulated in an mTORC1-dependent manner [124]. These mRNAs can be divided into two groups: (1) mRNA with short 5' UTR implicated in mitochondrial function and (2) long 5' UTR mRNA that play a role in proliferation and survival promoting functions [124]. In malignant cells, mTOR inhibition or eIF4E depletion suppressed the translation of both long and short 5' UTR mRNAs [124]. In turn eIF4A1 depletion or eIF4A inhibitors selectively suppressed long 5' mRNA, but not short 5'UTR mRNA translation [124]. In conclusion, alterations in mTOR activity have particularly dramatic effect on translation of a subset of mRNAs which harbor specific 5'UTR features.

1.5.1 Therapies Targeting mTOR in Cancer

Hyperactivated mTOR signaling commonly occurs in human diseases such as cancer, obesity, type II diabetes, and neurodegeneration [104]. Given the anti-proliferative potential of rapamycin, many rapamycin analogs (rapalogues) and derivatives have been developed and tested in clinical trials [125]. mTOR targeted therapies fall generally into two categories: allosteric mTOR inhibitors and mTOR kinase inhibitors [125]. Allosteric mTOR inhibitors include rapalogues such as temsirolimus, everolimus, and ridaforolimus; however, none of these significantly increase patient survival rates [125]. Everolimus is approved for therapy by the FDA for treatment of advanced stage renal cell carcinoma, hormone receptor positive, HER2-negative breast cancer in postmenopausal women; pancreatic neuroendrocrine tumour; adult renal angiomyolipoma

associated with TSC; and pediatric or adult subependymal giant cell astrocytoma with TSC [125]. Everolimus was shown to prolong patient survival by 2.1 months [125]. Temisorlimus is also approved for treatment of renal cell carcinoma, but only shows modest improvement of patient survival by around 3.6 months[125].

In pre-clinical models, active site mTOR inhibitors (asTORi) exhibit more potent anti-neoplastic efficacy than rapamycin through inhibition of both mTORC1 and mTORC2 [32]. Unlike rapamycin, which activates AKT via the S6K1/IRS-1/PI3K feedback, asTORi suppress AKT by inhibiting mTORC2 [126]. Although this was thought to explain stronger anti-neoplastic effects of asTORi as compared to rapamycin, it was found that the ability of asTORi to suppress rapamycin-insensitive mTORC1 outputs, including phosphorylation of 4E-BPs underpins higher potency of asTORi relative to rapamycin ([127, 128]. Vistusertib and Sapanisertib are two mTOR kinase inhibitors currently in phase II of clinical trials [126]. While these inhibitors are well-tolerated by patient, thus far the treatments have not been able to significantly improve patient outcome [126]. Low efficacy of mTOR inhibitors in patients may be attributed to the feedback inhibition of AKT by mTOR-activated S6K, thereby leading to increased AKT activation [129]. Activation of AKT opposes mTORC1 inhibition and functions to propagate signaling downstream through mTORC1.

1.6 PI3K/AKT/mTOR Signaling Pathway in Breast Cancer

PI3Ks are a family of intracellular lipid kinases that phosphorylate the 3' hydroxyl group of phosphatidylinositol (PI) [130]. Subsequent to this phosphorylation event extracellular signals are transmitted to intracellular secondary messengers that will transduce a variety of signaling

pathways involved in metabolism, cell-cycle regulation, differentiation, migration, survival, and growth [130]. PI3Ks exist in three classes (I-III) that differ in substrate specificity, sequence homology, expression, and regulation [130]. Class I PI3Ks are divided into two subclasses: IA and IB [130]. Class IA PI3Ks are activated by RTKs while class IB are activated by G-protein coupled receptors (GPCRs) [131, 132].

When receptor protein tyrosine kinases are activated by growth factors extracellularly, this results in the autophosphorylation on tyrosine residues in their phospho- YXXM motifs within the RTK [133]. Subsequently, PI3K is recruited to the membrane by binding directly to the phospho-tyrosine of RTKs through the C-terminal SH2 domain in its adaptor subunit [134, 135]. Class I PI3Ks are also recruited to the plasma membrane by adaptor proteins such as IRS family members, Shc, or Grb2 [126, 136]. For instance, growth factors and hormones stimulate RTK-mediated IRS-1 phosphorylation on tyrosine motifs and association of IRS-1 with the PI3K regulatory subunits at the plasma membrane [126, 136]. Adaptor proteins IRS-1 and Shc can also activate the RAS/MAPK pathway [134, 137]. This allows for allosteric activation of the p110 catalytic subunit [132]. The p110 catalytic subunits (α,β,δ) of class I PI3Ks phosphorylate phosphatidylinositol-4,5-biphosphate (PI-4,5-P_2) to phosphatidylinositol-3,4,5-triphosphate (PI3,4,5-P_3) [132]. PI3,4,5-P_3 then recruits a signaling proteins with pleckstrin homology (PH) domains to the membrane [134, 137]. Among these PH domain-signaling proteins is protein serine/threonine kinase 3-phosphoinositide-dependent protein kinase-1 (PDK1) and AKT/protein kinase B (PKB) [134, 137].

PI3K dysregulation is central in cancer. Indeed, PI3K activity was initially discovered in 1984 in purified preparations of oncoprotein $pp60^{v\text{-}src}$[138]. Others soon observed PI3K activity associated with oncoprotein, polyoma virus middle T antigen (PyV-MT) which is known to bind and activate $pp60^{c\text{-}src}$ [139, 140]. Constitutively activated p110α subunit of PI3K was shown to be capable of driving tumor formation in immortalized (via hTERT) human mammary epithelial (HMEC) cells [141]. Activating mutations in humans point to class IA PI3Ks as attractive cancer targets as the *PIK3CA* gene, encoding the p110α catalytic subunit, has been to discovered to be commonly mutated in most common cancers including: colon, breast, brain, liver, and prostate [142, 143]. The *PIK3CA* mutations lead to aberrant PI3K signaling, thereby rendering *PIK3CA* as an oncogene [142]. About 25% of breast cancers contain somatic mutations in *PIK3CA*, with the majority of these mutations being located in its kinase domain [144]. Creighton et al. proposed that luminal B tumors have hyperactive PI3K signaling which is associated with lower ER levels [31]. This is correlated with resistance to endocrine therapy. Targeting PI3K in these tumors may be key to restoring ER expression, signaling, and hormonal sensitivity [31]. This indicates that loss of ER signaling may be compensated by increased PI3K signaling [145].

AKT/PKB is involved in a variety of cell processes such as cell survival, metabolism and cell cycle progression [137]. It belongs to the AGC kinase family and consists of an N-terminal PH domain, a central kinase CAT domain, and a C-terminal extension (EXT), which contains a regulatory hydrophobic motif (HM) [137]. There are three highly homologous isoforms of AKT: AKT1, AKT2, AKT3 with some but not fully overlapping functions[146]. In general, AKT1 is considered to be the most involved in cellular growth and angiogenesis while AKT2 and AKT3 are most involved in glucose homeostasis and neuronal development, respectively [146].

AKT1 is phosphorylated by mTORC2 at its Ser473 (human) residue in its hydrophobic motif and by PDK1 on its Thr308 residue in its active site [137]. These phosphorylation events lead to AKT1 activation [147-149]. In general, AKT/PKB increases survival by inactivating pro-apoptotic factors such as Bad and procaspase-9 and Forkhead family transcription factors (FOXO) that induce the expression of other pro-apoptotic factors such as Fas-ligand [150]. Moreover, activated AKT1 promotes cell survival by phosphorylation and translocation of Mdm2 into the nucleus where it downregulates p53. As a result, p53-mediated cell cycle checkpoints are antagonized by AKT1 [151, 152].

AKT1 activates downstream mTORC1 kinase by inhibiting tuberous sclerosis complex (TSC) [146].The tumor suppressor TSC complex consists of TSC1 and TSC2 genes, which encodes for hamartin and tuberin, respectively [153]. As negative regulators of mTORC1, these tumor suppressors are critical regulators of cell growth and proliferation [153]. Mutations in either TSC1 or TSC2 result in an autosomal dominant disorder: TSC syndrome [153]. TSC syndrome can result in severe pathological consequences such as mental retardation, epilepsy, autism, hamartomas, as well as cardiac, pulmonary, and renal failure [153]. TSC2 contains a GTPase activating domain that was found to inactivate Rheb GTP-binding protein [154]. Rheb is a GTPase and member of the RAS super-family, which stimulates mTORC1 kinase activity [155-157]. AKT1 directly phosphorylates TSC2 at Ser939 and Thr1462 to relieve Rheb inhibition of mTOR. AKT1 activation has been identified in many common cancers including (but not limited to) multiple myeloma, lung, head and neck, breast, brain, gastric, endometrial, colon, ovarian, and prostate cancers [158]. Phosphorylation of AKT1 on Ser473 has been associated with poor prognosis in skin, pancreas, liver, and breast cancers [158].

PTEN (phosphatase and tensin homolog deleted from chromosome 10) was identified as a tumor suppressor which antagonizes PI3K signaling by removing the 3' phosphate from $PI(3,4,5)P_3$ [159-161]. PTEN, therefore acts as negative regulator of PI3K/AKT signaling [162]. PTEN has been reported to be inactivated in a significant of human cancers including brain (>30%), prostate (30-50%) and breast (>20%) [161, 163-165]. Mutations in PTEN can also result in a variety of PTEN hamartoma tumor syndrome (PHTS) which results in a spectrum of disorders including Cowden syndrome (CS) [166]. PHTS is passed down through autosomal dominant inheritance patterns and predisposes individuals to hamartomatous growths and malignancies in various organ systems [166]. Individuals with CS have an increased risk for female breast, endometrial, thyroid, colon, and renal cancers [166].

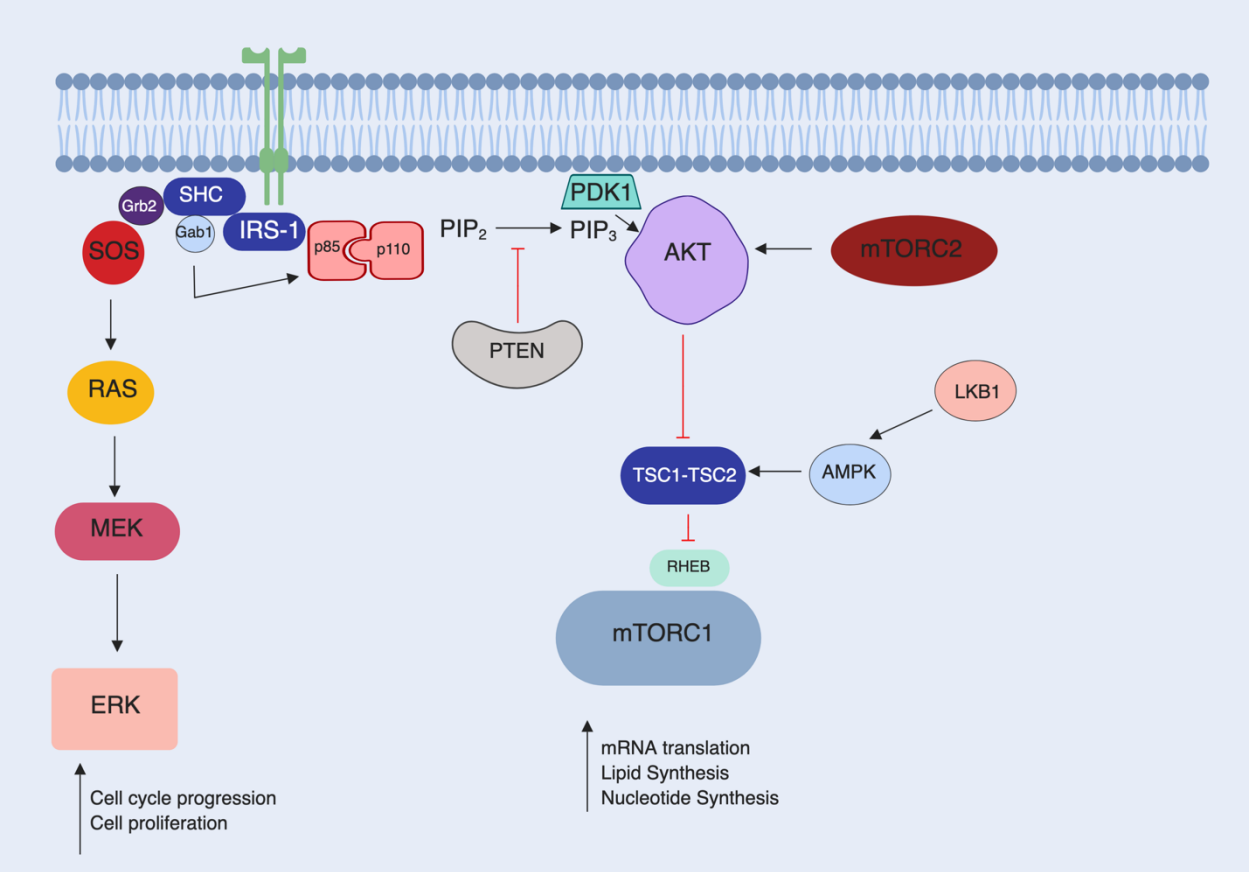

Figure 4. Receptor Tyrosine Kinase Signaling Through PI3K/AKT and RAS/ERK pathways Activation of RTKs by extracellular stimuli results in the auto-phosphorylation of tyrosine residues on RTKs. These tyrosine residues recruit adaptor proteins such as Shc and IRS-1 through their SH2 domain. Adaptor proteins recruit either other adaptor proteins such as Gab, Grb2 or the adaptor subunit of PI3K, p85. Recruitment of p85 allows p110 to phosphorylate PIP_2 to PIP_3 and leads to recruitment of AKT to the plasma membrane. At the plasma membrane, AKT is phosphorylated by mTORC2 and PDK1 which leads to its activation. Activated AKT represses TSC1/2. Repression of TSC1/2 by AKT allows for Rheb activation of mTORC1 and subsequent mRNA translation, lipid synthesis, and nucleotide synthesis, among other mTORC1 functions. RTKs can also activate the RAS/ERK pathway which leads to an increase in cell cycle progression and cell proliferation.

1.6.1 ShcA Adaptor Protein

The Src homology and Collagen (Shc) family of adaptor proteins is one of the most studied adaptor proteins which has been implicated in disease ranging from Alzheimer's to cancer[167]. Shc exerts its effects through activation of PI3K/AKT and MAPK/ERK signaling pathways. The adaptor protein has no intrinsic enzymatic activity, but instead serves as a docking site for protein-protein

interactions and propagates intercellular signaling downstream of RTKs such as ErB2/HER2 [167]. The Shc family of adaptor proteins consists of four members that are encoded by four separate genes: Shc/Shc1/ShcA, Sli/Shc2/ShcB, Rai/Shc3/ShcC and RaLP/Shc4/ShcD [168]. Among these Shc family members, ShcA has been the most widely studied given its ubiquitous expression in human tissue except for the adult human brain [167]. Notably, deletion of SHC1 is embryonically lethal in mice [169].

The ShcA protein is present in three isoforms: p46, p52, and p66ShcA. The three isoforms are produced through alternative promoter usage (p66) or alternative translation initiation start site (p46 and p52) [168]. p46ShcA and p52ShcA are involved in cell cycle progression and cell differentiation while p66ShcA plays a role in apoptosis and oxidative stress response [168] (Figure 5). ShcA protein isoforms share similar structure except for the extra 110 amino acids at the amino-terminus of p66 [168].

Isoforms of ShcA contain a phospho-tyrosine binding (PTB) domain, a carboxyterminal SH2 domain, and a collagen homology 1 (CH1) domain [168] and are involved in signal transduction pathways [168] (Figure 5). The CH1 domain contains three tyrosine phosphorylation sites: Tyr239/Tyr240 and Tyr317 (Tyr313 in mice) [168]. When phosphorylated at Tyr239 and Tyr317, p46/p52ShcA isoforms have been shown to specifically recruit Grb2/SOS complex to activate RAS/MAPK signaling [168]. Interestingly, phosphorylated p66ShcA can inhibit p46/p52ShcA signal transduction, particularly in periods of oxidative stress [170]. Further, phosphorylated ShcA on Tyr239/Tyr240 appears to induce transcriptional activity of c-myc [168]. In the context of

cancer, it has been shown that Tyr317 on ShcA is important for tumor cell survival while Tyr239/Tyr240 on ShcA are more important for tumor vascularization [171].

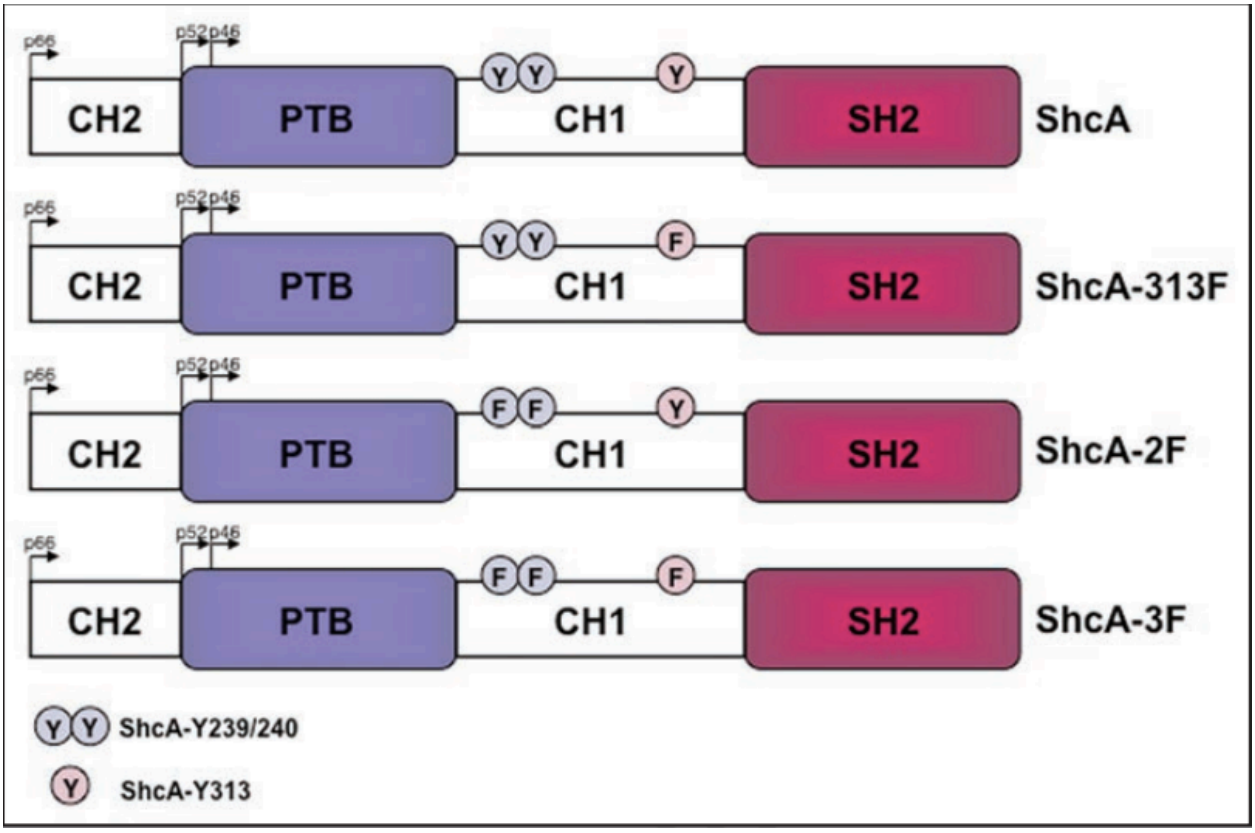

Figure 5. ShcA Structure and Mutations
The ShcA family of adaptor proteins has 3 family members: p66, p52, and p46. All family members contain a PTB, CH1, and SH2 domain while only p66 contains a CH2 domain on its amino-terminal end. Tyrosine in the CH1 domain are essential for downstream signaling of ShcA. Thus, tyrosine can be mutated to phenylalanine, non-phosphorylated mutants to study the role of each tyrosine in downstream signaling. Mutants generated are ShcA-313F containing a Y313F mutation of CH1 domain, ShcA 2F containing Y239F and Y240F mutation of CH1 domain, and ShcA3F containing Y239F, Y240F, and Y313F mutations of the CH1 domain. These are compared to wild-type ShcA cells. Adapted from Ursini-Siegel et. al (2008) [168].

ShcA plays an important role in breast cancer progression. Increased Y317 ShcA phosphorylation and reduced p66ShcA levels has been associated with early relapse in breast cancer patients [172, 173]. In mouse models, loss of ShcA expression in the mammary epithelium significantly decrease

tumor development [168]. Finally, ShcA stimulates breast tumor angiogenesis via the AKT/4E-BP axis, which mediated increase in vascular endothelial growth factor (VEGF) mRNA translation downstream of its phosphor-tyrosine residues [174]. Indeed, breast cancer cell lines expressing ShcA alleles that are debilitated in transducing phospho-tyrosine dependent signals (Shc3F) exhibited impaired tumor growth. However, depletion of 4E-BP1 is able to restore mammary tumor growth in a Shc3F context [174]. This was determined to be regulated, in part, via regulation of VEGF mRNA translation [174]. Thus, 4E-BPs play a role downstream of ShcA oncogenic signaling.

1.7 MMTV-PyV-MT Mouse Model of Breast Cancer

The MMTV-PyV-MT is an optimal model to study mammary tumorigenesis of the poor outcome breast cancers such as luminal B subtype. In this model, the PyV-MT oncogene is under the control of mouse mammary tumor virus long terminal repeat (MMTV LTR) promoter and thus preferentially expressed in the mammary epithelium [175]. Variable expression of promoter activity can be observed in the skin, salivary gland, ovary, lung, and B and T lymphocytes of female mice. The promoter is unresponsive to estrogen [176]. Mammary expression of the PyV-MT oncogene results in rapid induction of multi-focal, metastatic mammary tumors [177]. The PyV-MT mouse model is able to recapitulate four distinct steps of mammary tumorigenesis: hyperplasia, adenoma/mammary intraepithelial neoplasia (MIN), and early and late carcinoma [175] (Figure 6). Mammary hyperplasia can be detected in PyV-MT mice as early at 4 weeks and pulmonary lung metastasis can be observed by 12 weeks of age [178]. PyV-MT driven tumors are ER+ but undergo loss of ER receptors with persistent expression of HER2 throughout tumorigenesis.

PyV-MT is tethered to the plasma membrane and acts as an oncogene largely via its ability to act as an RTK-mimetic [179]. To this end, PyV-MT oncogene is an RTK-mimetic that is able to recruit signaling molecules such as c-Src to phosphorylate its tyrosine residues in particular, Tyr315, Tyr250, and Tyr322. [168]. These phosphorylated residues (Tyr315, Tyr250, and Tyr322) are then able to engage PI3K, ShcA, and phospholipase C-γ1 (PLC-γ1), respectively [180-183]. Phosphorylated tyrosine act as binding sites for the SH2 or PTB domains of these signaling molecules. In the case of PyV-MT, Tyr250 residues within a consensus NPxpY motif for the PTB domain of ShcA, which then recruits Grb2 [179]. Grb2 in turn engages guanine exchange factor SOS1 and adaptor molecule Gab1 [179]. Recruitment of Grb2/SOS complexes activates the RAS and MAPK/ERK kinase cascade [179]. Gab1 engages PI3K and leads to AKT/mTOR activation and activity [184]. Thus, the constitutive activation of signaling pathways often dysregulated in cancer makes the PyV-MT model a relevant and ideal model to study breast cancer.

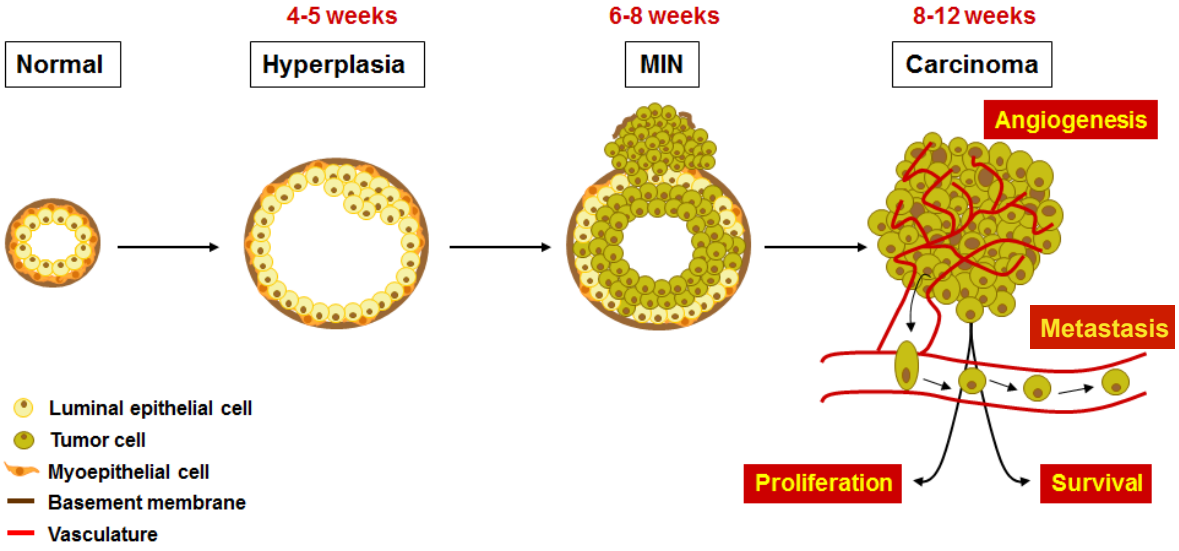

Figure 6. Transgenic PyV-MT Mouse Model Recapitulates Human Breast Cancer[168]
The MMTV-PyV-MT mouse model is a breast cancer model that represents the human luminal B molecular subtype of breast cancer. The PyV-MT oncogene is expressed preferentially in the mammary gland, where it drives cellular transformation. At 4-5 weeks of age, mice exhibit hyperplasia in luminal epithelial tissue followed by minimally invasive neoplasia by 6-8 weeks. By 6-8 weeks, tumors are physically palpable. After week 8, the mice will exhibit carcinoma. The PyV-MT mouse model is a metastatic mouse model that will display pulmonary metastases by or before 12 weeks of age.

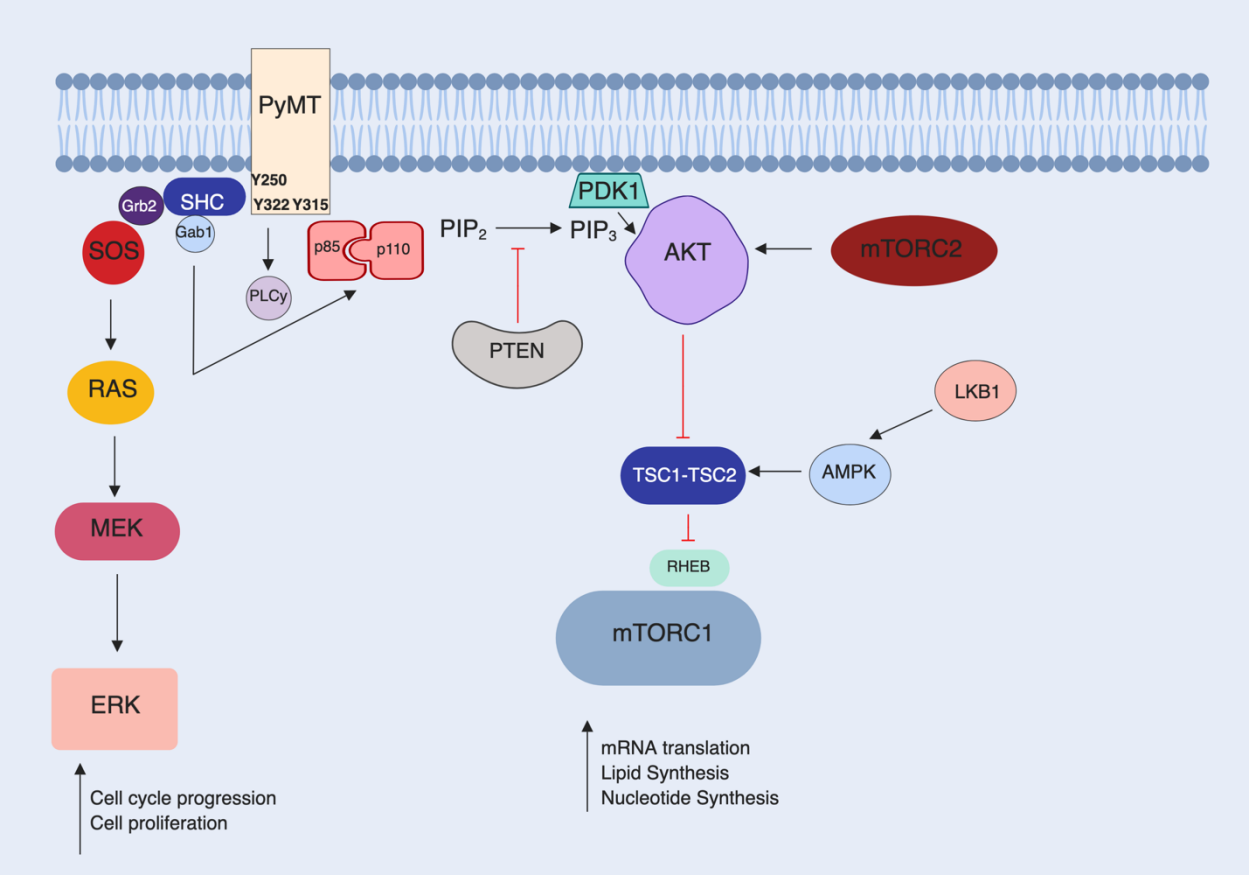

Figure 7. PI3K/AKT/mTOR Pathway Downstream of PyV-MT
The PyV-MT oncogene associates with the plasma membrane and acts as an RTK-mimetic, thereby mimicking constitutively active PI3K/AKT signaling. The PyV-MT oncogene has three tyrosine: Tyr250, Tyr322, and Tyr315 that interact with Shc, PLCy, and PI3K, respectively.

1.8 Metastasis

Metastasis is the leading cause of cancer-related deaths. Thus, understanding the metastatic process is imperative to reducing metastatic cancer-related deaths and unnecessary patient suffering. Metastasis is a multi-step process that requires successive changes in cell biology and gene expression to allow for local invasion, followed by intravasation into blood and lymphatic vessels, transit and survival of cancer cells in lymphatic and hematogenous systems, exit of cancer cells from such systems, and finally formation of secondary micro- and macro- metastatic tumors

in a new site[185]. The epithelial-mesenchymal transition (EMT) program is a program that has gained attention for its characteristic implication in metastasis and invasion. The EMT program is centered on the induction of transcriptional factors such as Snail, Slug, Twist, and Zeb1/2 that orchestrate the switch of cells from an epithelial to mesenchymal phenotype that will allow them to invade, resist cell death, and disseminate [186].

To metastasize, cancer cells must have the tumor intrinsic properties to do so in the proper microenvironment. The tumor microenvironment (TME) consists of the extracellular matrix (ECM), fibroblasts, adipose cells, immune-inflammatory cells, and the blood and lymphatic vascular networks [2]. The TME has been shown to play an important role in advanced malignancies and aggressive cancers [2]. An important part of the TME is oxygen supply.

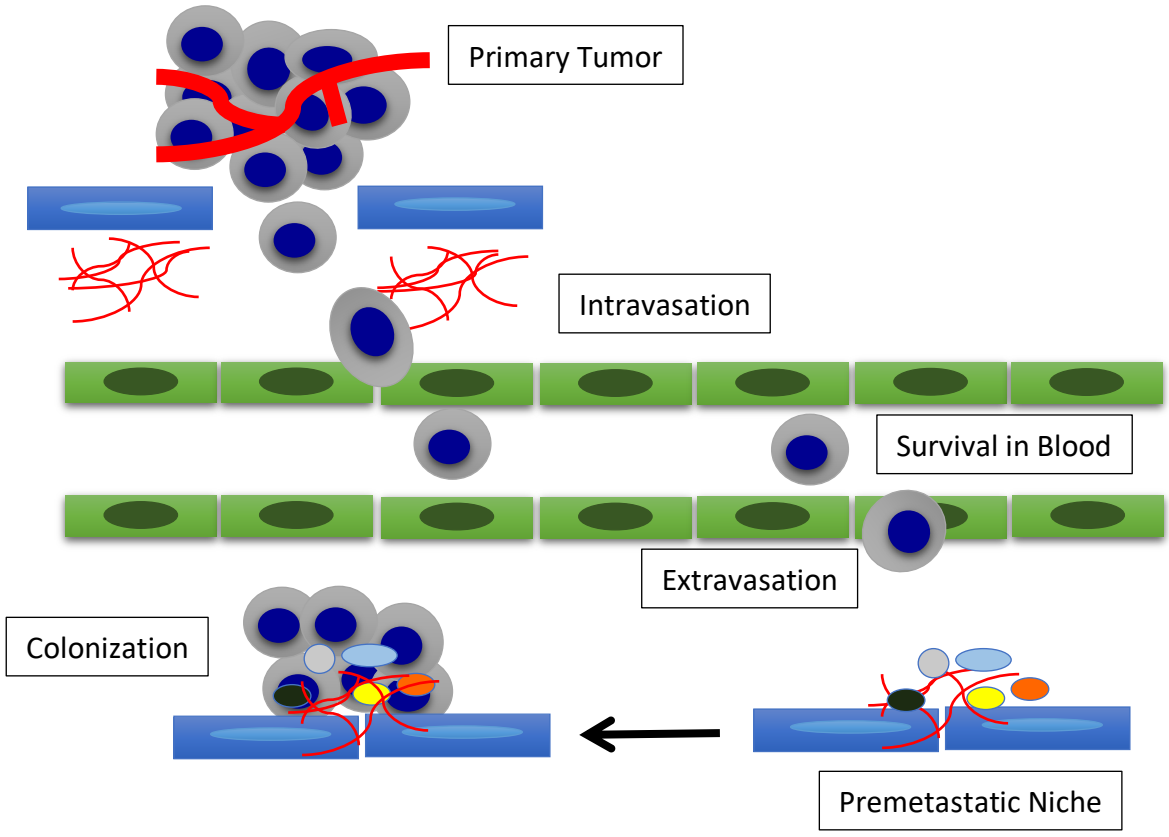

Figure 8. Metastatic Cascade
Each step of the metastatic cascade must occur for cancer to metastasize to a secondary site. These stages are: formation of a primary tumor, intravasation, survival in circulation, extravasation, existence of a premetastatic niche, and colonization. Once the primary tumor forms, the cells must be able to break through the basement membrane and intravasate into the bloodstream. Next, the cells must be able to survive in circulatory system. Then, cells that have arrived at a secondary location must be able to extravasate and colonize a secondary site. To be able to colonize, there also must be an apt environment, termed a premetastatic niche that will allow cells to grow in this secondary site.

1.9 Rationale/ Objectives

Previous research in the lab has shown that 4E-BPs play a major role in mediating the effects of ShcA, and more broadly PI3K signaling, in breast cancer [174]. Notably, loss of 4E-BP1 in cancers expressing inactive ShcA (ShcA-3F) was sufficient to rescue tumorigenesis. The ShcA-3F mutant has all three tyrosine (Tyr239, Tyr240, and Tyr313) mutated to phenylalanine, thereby abrogating downstream PI3K/AKT/mTOR and RAS/ERK signaling [171].

Following this discovery, we employed MMTV-PyMT model to establish the role of 4E-BPs in RTK-driven breast cancers. We initially hypothesized **that loss of 4EBPs may have tumor promoting effects in an aggressive MT mammary tumorigenesis model.**

Objective 1. To characterize mitogenic signaling response of ShcA mutant cell lines and determine phenotype of MMTV-PyMT/ ShcA-3F heterozygous /4E-BP1/4E-BP2 null mice

The primary aim of objective 1 was to establish the precise role for 4E-BPs in mediating the effects of ShcA signaling in breast cancer. This was achieved by employing breast cancer cells lines in which CH1 tyrosine residues (ShcA2F and Shc3A13F) in ShcA are mutated. ShcA mutated cell lines (ShcA2F and ShcA313F) were exposed to mitogens [i.e. epidermal growth factor (EGF)] and

pharmaceuticals that abrogate ShcA signaling towards the 4E-BPs (e.g. torin1). Moreover, we utilized primary cell lines from MMTV-PyMT/ ShcA3F heterozygous /4E-BP1/2 null mouse tumors. These cell culture-based assays were complemented by *in vivo* approaches whereby transgenic mice were developed by breeding MMTV-PyMT/ShcA3F heterozygous mice with ShcA3F heterozygous/4E-BP1/2 null mice to obtain MMTV-PyMT/Shc3Fhet/4E-BP1/2 null mice. ShcA3F heterozygous mice were used as ShcA3F homozygous mice die perinatally [171]. PyV-MT/4EBP1/2 null transgenic mice with mutated ShcA (Shc2F and Shc313F) were also generated in an effort to elucidate the mechanism linking ShcA activation of AKT and 4E-BP-dependent translation of VEGF.

Objective 2. To establish the role of 4E-BP1 and 2 in breast cancer progression using MMTV/PyV-MT/4E-BP1/2 null mice

Herein, we set out to establish the role that 4E-BP1 and 2 play at every step of mammary tumorigenesis from initiation to metastatic spread. To this end, MMTV-PyV-MT/4E-BP1/2 null transgenic mice were generated by crossing a MMTV-PyV-MT mouse with 4E-BP1/2 null mice to obtain MMTV-PyV-MT/4E-BP1/2 null mice that were monitored for tumor development and progression. These studies were complimented by cell culture studies in which cell lines derived from MMTV-PyMT wild-type and MMTV-PyV-MT/4E-BP1/2 null tumors were queried to dissect corresponding mechanisms.

Chapter Two: Methods

Cell Culture

Primary cell lines were cultured in 2.5% fetal bovine serum (FBS) (Wisent Bio) Dulbecco's modified Eagle's medium (DMEM) (Wisent Bio) containing 100 UI penicillin/100 ug/mL streptomycin (Wisent Bio), 50 ug/ml gentamycin (Wisent Bio), supplemented with mammary epithelial growth supplement (MEGS). MEGS is made up of 3 ng/mL epidermal growth factor (EGF), 0.5 μg/mL hydrocortisone, 5 μg/mL insulin, and 0.4% bovine pituitary extract (BPE). NMuMG-NT2197 CRISPR/Cas9 knock-out 4E-BP1/2 cells were cultured 10% FBS in DMEM supplemented with 10 μg/ml insulin 20 mM HEPES, pH 7.5, 100 UI penicillin/100 ug/mL streptomycin (Wisent Bio), and 50 ug/ml gentamycin (Wisent Bio). For experimental purposes, cells were cultured in 0.5% FBS in DMEM prior to treating with 50 ng/mL EGF. Inhibitors used in *in vitro* experiments include: LY294002 (Tocris), Torin1 (Tocris), cycloheximide (Sigma-Aldrich), and MG132 (Sigma-Aldrich). All cells lines were routinely tested for mycoplasma using Mycoprobe Mycoplasma Detection Kit (R&D Systems) at least once a month.

Generation of 4E-BP1/2 knock-out cells by CRISPR-Cas9

Described in (Hulea, 2018) [102]

Primary Cell Line Generation from Mouse

Mice were sacrificed and mammary tumors removed. Mammary tumors were kept in ice cold PBS. Subsequently, tissue was finely chopped using McIIwain tissue chopper (Campden Instruments) and scissors. Tissue ($1cm^3$) was incubated at 37^oC on a shaker for 2.5 hours in plain DMEM containing penicillin/streptomycin and gentamycin and 2.4 mg/ml Dispase (Roche; neutral protease, grade II) and 2.4 mg/ml Collagenase B (Roche). After incubation, tissue was centrifuged for 3 min at 800 rpm. After centrifugation, the supernatant was removed, and tissue was washed

2x with 1mM EDTA/PBS. Tissue/cells were resuspended in 1% FBS DMEM supplemented with MEGS at a density of 800,000 cells/mL. After 24 hours, the medium was changed to 2.5% FBS DMEM supplemented with MEGS. Cells were left in culture for a couple weeks to stabilize before splitting.

Retroviral Production and Infection

Transfection was performed using Opti-MEM (Life Technologies) media, lipofectamine 2000 (Invitrogen), Phoenix (293T) packaging cells. Phoenix cells were transfected with 20 μg of retroviral plasmid (pBabe empty vector and pBabe-4E-BP1). After 24h, virus-containing medium as filtered (0.45 μM), collected and used to infect recipient cells. Recipient cells were treated with 4 μg/uL polybrene prior to infection and subjected to two rounds of infection over 48 hours. Following infection, cells were selected using 1μg/mL puromycin.

Transgenic Mice

MMTV/PyV-MT mice have been described [177]. The 4E-BP1/4E-BP2 null mice were a generous donation from the Sonenberg Lab and previously described [86, 187]. All mice were on an FVB background. Experimental transgenic mice were monitored for tumor onset by physical palpation twice a week. Mice were necropsied at 8-weeks post tumor onset or if tumor burden exceeded 6 cm^3. At time of necropsy, tumors were measured using a caliper. Mammary glands/tumors and lungs were harvested from mice. Tumor and lung tissues were fixed in 10% buffered formalin for 16 hours before paraffin embedding. Tumor tissue from each mouse was also flash frozen in liquid nitrogen and stored at -80^{o}C. All animal studies were approved by the Animal Resources Council

at McGill University and comply with guidelines set by the Canadian Council of Animal Care. Results were analyzed on Prism7 by GraphPad.

PCR Genotyping

Tails were collected from transgenic mice to determine genotypes. About 1 mm of tail was collected from mice at 3 weeks of age and digested in 500 μL of tail digestion buffer (consisting of 10 mM Tris pH 8.0, 100 mM NaCl, 10 mM EDTA, pH 8, 5% SDS. DNA was isolated from tails using ethanol. PCR was performed using following primers:

MT FWD: 5'GGA AGC AAG TAC TTC ACA AGG G 3'

MT REV: 5' GGA AAG TCA CTA GGA GCA GGG 3'

4E-BP1 FWD: 5' GAT GGA GTG TCG GAA CTC ACC 3'

4E-BP1 REV: 5' GAC CTG GAC AGG ACT CAC CGC 3'

Neo-FWD: 5' GCA TCG AGC GAG CAC GTA CTC 3'

4E-BP2 FWD: 5' GGT GGG ACT GTG GGT CTT CTG 3'

4E-BP2 REV: 5' CAG CAC CTG GTC ATA GCC GTG 3'

Neo-FWD: 5' GCA TCG AGC GAG CAC GTA CTC 3'

ShcA Wild-Type FWD: 5' CTG CAA AGG GCT TGC AAG TGT G 3'

ShcA Wild-type REV: 5' AAC ACC ATC AAATGC CCA ACT TCC 3'

ShcA Knock-In (KI) FWD: 5' GGT CGC TAC CAT TAC CAG TTG GTC TGG 3'

ShcA KI REV: 5' TAC CCG GTA GAA TTA ATT CCT CGA CCG 3'

PCR products were run a 1% agarose gel containing ethidium bromide in TAE (Tris-Base, acetic acid, EDTA) buffer.

Cell Viability Assays

PyV-MT (MT), PyV-MT/ShcA2F (2F), and PyVMT/ShcA313F (313F) cells were seeded 50,000 cells per well in a 24-well plate. Cells were either treated with torin1 (100 nM) or DMSO for 24h. After 24h, cells were detached from wells using trypsin and viable cells were counted using the method of trypan blue exclusion. Cells were counted using a hemocytometer (Hausser Scientific).

Immunoblotting

Cells were lysed in whole lysis buffer (PLCγ lysis buffer) comprised of 20 mM Tris pH 7.5, 420 mM NaCl, 2 mM $MgCl_2$, 1 mM EDTA, 10% glycerol, 0.5% NP40, 0.5% Triton) supplemented with 5 mM NaF, PIN (1 μg/mL Chymostatin, 2 μg/mL Antipain, 2 μg/mL Leupeptin, 1 μg/mL Pepstatin, 2 μg/mL Aprotinin) and 5 mM $NaVO_4$. Flash-frozen tumor pieces were crushed using a mortar and pestle in liquid nitrogen. Crushed tumor pieces were subsequently lysed in whole lysis buffer (PLCγ).

Lysates were centrifuged at 16,000 g for 10 minutes at 4^{o}C. Supernatant was collected and protein concentration measured by Bradford assay using Bradford reagent (Bio-Rad). Protein was loaded into 10% or 15% acrylamide gels and transferred onto PDVF membranes 65V for 2h. Subsequently, membranes were blocked in 3% bovine serum albumin (BSA) dissolved in TBST (100 mM Tris pH 8, 1.5 M NaCl, 0.05% Tween 20). Membranes were incubated overnight in primary antibodies in 3% BSA/TBST and then probed using secondary IgG antibodies (Jackson ImmunoResearch dilution 1:10,000) conjugated to horseradish peroxidase. ECL (GE healthcare) was used for protein detection. Membranes were exposed using the Azure c300 Chemiluminescent Western Blotting Imaging System. Primary antibodies used: eIF4E (1:1000 dilution, Cell

Signaling #9742S), p-eIF4E S209 (1:1000 dilution, Cell Signaling #9741L), eIF4G1 (1:1000 dilution, Cell Signaling #2858S), Cyclin D1 (1:1000 dilution, Cell Signaling #2978S), pAKT S473 (1:1000 dilution, Cell Signaling #9271S), pAKT T308 (1:1000 dilution, Cell Signaling #2965S), AKT1 (1:1000 dilution, Cell Signaling #2938S), p4E-BP1 S65 (1:1000 dilution, Cell Signaling #9456S), p-4E-BP1 T37/46 (1:1000 dilution, Cell Signaling #2855S), p-S6 ribosomal protein S240/244 (1:1000 dilution, Cell Signaling #2215S), S6 ribosomal protein (1:1000 dilution, Cell Signaling #2217), p-p70S6 Kinase (T389) (1:1000 dilution, Cell Signaling #9205S), p70S6 Kinase (1:1000 dilution, Cell Signaling #2708), 4E-BP1 (1:1000 dilution, Cell Signaling #9644S), 4E-BP2 (1:1000 dilution, Cell Signaling # 2845S), tubulin (1:15,000, Sigma Aldrich, #T5168).

RNA Extraction/ RT-qPCR

Total RNA was extracted from tumor tissue using RNeasy Midi Kit (Qiagen) following protocol indicated in kit. Following RNA extraction, RT-qPCR was performed using BrightGreen 2X qPCR MasterMix-Low ROX (abcam). The following primers were used: eIF4E, Actin, GAPDH

eIF4E FWD: 5’ CTG TGC CTT ATT GGA GAA T 3’

eIF4E REV: 5’ GGA GGA AGT CCT AAC CTT T 3’

B-ACTIN FWD: 5’ TTC CTT CTT GGG TAT GGA A 3’

B-ACTIN REV: 5’ CCA CGA TCC ACA CAG ACT A 3’

GAPDH FWD: 5’ TGT GTC CGT CGT GGA TCT GAC 3’

GAPDH REV: CAC CCT GTT GCT CTA GCC GTA 3’

Immunohistochemistry

Tissues analyzed by immunohistochemistry were paraffin-embedded and sectioned (4 μM) using a microtome and blade. Prior to IHC, tissue samples were deparaffinized on the slides using xylene

and ethanol washes. Antigen retrieval was performed in a pressure cooker for approximately 25 minutes in 1X Citrate Antigen Retrieval Solution. Primary antibody eIF4E (Cell Signaling #9742, 1:100 dilution) was used on slides. Slides were then probed with biotinylated secondary antibody (Vector). Avidin/Biotin (Vectastatin) complex was used to amplify signal from biotinylated secondary antibody. Slides were developed using DAB substrate (Vector) and counterstained with 20% hematoxylin.

Slides were scanned using a ScanScope XT Digital Slide Scanner (Aperio) and data analyzed using Image Scope software. Images were analyzed by categorizing strong, weak, and negative signals in the samples.

Figures

Unless figures have been adapted from previous publications and referenced in the caption, the figures presented in this thesis have been created using Microsoft Powerpoint and Biorender (biorender.com)

Chapter Three: Results

3.1 PyV-MT cells exhibit low responsiveness to mitogenic stimulation

To understand the wiring of signaling pathways in the PyV-MT model, we used three mutant cell lines to characterize their basal mitogenic signaling. Epidermal growth factor (EGF), 50 ng/ml [188], was used to stimulate EGFR signaling in two ShcA mutated PyV-MT cell lines: ShcA with CH1 domain Tyr239 mutated to Phe and Tyr240 mutated to Phe (2F) and ShcA with CH1 domain Tyr313 mutated to Phe (313F). Importantly, these are knock in cell lines in which both endogenous *ShcA* alleles express the various point mutants [171]. Phosphorylated tyrosine (Tyr239/240/313) in the ShcA CH1 domain bind Grb2/SOS and Grb2/Gab1 complexes to activate the RAS/ERK and PI3K/AKT pathways, respectively. The Tyr313 residue of ShcA is necessary for ShcA RAS/ERK signaling while Tyr239 and Tyr240 seem to be dispensable for engaging this signaling pathway [189]. Thus, it is predicted that 313F cells will exhibit a greater induction of RAS/ERK signaling upon starvation and stimulation than 2F cells, respectively. These cells lines were compared to a PyV-MT ShcA wild type cell line (MT).

Prior to EGF stimulation, cells were starved in 0.5% FBS media with no additional mammary epithelial growth supplement (MEGS) added for 24 hours. Phosphorylated AKT, indicating PI3K (Thr308) and mTORC2 (S473) activity, as well as phosphorylated 4E-BP indicative of mTORC1 activity was largely unchanged in MT cell lines subjected to starvation and EGF stimulation (Figure 9). This indicates that MT cells are minimally responsive to both starvation and EGF stimulation irrespective of their ShcA status, which can be explained by constitutive activation of the PI3K/AKT/mTOR axis independently of extracellular signal via the RTK-mimicry of PyV-MT oncogene.

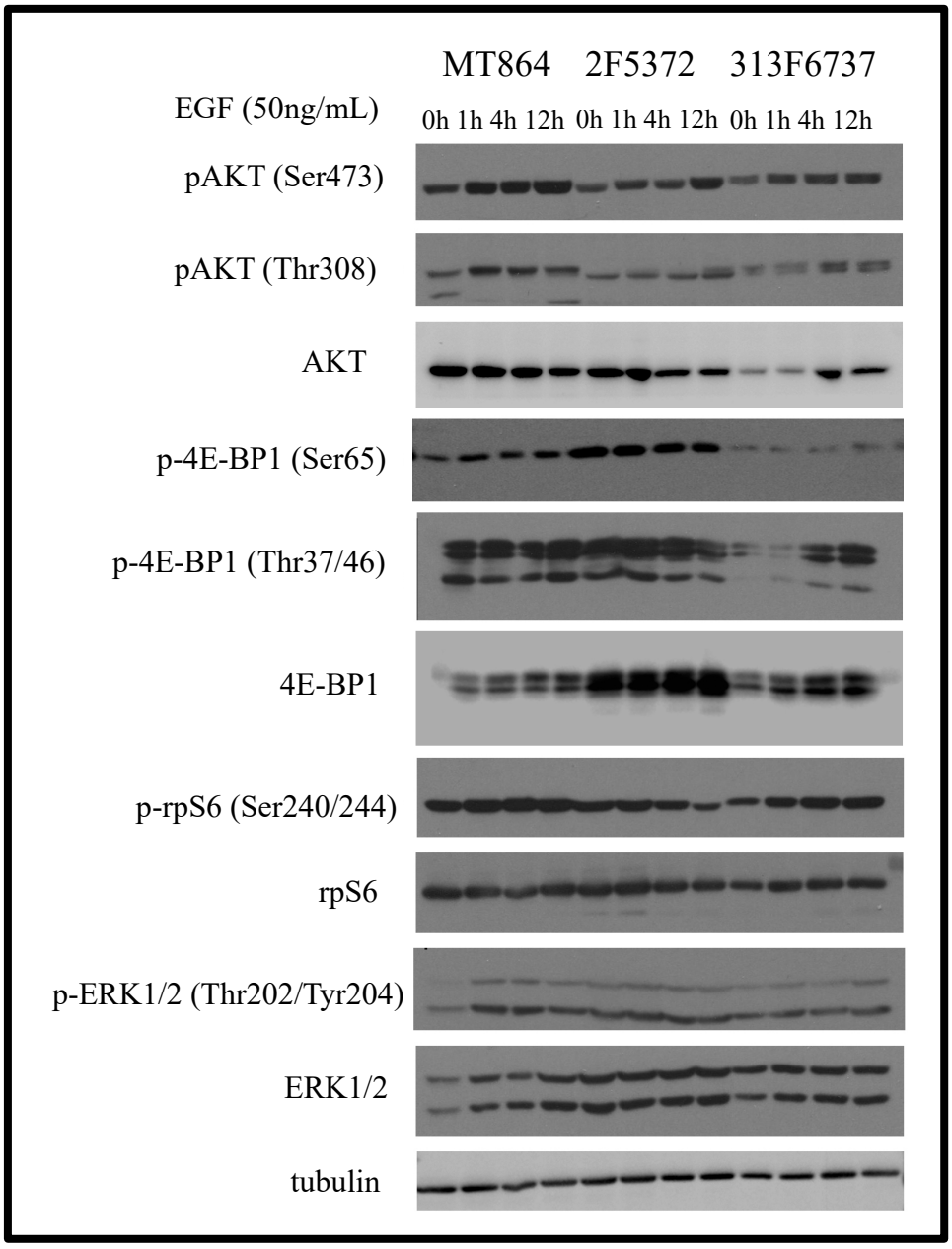

Figure 9. PyV-MT cells unresponsive to mitogenic stimulation
MT, 2F, and 313F cells were starved in 0.5% FBS (no MEGS) for 24h and then stimulated with 50 ng/ml EGF for 1-hour, 4-hour, and 12-hour in 2.5% FBS DMEM. The numbers besides each cell line correspond to the mouse number from which the cells were isolated. Lysates were analyzed by western blotting on SDS-PAGE gels. (n=3)

3.2 PyV-MT/ShcA2F cell line most responsive to mTOR inhibition

To establish the role of mTOR signaling in mediating the oncogenic PyV-MT/ShcA signaling we next investigated the effects of mTOR inhibitors on proliferation of PyV-MT cells expressing wild-type ShcA or ShcA mutants. 50,000 MT, 2F, and 313F cells were treated with 100 nM and 250 nM of torin1 for 24h and the number of remaining viable cells was determined by trypan blue exclusion method. Consistently with previous publications [188], 2F cells exhibited the highest mTOR activity as illustrated by higher 4E-BP1 phosphorylation relative to other cell lines (Figure 10) Accordingly, cells expressing 2F were the most susceptible to antiproliferative effects of torin1, which abolished mTOR signaling in all 3 cell lines (Figure 10).

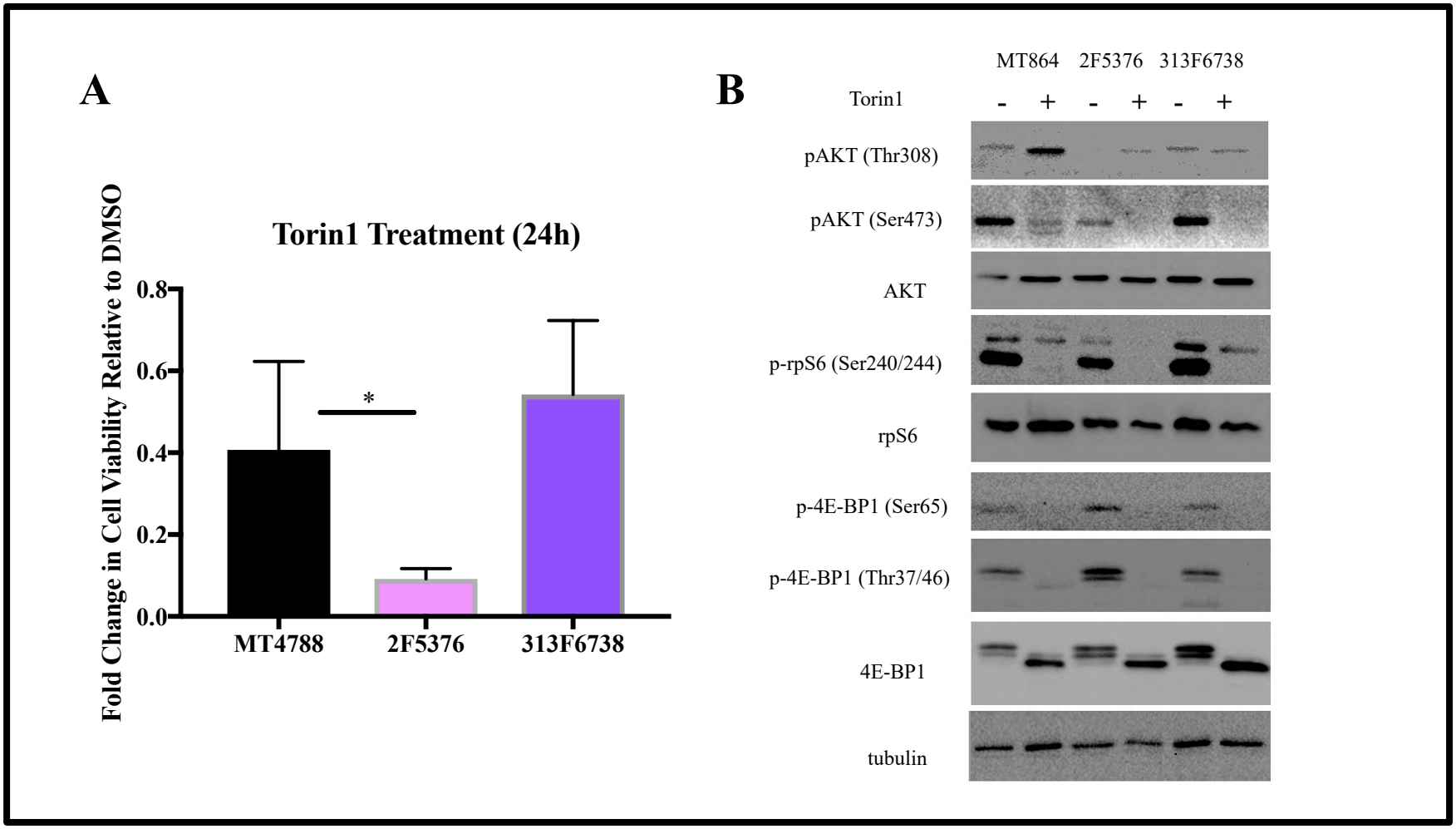

Figure 10. ShcA2F Mutant Sensitive to Torin1 Treatment of PyV-MT cell lines
(A) Cells were treated for 24 hours with torin1 at 100 nM. Viable cells were quantified by trypan blue exclusion. Data is shown as fold change from DMSO-treated controls at 24 hours. *, $p<0.05$ (unpaired t-test) This data is representative of an n=2, 4 wells per condition (B) MT, 2F, and 313F cells were treated for 4 hours with 250 nM Torin1 and lysed with PLCγ lysis buffer and analyzed by western blotting. (n=2)

3.3 4E-BPs mediate the effects of ShcA on breast cancer tumor onset in PyV-MT model

Despite the fact that 4E-BP1/2 null mice have been characterized in context of insulin resistance, prostate cancer, and mutated p53 [93-95], to our knowledge, the 4EBP1/2 knock out mice have not been characterized in the context of dysregulated RTK signaling. Thus, transgenic mice were generated to investigate the effect of 4E-BP1/2 loss in mammary tumorigenesis in wild-type PyV-MT and PyV-MT/Shc3F heterozygous mice, which are defective in ShcA signaling and exhibit delayed tumor onset [171]. Mice were physically palpated for tumor onset starting at 5 weeks of age and sacrificed at 8 weeks post-tumor onset or when total tumor volume reached 6 cm^3. A tumor curve was generated to evaluate tumor onset and tumor burden. PyV-MT/Shc3F heterozygous mice exhibit delayed tumor onset [171] due to impaired signaling through ShcA. Deletion of the *EIF4EBP1* and *EIF4EBP2* genes led to acceleration of tumor onset compared to controls (Figure 11). Thus, 4E-BP1 and/or 2 may play a role in ShcA-driven oncogenic signaling in the stage of tumor initiation. In contrast, deletion of the *EIF4EBP1* and *EIF4EBP2* genes had no effect on tumor burden compared to controls. This suggests that 4E-BPs may be less important in an already established tumor program.

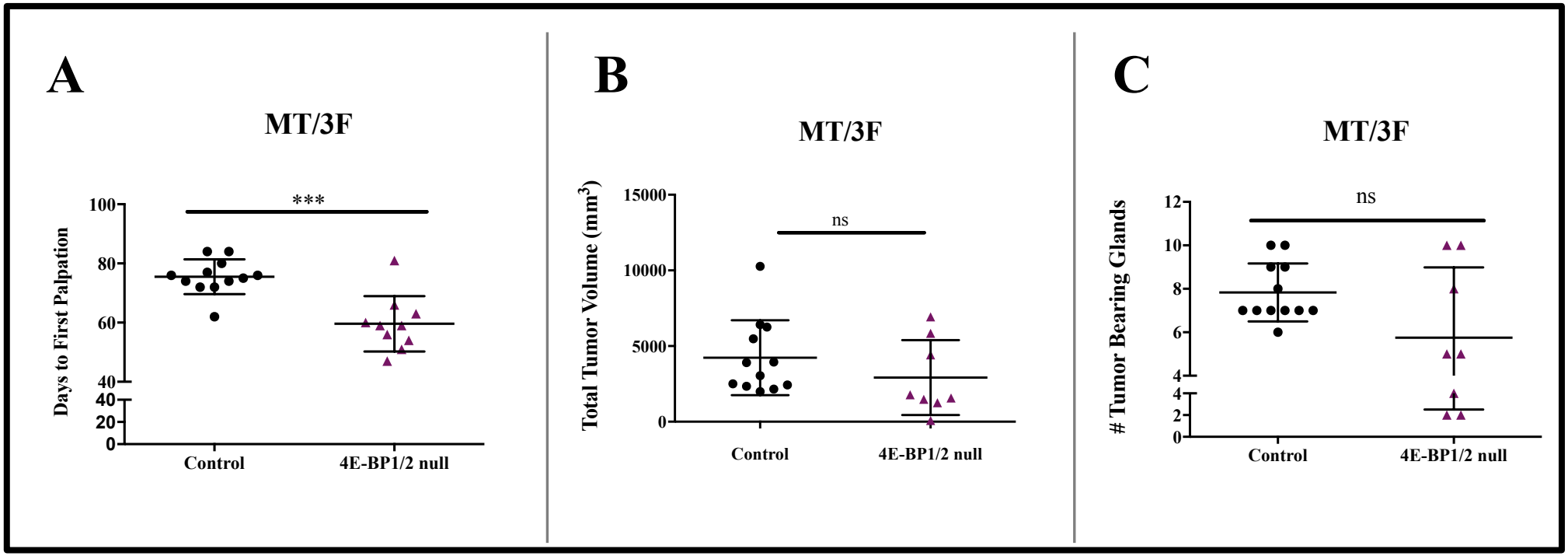

Figure 11. Loss of 4E-BP1/2 rescues PyV-MT/Shc3F heterozygous phenotype A) PyV-MT (MT (n=12), PyV-MT/Shc3F heterozygous (MT/3F) (n=10) and MT/Shc3F heterozygous/4E-BP1/2 null (MT/3F/4E-BP1/2 null) (n=8) mice were palpated for onset of tumor. B) Mice were euthanized at humane end-point (12-16 weeks old), primary mammary tumor volumes were measured by caliper and C) tumor burden was noted, $p < 0.0001$ *** (two-tailed t-test)

3.4 The Loss of 4E-BP1 and 2 Accelerates Primary Tumor Growth but Dramatically Decreases Lung Metastasis in PyV-MT/4E-BP1/2 null mice

To investigate the role of 4E-BPs in mediating the effects of oncogenic RTK signaling in the context of wild-type ShcA, we further characterized a PyV-MT/4E-BP1/2 null female mouse cohort. These mice were monitored for tumor onset starting at 5 weeks by physical palpation. Mice were necropsied at 8 weeks post-tumor onset. Contrary to the PyV-MT/Shc3F heterozygous /4E-BP1/2 null mice, the PyV-MT/4E-BP1/2 null animals did not exhibit accelerated tumor onset compared to control PyV-MT wild-type mice (Figure 12). Moreover, 4E-BP1/2 status of the tumor did not appear to have a major impact on the number of tumor-bearing glands (Figure 12). In contrast, tumor volumes in MT/4E-BP1/2 null mice were significantly higher than in control mice (Figure 12). The latter result is in line with the role of the 4E-BPs as translational repressors, since it is well established that high levels of protein synthesis are required to support tumor growth [190].

The number of pulmonary metastases were counted, and total area of metastases measured using ImageScope (Figure 13). Upon necropsy of PyV-MT/4E-BP1/2 null mice at 14-16 weeks of age (8 weeks post-tumor onset), the lungs of PyV-MT/4E-BP1/2 null mice appeared to be absent of pulmonary metastases (Figure 13). This finding was in contrast to wild-type PyV-MT mice that showed significant metastases to the lung at 14 weeks of age (Figure 13). These macroscopic observations were confirmed by H&E staining of step-sectioned lung tissue of PyV-MT/4E-BP1/2 null and wild-type mice (Figure 13). Collectively, these findings revealed that notwithstanding that 4E-BPs exert tumor-suppressive properties, their loss in the PyV-MT model impedes metastatic dissemination of breast cancer cells.

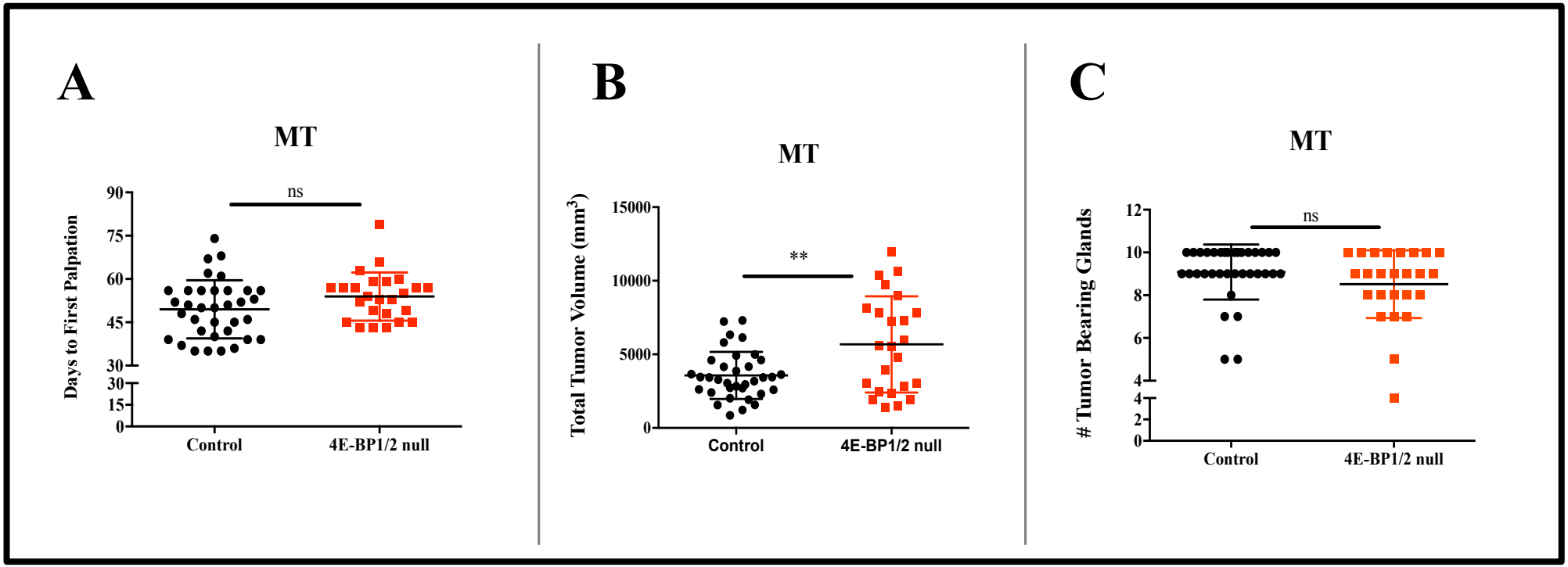

Figure 12. Loss of 4E-BP1/2 does not change tumor onset, tumor burden, nor tumor bearing glands A) PyV-MT (n=35) and PyV-MT/4E-BP1/2 null (n=25) mice were palpated for onset of tumor. B) Mice were euthanized at humane end-point (12-16 weeks old), primary mammary tumor volumes were measured by caliper and C) tumor burden was noted, $p < 0.002$ **

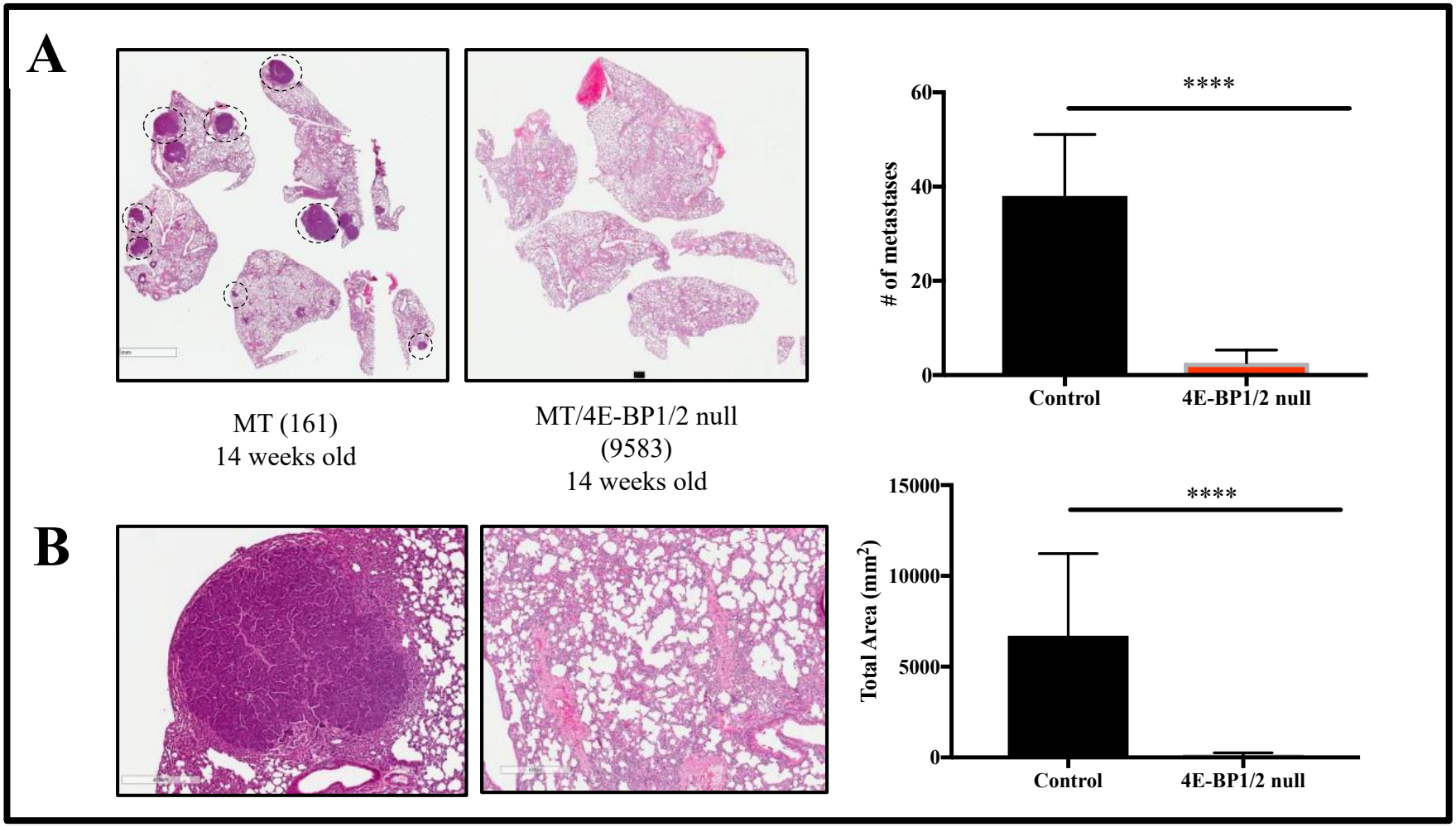

Figure 13. Loss of 4E-BP1/2 impairs metastasis

A) Metastases from each mouse was counted from hematoxylin and eosin (H&E) stained lung step sections, number of metastasis indicated in top right corner. B) Scaled representative sections of PyV-MT and PyV-MT/4E-BP1/2 null C) Counted number of metastases in lungs at 12-16 weeks of age D) Quantification of total metastases area in the lung. (n=9 for each group) Analyses done using Image Scope.

3.5 Decreased Metastasis Phenotype in PyV-MT/4E-BP1/2 null Mice Is Correlated with Decreased eIF4E Levels in Primary Tumor

The surprising finding that the loss of 4E-BP1 and 2 abrogates lung metastases in the PyV-MT model has led us to diverge from our original objective 1 and turn our focus to investigating the molecular underpinnings of this unexpected phenomenon. Considering previous reports which indicate that the changes in eIF4E or 4E-BP levels may induce mechanisms which adjust the eIF4E/4E-BP ratio [101], we first investigated the effects of 4E-BP loss on eIF4E levels. To this end, we generated tumor lysates (see methods) and analyzed them by western blotting. Strikingly, these experiments revealed a significant decrease in total eIF4E protein levels in PyV-MT/ 4EBP1/2 null breast tumors as compared to their 4E-BP proficient counterparts (Figure 14). This was confirmed by IHC on age-matched breast tumors from PyV-MT wild-type and PyV-MT/4EBP1/2 null mice (Figure 14).

eIF4E levels were decreased in 14 primary tumors without major reduction in other eIF4F subunits (Figure 15, n=6 for each transgenic mouse shown). Thus, this suggests that the loss of 4E-BP1/2 expression in the PyV-MT mouse model has a major impact on eIF4E levels, while only marginally affecting eIF4G1 and eIF4A levels.

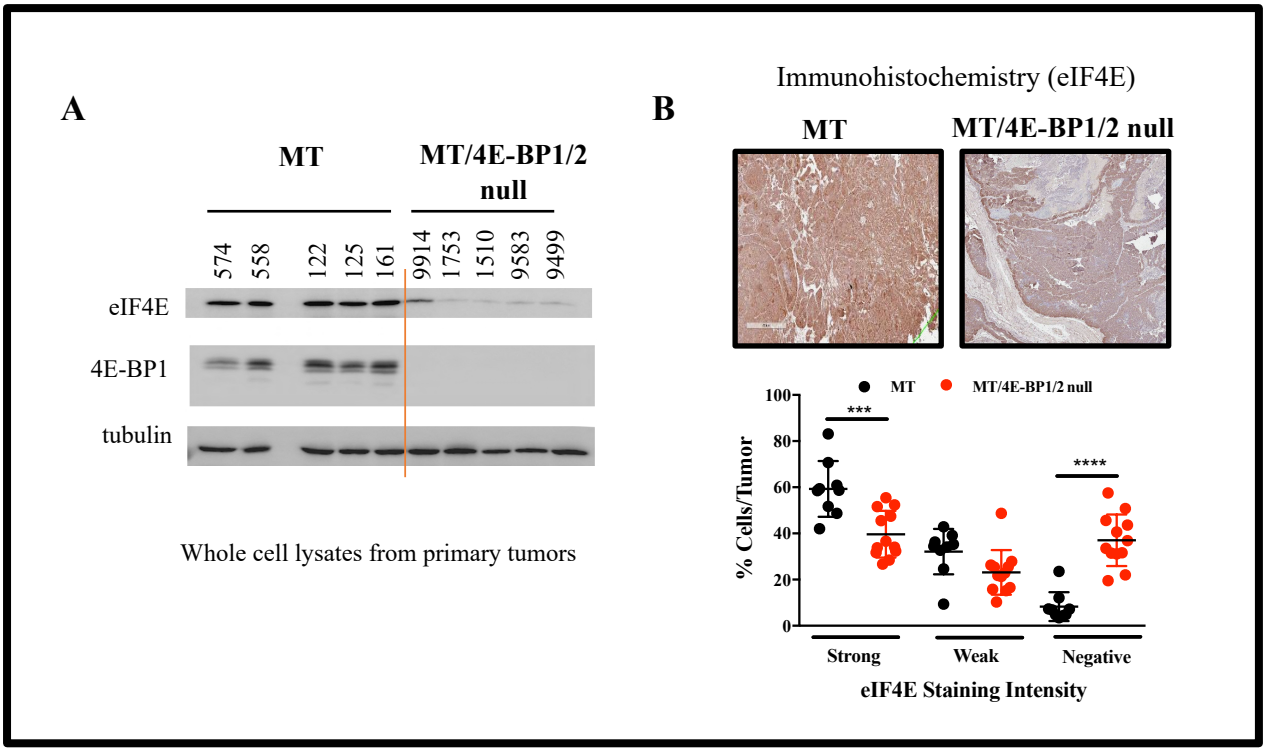

Figure 14. Loss of 4E-BPs *in vivo* leads to reduced total eIF4E protein levels in tumors
(A)Tumor from PyV-MT (n=5) and PyV-MT/4E-BP1/2 null mice (n=5) were lysed in PLCγ lysis buffer, run on an SDS-PAGE gel and probed for eIF4E, 4E-BP1, and tubulin using immunoblotting techniques. Each horizontal number above blot corresponds to mouse number (B) Paraffin-embedded tumor samples were analyzed by IHC to examine levels of eIF4E staining. Quantification of positive eIF4E staining is shown below (n=9 (PyV-MT), n=12 (PyV-MT/4E-BP1/2 null). ***, *p=0.0007*,****, *p<0.0001* (two-tailed t-test) (n=5)

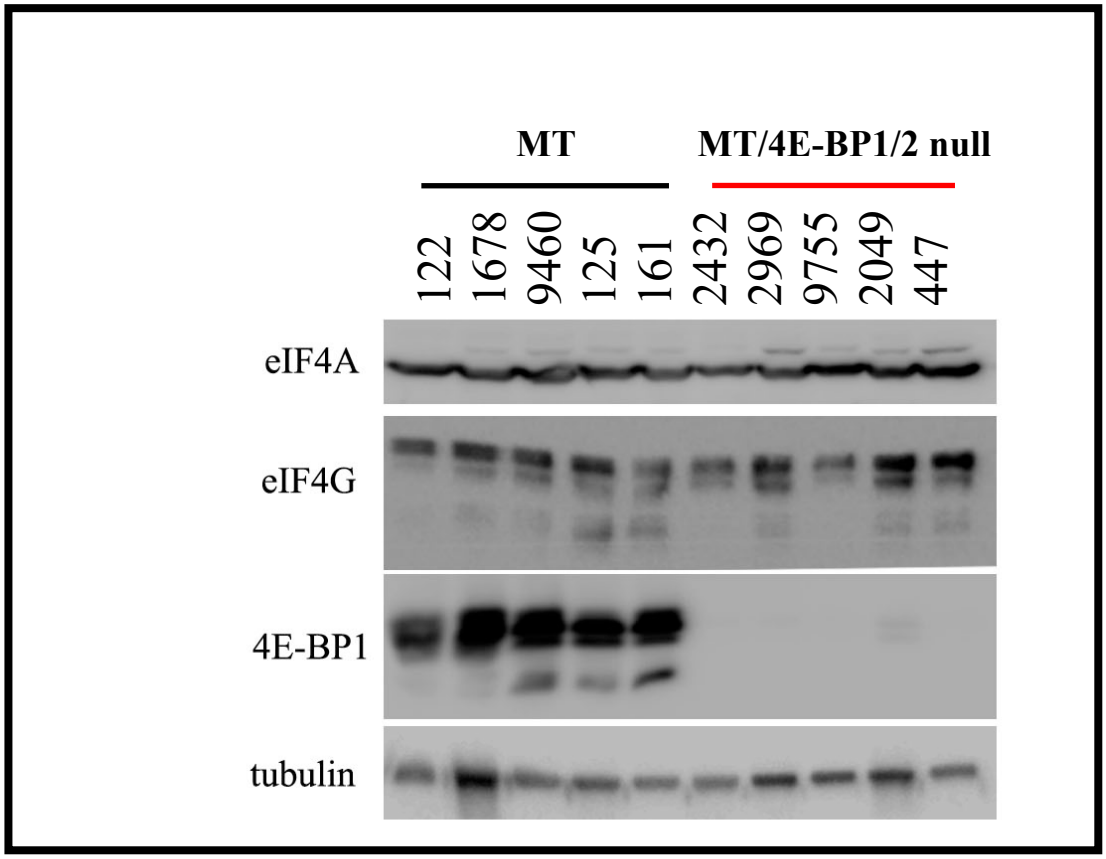

Figure 15. Protein Levels of Translation Initiation Machinery are Unchanged in PyV-MT 4E-BP1/2 null Tumors

Primary tumor from PyV-MT (n=5) and PyV-MT/4E-BP1/2 (n=5) null mice aged 14-16 weeks were lysed with PLCγ lysis buffer and analyzed by western blotting to evaluate relative levels of translation initiation machinery.

3.6 4E-BP1 status, not PI3K signaling, modulates eIF4E levels

eIF4E is thought to exert pro-metastatic properties [62, 75]. We postulated that eIF4E downregulation dramatically reduces the metastatic potential of 4E-BP1/2 null cells. Primary cell lines (155, 447, 5239, 451, and 160) were made from PyV-MT wild-type and PyV-MT/4E-BP1/2 null mammary tumors isolated at the time of necropsy. PyV-MT/4E-BP1/2 null cells exhibited decreased eIF4E levels in cell culture as compared to 4E-BP1/2 proficient cells (Figure 16). In contrast, the 4E-BP1/2 status did not seem to affect mTOR and ERK signaling (Figure 16). Since PyV-MT acts as an RTK mimetic which hyperactivates PI3K, we next investigated the effects of inhibiting PI3K on eIF4E levels. The eIF4E protein levels in PyV-MT/4E-BP1/2 null cells were, however, not affected by PI3K inhibition using LY290042 (Figure 16).

To confirm that the reduction in eIF4E levels is caused by 4E-BP loss and not caused by inadvertent events, 4E-BP1 was reintroduced in primary MT/4E-BP1/2 null cell line (155) using a retroviral infection. Re-expression of 4E-BP1 resulted in increased eIF4E protein levels as compared to the vector control (Figure 17). Collectively, these results show the co-dependence between eIF4E and 4E-BP levels which is consistent with previous publications [100, 101].

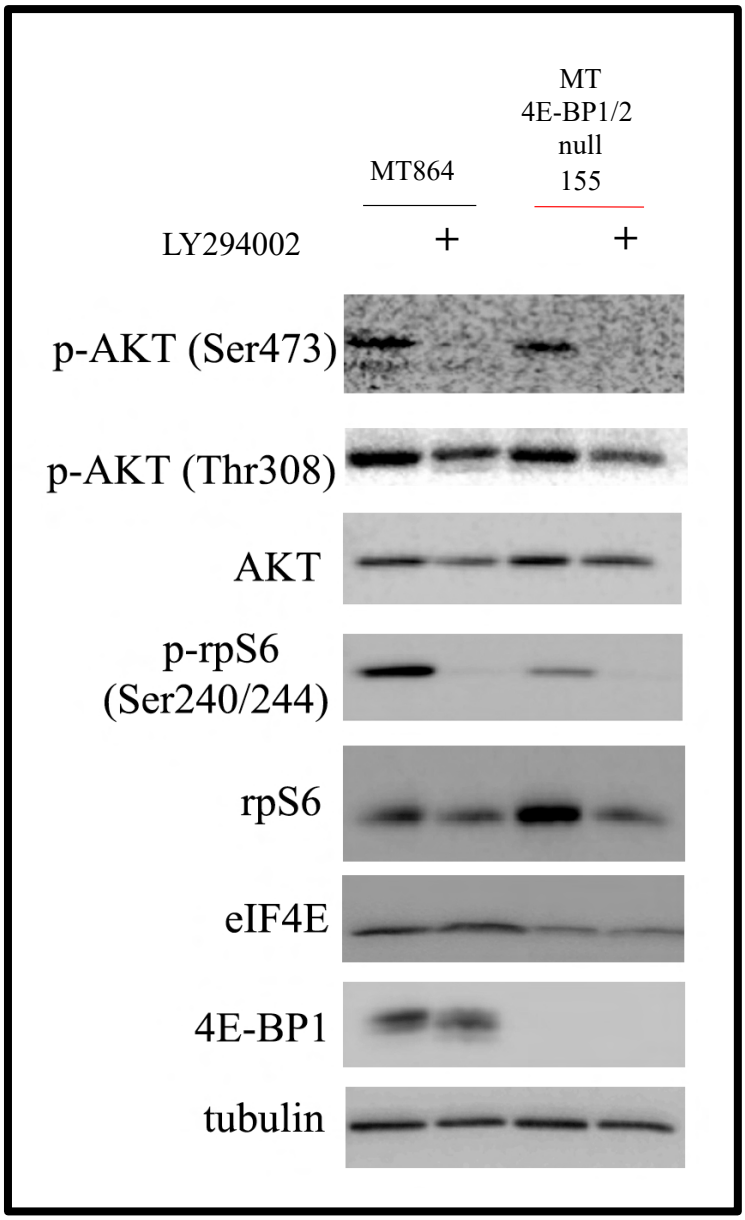

Figure 16. 4E-BP status in the cell does not affect PI3K/AKT/mTOR signaling
Primary cell lines (155, 447, 451) were established from PyV-MT 4E-BP1/2 null mouse tumors at necropsy. These cell lines were compared to established MT cell line, 864. MT 864 and MT/4E-BP1/2 null cells, cultured in 2.5% FBS, MEGS supplemented DMEM media, were treated with LY294002 at a concentration of 20 uM for 20 hours. Lysates were analyzed by western blotting. (n=3)

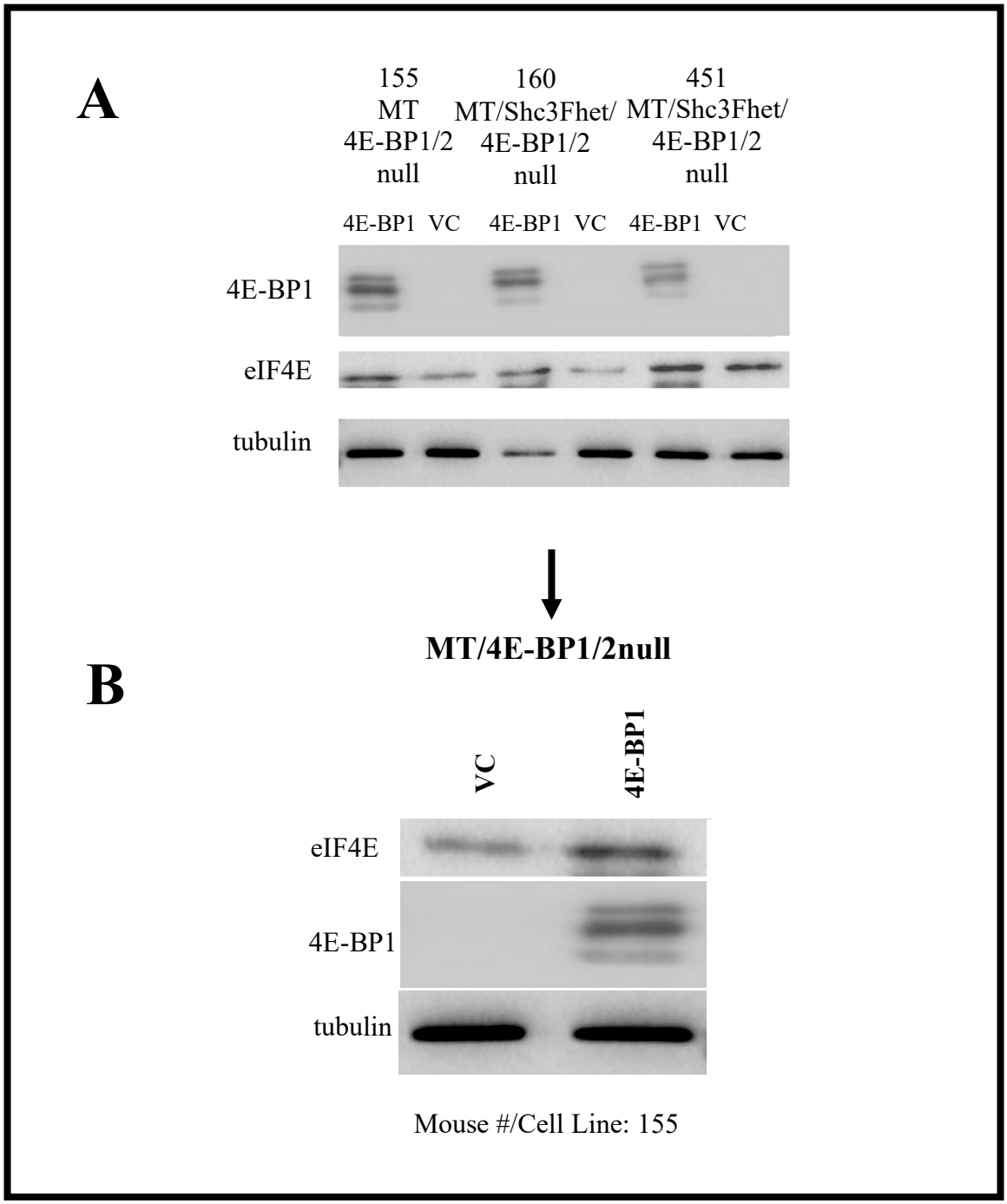

Figure 17. 4E-BP1 Re-expression Increases eIF4E Levels
(A) 4E-BP1 was expressed in primary PyV-MT/4E-BP1/2 null cell lines. Cells were maintained in 2.5% FBS, MEGS supplemented DMEM media and lysed at 80% confluency. Lysates were analyzed using western blotting. The re-expression of 4E-BP1 in each cell line is shown besides its respective vector control (VC) (B) Zoom of cell line 155 from panel (A) (n=3)

3.7 Dissecting the mechanisms of 4E-BP-loss induced eIF4E downregulation.

We next sought to identify the mechanism which underpin reduction in eIF4E levels in 4E-BP1/2 null PyV-MT breast cancer cells. It has been reported that eIF4E is regulated transcriptionally by c-myc [51] and that its mRNA stability is regulated by HuR and AUF1 proteins [53]. Both of these mechanisms are reflected in steady-state mRNA levels, and thus we compared eIF4E mRNA levels between PyV-MT wild-type and PyV-MT/4E-BP1/2-null tumors using RT-qPCR. These experiments revealed that eIF4E mRNA levels are not affected by 4E-BP status in the cells (Figure 18).

Next, to investigate whether the downregulation of eIF4E in 4E-BP deficient cells is mediated by protein degradation, we employed cycloheximide chase experiments in PyV-MT wild-type or PyV-MT/4E-BP1/2 null primary breast cancer cell lines. At basal conditions, previous studies have reported that the half-life of eIF4E is > 14 hours [191]. Strikingly, in the PyV-MT/4E-BP1/2 null context, the eIF4E protein levels significantly decreased by 18 hours of cycloheximide (CHX) treatment, but not in 4E-BP wild-type context (Figure 19). Co-treatment with cycloheximide and the proteasome inhibitor MG132 rescued eIF4E in MT 4E-BP1/2 null cells to the levels observed in a control (Figure 20). This suggest that the ubiquitin-proteasome systems, at least, in part mediates the effects of 4E-BP loss on eIF4E protein levels.

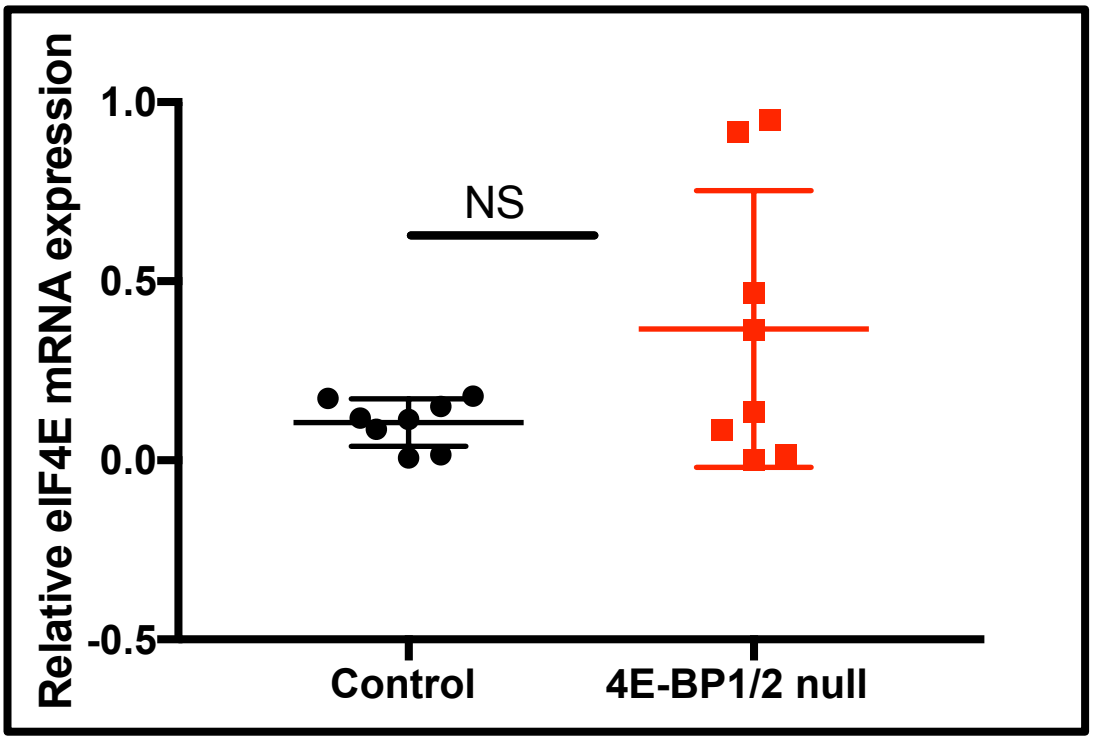

Figure 18. eIF4E mRNA levels are unchanged by loss of 4E-BP1/2 (n=8)
Total RNA was isolated PyV-MT and PyV-MT/4E-BP1/2 mouse tumors of 14-16 weeks of age (n=8). RT-qPCR was performed on these tumors using primers for eIF4E. Data is shown as fold change compared to actin and GAPDH controls.

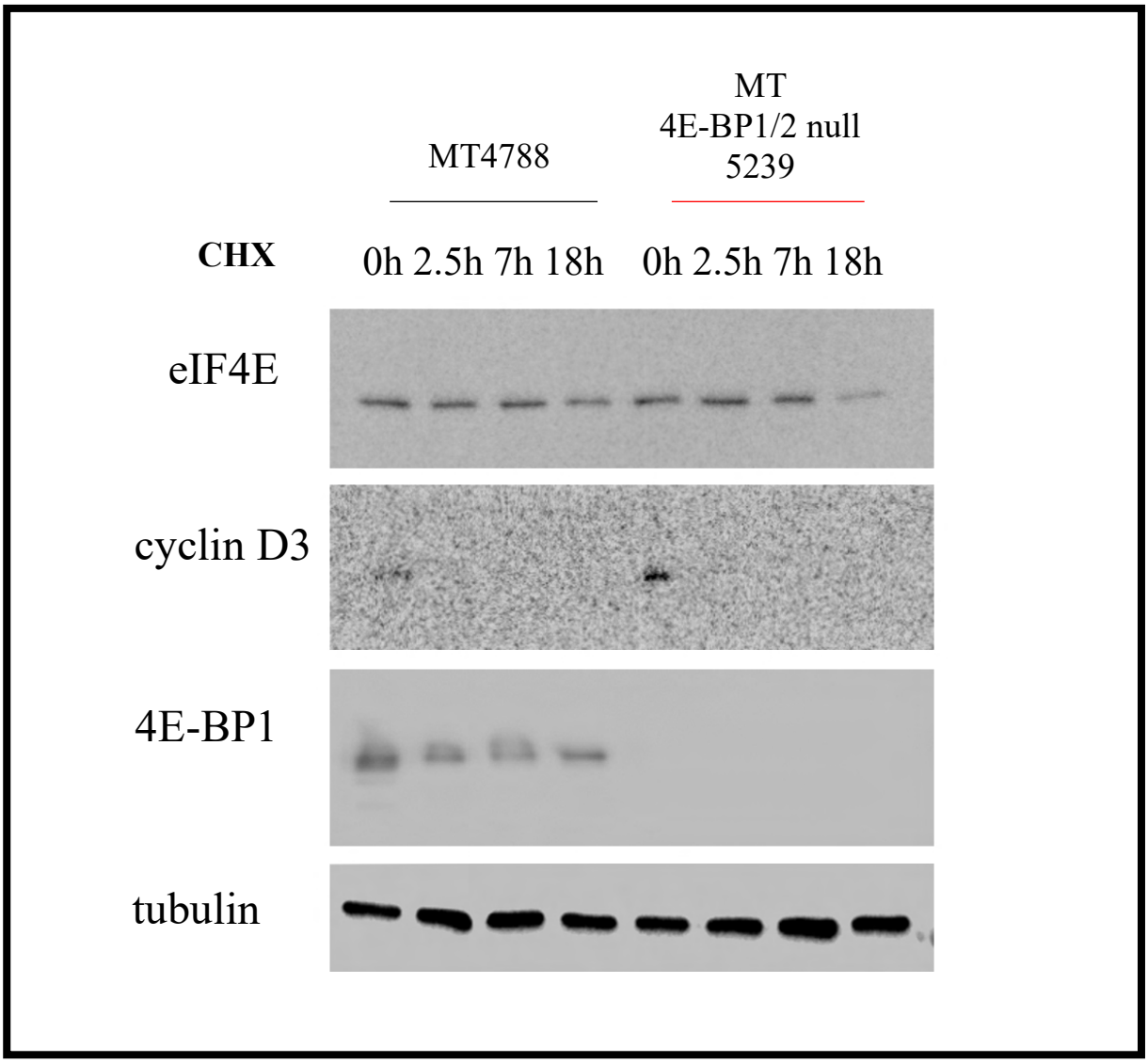

Figure 19. Loss of 4E-BP1/2 leads to decreased eIF4E protein stability
PyV-MT4788 and PyV-MT/4E-BP1/2 null 5239 cell lines were treated with CHX in 2.5% FBS DMEM (+MEGS). Cells were treated with CHX for 2.5h, 7h, and 18h. Cyclin D3 was used a positive control for CHX treatment. (n=2)

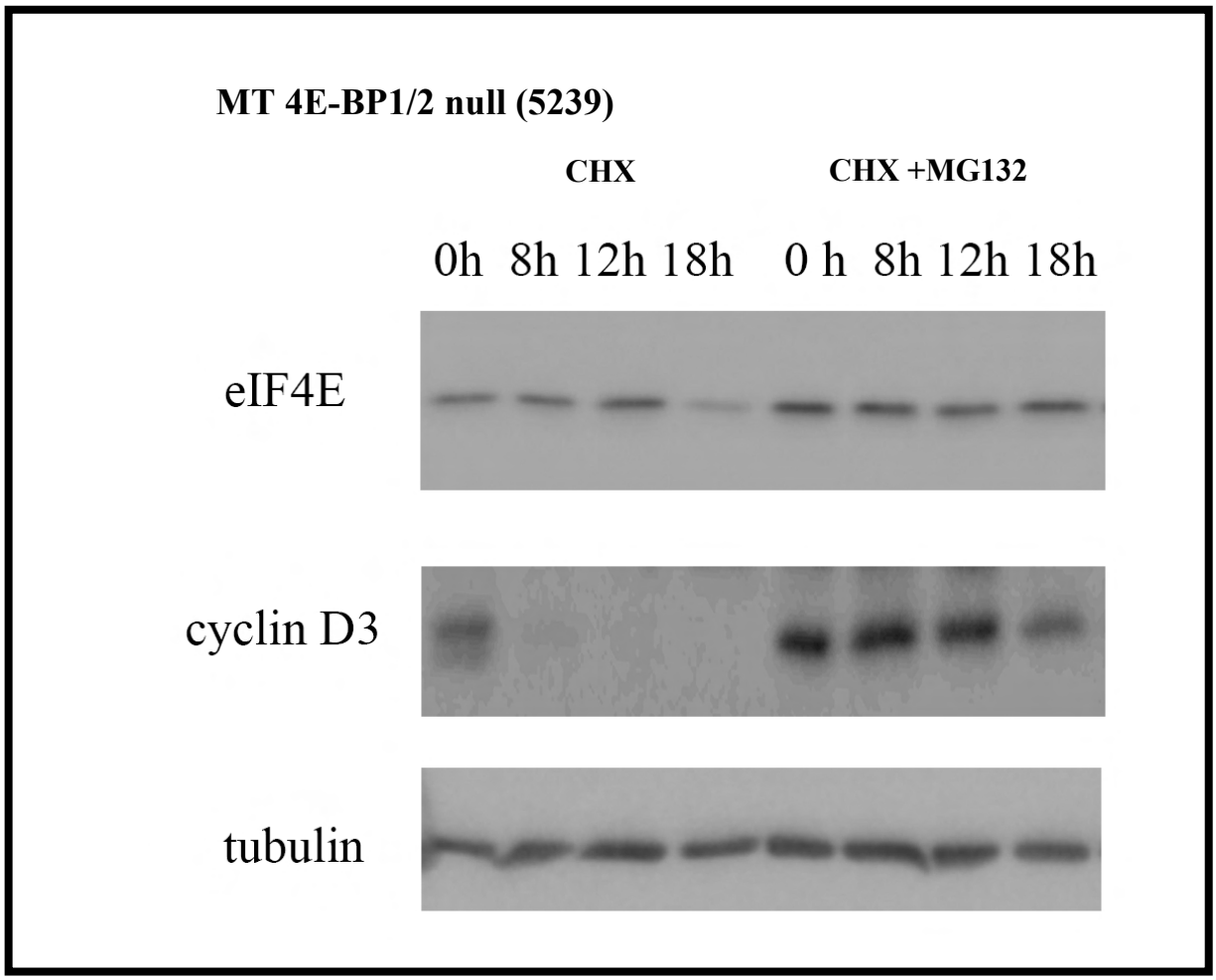

Figure 20. eIF4E stability is rescued by blocking proteasome in PyV-MT 4E-BP1/2 null cell line

PyV-MT/4E-BP1/2 null 5239 cells were treated with CHX and CHX+MG132 for 0h, 8h, 12h, and 18h. Cells were treated in 2.5% FBS DMEM (+MEGS). Cyclin D3 was used as a positive control for CHX and MG132 treatment. (n=2)

3.8 Correlative decrease of eIF4E levels in 4E-BP1/2 null contexts is not conserved across model systems

The dramatic decrease in eIF4E levels within primary tumors of PyV-MT/4E-BP1/2 null mice has not been reported to our knowledge. While decreased 4E-BP1 levels in contexts of eIF4E depletion have been observed [101], there have been no reports illustrating the inverse phenomenon. To establish whether or not this was a context/model specific phenomenon, an additional mouse breast cancer cell line was employed. To this end we utilized HER2 amplified NT2197 cells in which *EIF4EBP1* and *EIF4EBP2* were deleted by CRISPR ([102]). In NT2197 4E-BP1/2 depleted cells, there was only minimal decrease in eIF4E levels compared to the NT2197 control (Figure 23). This is in stark contrast to the dramatic reduction in eIF4E levels exhibited by PyV-MT/4E-BP1/2 cells compared to PyV-MT controls (Figure 23). PyV-MT/4E-BP1/2 null cells are derived from transgenic mice with a germline deletion of *EIF4EBP1* and *EIF4EBP2* while *EIF4EBP1* and *EIF4EBP2* deletion in NT2197 cells was induced later, in an already established cancer cell line. The time point at which 4E-BPs were lost may account for the inconsistent decrease in eIF4E levels across 4E-BP1/2 null systems.

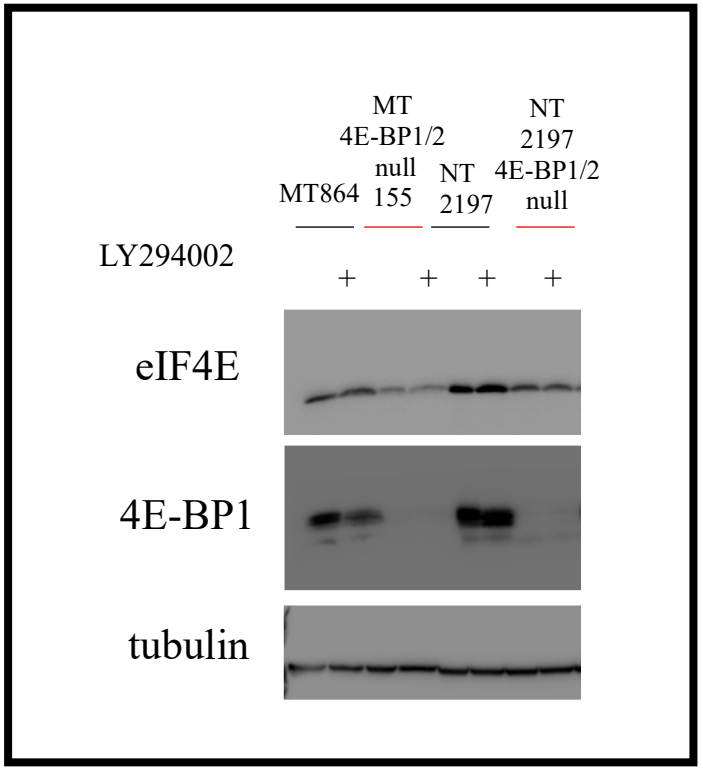

Figure 21. Decreased eIF4E protein levels does appear in NT2197 cells
PyV-MT864, PyV-MT/4E-BP1/2 null, NT2197, and NT2197 CRISPR /Cas9 edited 4E-BP1/2 null cells were treated with LY294002, PI3K inhibitor, for 20 hours at 20 uM. Lysates were analyzed by western blotting. (n=2)

Chapter Four: Discussion

In this project, we aimed to characterize the mitogenic signaling response of ShcA mutant cell lines (2F and 313F) and determine the phenotype of PyV-MT/ShcA-3F heterozygous/4E-BP1/2 null mice. In parallel, our second objective was to establish the role of 4E-BP1 and 2 in breast cancer progression using the PyV-MT model. 4E-BPs have been long-characterized as repressors of mRNA translation [50, 91]. Studies have shown that 4E-BP1/2 loss is paralleled by increased proliferation in cell culture and increased anchorage-independent growth [190]. However, according to Cancer Genome Atlas, EIF4EBP1 copy number is increased in 18.38% of breast cancer cases and decreased in only 4.48% cases. High 4E-BP1 mRNA expression levels were also found to associate with poor outcome in breast cancer [192]. In this thesis, we set out to determine the role of 4E-BPs in breast cancer in the context of dysregulated RTK signaling.

Previous work in the lab demonstrated that ShcA-driven AKT activation potentiates breast tumor angiogenesis in a 4E-BP dependent manner [174] In PyV-MT/Shc3F heterozygous transgenic mice, the germline loss of 4E-BP1/2 led to accelerated tumor onset as compared to 4E-BP1/2-proficient mice (Figure 11a). This confirms that ShcA-driven breast tumor angiogenesis functions through 4E-BPs as loss of 4E-BPS is able to accelerate delayed tumor onset observed in ShcA3F heterozygous mice [171]. Further experiments are carried out to identify the ShcA CH1 tyrosine responsible for downstream signaling through 4E-BPs. We predict that the phosphorylation of ShcA Tyr239 and 240 is likely to be the event which triggers downstream signaling via 4E-BPs. This is based on our observations that ShcA 313F cells (with intact Tyr239/240) possess high AKT activation when compared to ShcA 2F cells (herein Tyr239/240 were mutated to Phe) (Figure 10b). ShcA2F cells heightened sensitivity to asTORi-torin1 can be explained by a compensatory

mechanism by which ShcA2F cells activate mTOR signaling through its Tyr313 residue to compensate for loss of reduction of AKT signaling through ShcA Tyr239/240 residues (Figure 10a). Therefore, we postulate that Tyr239 and Tyr240 of ShcA plays a major role in modulating 4E-BP phosphorylation status downstream of ShcA, and thus eIF4F levels.

We also show that in an MMTV-PyV-MT breast cancer mouse model, the loss of 4E-BP1 and 4E-BP2 increases tumor volume while not affecting tumor onset and the number of tumor bearing glands (Figure 12). Thus, in the context of the MMTV-PyV-MT model, 4E-BPs do not appear implicated in tumor initiation. This can be explained by the constitutive activation of RTK signaling in MMTV-PyV-MT model which inactivates 4E-BPs via mTORC1 [104, 179]. Indeed, we have demonstrated that mTOR signaling is hyperactivated in cells isolated from PyV-MT-driven tumors, and largely unresponsive to nutrient and/or growth factor depletion (Figure 9 and 10). In this manner, even in wild-type MMTV-PyV mice, 4E-BPs are inactivated by hyperactive mTOR signaling. In contrast, we made an unexpected observation that the germline loss of *EIF4EBP1* and *EIF4EBP2* genes also led to the unexpected reduction in pulmonary metastases in the MMTV-PyV-MT model (Figure 13). Strikingly, impaired pulmonary metastasis was accompanied by a significant decrease in eIF4E protein levels in primary tumors of PyV-MT/4E-BP1/2 null mice as compared to 4E-BP1/2 proficient mice (Figure 13).

The reduction in pulmonary metastases of transgenic PyV-MT/4E-BP1/2 null mice was unpredicted given similar studies done in different mouse models. For example, in a PTEN null prostate cancer model that in part mimics constitutive AKT activation, the germline loss of *EIF4EBP1* and *EIF4EBP2* genes led to increased tumor invasiveness [95]. Using the same PyV-

MT mouse model, Nasr et. al demonstrated that hyperactive mTORC1 in a PyV-MT/Tsc2 heterozygous mouse results in greater number of pulmonary metastases [65]. There are multiple possibilities to explain for the unexpected reduction in metastatic burden in the MMTV/PyV-MT/4E-BP1/2 null mouse. Here, we elaborate on two of these possible explanations.

4.1 Two-Potent Oncogenic "Hits"

The loss of pulmonary metastases in the PyV-MT/4E-BP1/2 null transgenic mice may be due to an exceeded oncogenic threshold. Surpassing this oncogenic stress threshold, in particular in tumors which are nutrient and/or oxygen deprived due to the outstripping of the vasculature, may lead to energetic crisis, which if unchecked would lead to increased apoptosis. MMTV-PyV-MT mouse model contains two oncogenic "hits" or stressors that may push tumor cells into crisis. The first "hit" is the PyV-MT oncogene, which has very potent transforming activity. Associating with a number of c-src family members and the 85-kDa subunit of PI3K, the PyV-MT oncogene introduces an oncogenic stress on a cell that can result in genomic instability and increased energy consumption to sustain growth and proliferation [177, 179]. Accordingly, PyV-MT cells are unresponsive to serum deprivation and growth factor stimulation confirming continuous PI3K/AKT and RAS/ERK signaling (Figure 9).

The second "hit" is the loss of 4E-BPs, a negative repressor of mRNA translation. Germline deletion of *EIF4EBP1/2* leads to elevated eIF4F complex levels [32]. Abundant eIF4E allows for cells to translate eIF4E-sensitive mRNA that enable cellular proliferation and growth, an overall energy consuming process [55, 72, 193]. We hypothesize that the additive effects of the PyV-MT oncogene and germline loss of negative regulator, *EIF4EBP1/2*, surpasses a potential oncogenic

threshold and requires a cellular coping mechanism in order to adapt and survive. The downregulation of eIF4E protein levels in primary PyV-MT/4E-BP1/2 null tumors may be one such adaptive mechanism (Figure 14).

To summarize, adaptive decrease in total eIF4E levels likely reduces metastatic potential in the PyV-MT/4E-BP1/2 null mice. This is consistent with previous reports [67, 68, 75]. Importantly, the adaptive response observed is unique to the PyV-MT/4E-BP1/2 null model as significant decreases in eIF4E levels are not seen upon *EIF4EBP1/2* ablation in HER2 amplified NT2197 cells (Figure 21).

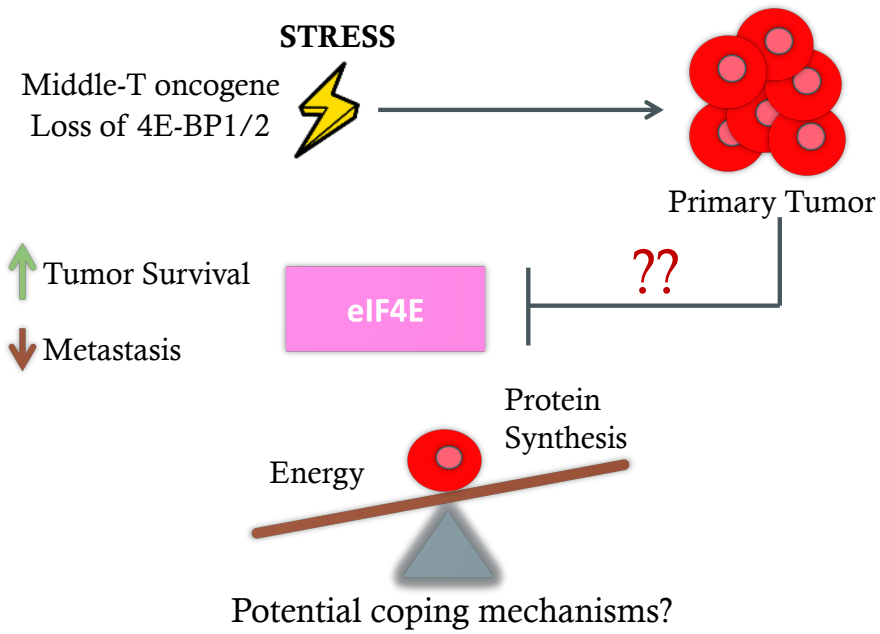

Figure 22. Working Model
In this working model, we propose that oncogenic stress in the form of the PyV-MT oncogene and loss of 4E-BP1 and 4E-BP2 leads to formation of a primary tumor. The primary tumor grows until a certain point in which eIF4E is downregulated by an unestablished mechanism. The downregulation of eIF4E is a coping/adaptive mechanism that allows for tumor survival and evasion of cell death. However, as a consequence, the tumor has to sacrifice metastasis in order to survive. Thus, in a tumor, the eIF4E/4E-BP ratio may be important not only in maintaining translational homeostasis, but for metastatic potential.

4.2 eIF4E/4E-BP Equilibrium

It is likely that eIF4E downregulation in PyV-MT/4E-BP1/2 null primary tumors occur both in response to germline loss of *EIF4EBP1* and *EIF4EBP2* and nutrition and growth factor depletion due to aberrant tumor growth. Co-dependence of 4E-BPs and eIF4E has already been reported in the literature [54, 101]. For example, depletion of eIF4E led to increased 4E-BP1 degradation by the proteasome which is mediated by the KLHL25-CUL3 complex-dependent ubiquitination [101]. In our results, we demonstrate that re-expression of 4E-BP1 in a PyV-MT/4E-BP1/2 null cell line leads to a rise in eIF4E levels compared to the vector control (Figure 17). This suggests an unknown potential sensing mechanism that exists between 4E-BPs and eIF4E which activates degradation pathways during eIF4E/4E-BP disequilibrium. We propose the PyV-MT/4E-BP1/2 null tumors may have an activated adaptive mechanism that degrades excess eIF4E through a ubiquitin-proteasome degradation pathway in an effort to restore eIF4E/4E-BP equilibrium (Figure 19, 20). eIF4E has already been reported to be targeted for degradation through ubiquitination of its Lys 159 residue by the Chip E3 ligase [54]. Further experiments should aim to confirm eIF4E degradation through ubiquitination in the PyV-MT/4E-BP1/2 null context. We predict that inhibition of eIF4E ubiquitination through mutagenesis may have the capacity to restore metastasis in PyV-MT-4E-BP1/2 null mice but are also aware of the difficulties pertinent to the potential inadvertent effects of mutation of Lys 159 residue on the cap binding activity of eIF4E [196].

4.3 Other Potential Factors

The reduction of pulmonary metastases in PyV-MT/4E-BP1/2 null mice may also be multifactorial. For instance, 4E-BPs have been suggested to play a significant role in hypoxia tolerance and regulation of reactive oxygen species (ROS) [95, 197]. The ability to recognize and deal with ROS is essential for oncogenic transformation and metastatic progression. Thus, loss of 4E-BPs may impair hypoxia tolerance and consequently metastasis. Impaired response to ROS has been shown to result in an impaired tumorigenesis program [68]. Genes involved in regulation and response to ROS are sensitive to eIF4E levels in a cell [68]. Therefore, loss of 4E-BPs that lead to a downregulation of eIF4E may result in impaired translation of ROS regulatory genes and hypoxia tolerance. In turn, metastasis is impaired.

Although the objectives of this thesis were originally centered around characterizing the role of 4E-BPs in the mammary tumorigenesis process of a wild-type and ShcA signaling-depleted MMTV-PyV MT mouse model, our objective shifted upon the discovery of reduced pulmonary metastases in the PyV-MT/4E-BP1/2 null model. We postulate that extreme oncogenic stress exerted by the PyV-MT oncogene, loss of 4E-BPs, and a potential inability to cope with ROS and hypoxia, leads cells to attempt regulation of the eIF4E/4E-BP ratio in cells, in order to avoid energy crisis and cell death. As a consequence, the tumor has reduced metastatic potential.

4.4 Limitations

This thesis contains certain limitations that are addressed here. First, our study is limited by the physiological relevance of our model. The PyV-MT/4E-BP1/2 null model does not reflect a physiologically relevant breast tumor. Tumors do not lose 4E-BPs during the tumorigenesis process, but rather increase 4E-BP levels in many instances [99]. While the PyV-MT model recapitulates a relevant human luminal B breast cancer process, the loss of 4E-BPs does not model human biology. While the model may not be relevant for clinical intervention, the results generated from studying the unexpected phenotype may shed light on mechanisms of tumor adaptation in the face of potent oncogenic stress, which is of high relevance to the understanding the molecular underpinnings of the neoplasia of the breast in humans.

Further, the PyV-MT/4E-BP1/2 null lung metastases phenotype is limited by the time that the tumor is allowed to grow. Mice were euthanized and necropsied at 8-weeks post tumor onset or when total tumor volume was 6 cm^3. While it was not possible to allow tumors to grow longer in mice due to the ethical endpoints, the study may have yielded different results if mice were not sacrificed at this time. By microscopic examination of H&E tumor sections, we saw little to no pulmonary lung metastases in the PyV-MT/4E-BP1/2 null mice. However, it is possible that metastasis is severely delayed in these mice or unable to colonize and grow in the lung. To address this limitation, we can inject PyV-MT/4E-BP1/2 null cells into the mammary fat pad of 4E-BP1/2 null mice. Once tumors reach ethical endpoint, we can resect tumors. Tumor resection would allow for the deciphering of the loss of metastatic potential from delayed metastasis in these 4E-BP1/2 null mice.

4.5 Conclusion

Oncogenic stress characterized by the potent PyV-MT oncogene and loss of 4E-BPs paradoxically leads to reduced capacity of breast cancers to metastasize. This phenotype may be due to downregulation of eIF4E and thus translational perturbations. As eIF4E plays a central role in translational reprogramming which underpins metastatic progression [68], reduction of eIF4E levels caused by the 4E-BP1/2 loss is expected to impede metastasis. Although the mechanism of eIF4E reduction caused by the loss of 4E-BP1/2 expression remains unclear, it appears that eIF4E protein is degraded at the faster rate in 4E-BP1/2-deficient compared to 4E-BP1/2 proficient cells, which is likely mediated by the ubiquitin-proteasome system. Considering that reduction in eIF4E levels becomes prominent only when the 4E-BP1/2-deficient tumors reach size when tumors typically outstrip their vasculature, it is plausible that downregulation of eIF4E serves as a compensatory mechanism which prevents nutrient deprived breast cancer cells to undergo energy crisis due to their inability to harness excessive energy consumption by translational apparatus. Indeed, it has been proposed that 4E-BPs may serve as a metabolic break, whereby loss of 4E-BP1/2 expression has been demonstrated to reduce prostate tumor growth under certain contexts [197]. Potential adaptation of 4E-BP1/2-deficient tumors to energy stress by decreasing eIF4E levels is therefore expected to result in reduced metastatic potential. Future work is required to establish the mechanisms that affect eIF4E/4E-BP ratio in tumors and their impact on tumor biology.

Literature Cited

1. Bray, F., et al., *Global cancer statistics 2018: GLOBOCAN estimates of incidence and mortality worldwide for 36 cancers in 185 countries.* CA Cancer J Clin, 2018. **68**(6): p. 394-424.
2. Bertos, N.R. and M. Park, *Breast cancer - one term, many entities?* J Clin Invest, 2011. **121**(10): p. 3789-96.
3. Perou, C.M., et al., *Molecular portraits of human breast tumours.* Nature, 2000. **406**(6797): p. 747-52.
4. Sorlie, T., et al., *Gene expression patterns of breast carcinomas distinguish tumor subclasses with clinical implications.* Proc Natl Acad Sci U S A, 2001. **98**(19): p. 10869-74.
5. Perou, C.M., et al., *Distinctive gene expression patterns in human mammary epithelial cells and breast cancers.* Proc Natl Acad Sci U S A, 1999. **96**(16): p. 9212-7.
6. Vallejos, C.S., et al., *Breast cancer classification according to immunohistochemistry markers: subtypes and association with clinicopathologic variables in a peruvian hospital database.* Clin Breast Cancer, 2010. **10**(4): p. 294-300.
7. Kennecke, H., et al., *Metastatic behavior of breast cancer subtypes.* J Clin Oncol, 2010. **28**(20): p. 3271-7.
8. Voduc, K.D., et al., *Breast cancer subtypes and the risk of local and regional relapse.* J Clin Oncol, 2010. **28**(10): p. 1684-91.
9. Park, S., et al., *Characteristics and outcomes according to molecular subtypes of breast cancer as classified by a panel of four biomarkers using immunohistochemistry.* Breast, 2012. **21**(1): p. 50-7.
10. Loi, S., et al., *Gene expression profiling identifies activated growth factor signaling in poor prognosis (Luminal-B) estrogen receptor positive breast cancer.* BMC Med Genomics, 2009. **2**: p. 37.
11. Tran, B. and P.L. Bedard, *Luminal-B breast cancer and novel therapeutic targets.* Breast Cancer Res, 2011. **13**(6): p. 221.
12. Cancer Genome Atlas, N., *Comprehensive molecular portraits of human breast tumours.* Nature, 2012. **490**(7418): p. 61-70.
13. Moasser, M.M., *The oncogene HER2: its signaling and transforming functions and its role in human cancer pathogenesis.* Oncogene, 2007. **26**(45): p. 6469-87.
14. Bianchini, G., et al., *Triple-negative breast cancer: challenges and opportunities of a heterogeneous disease.* Nat Rev Clin Oncol, 2016. **13**(11): p. 674-690.
15. Herschkowitz, J.I., et al., *Identification of conserved gene expression features between murine mammary carcinoma models and human breast tumors.* Genome Biol, 2007. **8**(5): p. R76.
16. Dias, K., et al., *Claudin-Low Breast Cancer; Clinical & Pathological Characteristics.* PLoS One, 2017. **12**(1): p. e0168669.
17. Waks, A.G. and E.P. Winer, *Breast Cancer Treatment: A Review.* JAMA, 2019. **321**(3): p. 288-300.
18. Jordan, V.C., *Tamoxifen: a most unlikely pioneering medicine.* Nat Rev Drug Discov, 2003. **2**(3): p. 205-13.

19. Early Breast Cancer Trialists' Collaborative, G., *Aromatase inhibitors versus tamoxifen in early breast cancer: patient-level meta-analysis of the randomised trials.* Lancet, 2015. **386**(10001): p. 1341-1352.
20. Tolaney, S.M., et al., *Adjuvant paclitaxel and trastuzumab for node-negative, HER2-positive breast cancer.* N Engl J Med, 2015. **372**(2): p. 134-41.
21. Geyer, C.E., et al., *Lapatinib plus capecitabine for HER2-positive advanced breast cancer.* N Engl J Med, 2006. **355**(26): p. 2733-43.
22. Slamon, D.J., et al., *Use of chemotherapy plus a monoclonal antibody against HER2 for metastatic breast cancer that overexpresses HER2.* N Engl J Med, 2001. **344**(11): p. 783-92.
23. Mariotto, A.B., et al., *Estimation of the Number of Women Living with Metastatic Breast Cancer in the United States.* Cancer Epidemiol Biomarkers Prev, 2017. **26**(6): p. 809-815.
24. Weigelt, B., et al., *Molecular portraits and 70-gene prognosis signature are preserved throughout the metastatic process of breast cancer.* Cancer Res, 2005. **65**(20): p. 9155-8.
25. Pollak, M., *Insulin and insulin-like growth factor signalling in neoplasia.* Nat Rev Cancer, 2008. **8**(12): p. 915-28.
26. Heuson, J.C., N. Legros, and R. Heimann, *Influence of insulin administration on growth of the 7,12-dimethylbenz(a)anthracene-induced mammary carcinoma in intact, oophorectomized, and hypophysectomized rats.* Cancer Res, 1972. **32**(2): p. 233-8.
27. Law, J.H., et al., *Phosphorylated insulin-like growth factor-i/insulin receptor is present in all breast cancer subtypes and is related to poor survival.* Cancer Res, 2008. **68**(24): p. 10238-46.
28. Pollak, M.N., E.S. Schernhammer, and S.E. Hankinson, *Insulin-like growth factors and neoplasia.* Nat Rev Cancer, 2004. **4**(7): p. 505-18.
29. Yerushalmi, R., et al., *Insulin-like growth factor receptor (IGF-1R) in breast cancer subtypes.* Breast Cancer Res Treat, 2012. **132**(1): p. 131-42.
30. Gonzalez-Angulo, A.M., et al., *PI3K pathway mutations and PTEN levels in primary and metastatic breast cancer.* Mol Cancer Ther, 2011. **10**(6): p. 1093-101.
31. Creighton, C.J., et al., *Proteomic and transcriptomic profiling reveals a link between the PI3K pathway and lower estrogen-receptor (ER) levels and activity in ER+ breast cancer.* Breast Cancer Res, 2010. **12**(3): p. R40.
32. Bhat, M., et al., *Targeting the translation machinery in cancer.* Nat Rev Drug Discov, 2015. **14**(4): p. 261-78.
33. Buttgereit, F. and M.D. Brand, *A hierarchy of ATP-consuming processes in mammalian cells.* Biochem J, 1995. **312 (Pt 1)**: p. 163-7.
34. Hinnebusch, A.G., *eIF3: a versatile scaffold for translation initiation complexes.* Trends Biochem Sci, 2006. **31**(10): p. 553-62.
35. Shatkin, A.J., *Capping of eucaryotic mRNAs.* Cell, 1976. **9**(4 PT 2): p. 645-53.
36. Imataka, H. and N. Sonenberg, *Human eukaryotic translation initiation factor 4G (eIF4G) possesses two separate and independent binding sites for eIF4A.* Mol Cell Biol, 1997. **17**(12): p. 6940-7.
37. Gingras, A.C., B. Raught, and N. Sonenberg, *eIF4 initiation factors: effectors of mRNA recruitment to ribosomes and regulators of translation.* Annu Rev Biochem, 1999. **68**: p. 913-63.

38. Sonenberg, N., et al., *Differential stimulation of capped mRNA translation in vitro by cap binding protein.* Nature, 1980. **285**(5763): p. 331-3.
39. Tahara, S.M., M.A. Morgan, and A.J. Shatkin, *Two forms of purified m7G-cap binding protein with different effects on capped mRNA translation in extracts of uninfected and poliovirus-infected HeLa cells.* J Biol Chem, 1981. **256**(15): p. 7691-4.
40. Sonenberg, N., et al., *A polypeptide in eukaryotic initiation factors that crosslinks specifically to the 5'-terminal cap in mRNA.* Proc Natl Acad Sci U S A, 1978. **75**(10): p. 4843-7.
41. Imataka, H., A. Gradi, and N. Sonenberg, *A newly identified N-terminal amino acid sequence of human eIF4G binds poly(A)-binding protein and functions in poly(A)-dependent translation.* EMBO J, 1998. **17**(24): p. 7480-9.
42. Pelletier, J. and N. Sonenberg, *Internal initiation of translation of eukaryotic mRNA directed by a sequence derived from poliovirus RNA.* Nature, 1988. **334**(6180): p. 320-5.
43. Hellen, C.U. and P. Sarnow, *Internal ribosome entry sites in eukaryotic mRNA molecules.* Genes Dev, 2001. **15**(13): p. 1593-612.
44. Duncan, R., S.C. Milburn, and J.W. Hershey, *Regulated phosphorylation and low abundance of HeLa cell initiation factor eIF-4F suggest a role in translational control. Heat shock effects on eIF-4F.* J Biol Chem, 1987. **262**(1): p. 380-8.
45. Osborne, M.J., et al., *eIF4E3 acts as a tumor suppressor by utilizing an atypical mode of methyl-7-guanosine cap recognition.* Proc Natl Acad Sci U S A, 2013. **110**(10): p. 3877-82.
46. Marcotrigiano, J., et al., *Cocrystal structure of the messenger RNA 5' cap-binding protein (eIF4E) bound to 7-methyl-GDP.* Cell, 1997. **89**(6): p. 951-61.
47. Matsuo, H., et al., *Structure of translation factor eIF4E bound to m7GDP and interaction with 4E-binding protein.* Nat Struct Biol, 1997. **4**(9): p. 717-24.
48. Pyronnet, S., et al., *Human eukaryotic translation initiation factor 4G (eIF4G) recruits mnk1 to phosphorylate eIF4E.* EMBO J, 1999. **18**(1): p. 270-9.
49. Gruner, S., et al., *The Structures of eIF4E-eIF4G Complexes Reveal an Extended Interface to Regulate Translation Initiation.* Mol Cell, 2016. **64**(3): p. 467-479.
50. Pause, A., et al., *Insulin-dependent stimulation of protein synthesis by phosphorylation of a regulator of 5'-cap function.* Nature, 1994. **371**(6500): p. 762-7.
51. Jones, R.M., et al., *An essential E box in the promoter of the gene encoding the mRNA cap-binding protein (eukaryotic initiation factor 4E) is a target for activation by c-myc.* Mol Cell Biol, 1996. **16**(9): p. 4754-64.
52. Rosenwald, I.B., et al., *Increased expression of eukaryotic translation initiation factors eIF-4E and eIF-2 alpha in response to growth induction by c-myc.* Proc Natl Acad Sci U S A, 1993. **90**(13): p. 6175-8.
53. Topisirovic, I., et al., *Stability of eukaryotic translation initiation factor 4E mRNA is regulated by HuR, and this activity is dysregulated in cancer.* Mol Cell Biol, 2009. **29**(5): p. 1152-62.
54. Murata, T. and K. Shimotohno, *Ubiquitination and proteasome-dependent degradation of human eukaryotic translation initiation factor 4E.* J Biol Chem, 2006. **281**(30): p. 20788-800.

55. Lazaris-Karatzas, A., K.S. Montine, and N. Sonenberg, *Malignant transformation by a eukaryotic initiation factor subunit that binds to mRNA 5' cap.* Nature, 1990. **345**(6275): p. 544-7.
56. Lazaris-Karatzas, A. and N. Sonenberg, *The mRNA 5' cap-binding protein, eIF-4E, cooperates with v-myc or E1A in the transformation of primary rodent fibroblasts.* Mol Cell Biol, 1992. **12**(3): p. 1234-8.
57. Rousseau, D., et al., *Translation initiation of ornithine decarboxylase and nucleocytoplasmic transport of cyclin D1 mRNA are increased in cells overexpressing eukaryotic initiation factor 4E.* Proc Natl Acad Sci U S A, 1996. **93**(3): p. 1065-70.
58. Sonenberg, N., *eIF4E, the mRNA cap-binding protein: from basic discovery to translational research.* Biochem Cell Biol, 2008. **86**(2): p. 178-83.
59. De Benedetti, A. and A.L. Harris, *eIF4E expression in tumors: its possible role in progression of malignancies.* Int J Biochem Cell Biol, 1999. **31**(1): p. 59-72.
60. Scott, P.A., et al., *Differential expression of vascular endothelial growth factor mRNA vs protein isoform expression in human breast cancer and relationship to eIF-4E.* Br J Cancer, 1998. **77**(12): p. 2120-8.
61. Li, B.D., et al., *Overexpression of eukaryotic initiation factor 4E (eIF4E) in breast carcinoma.* Cancer, 1997. **79**(12): p. 2385-90.
62. De Benedetti, A. and J.R. Graff, *eIF-4E expression and its role in malignancies and metastases.* Oncogene, 2004. **23**(18): p. 3189-99.
63. Koromilas, A.E., A. Lazaris-Karatzas, and N. Sonenberg, *mRNAs containing extensive secondary structure in their 5' non-coding region translate efficiently in cells overexpressing initiation factor eIF-4E.* EMBO J, 1992. **11**(11): p. 4153-8.
64. Graff, J.R., et al., *Therapeutic suppression of translation initiation factor eIF4E expression reduces tumor growth without toxicity.* J Clin Invest, 2007. **117**(9): p. 2638-48.
65. Nasr, Z., et al., *eIF4F suppression in breast cancer affects maintenance and progression.* Oncogene, 2013. **32**(7): p. 861-71.
66. Pettersson, F., et al., *Ribavirin treatment effects on breast cancers overexpressing eIF4E, a biomarker with prognostic specificity for luminal B-type breast cancer.* Clin Cancer Res, 2011. **17**(9): p. 2874-84.
67. Ruggero, D., et al., *The translation factor eIF-4E promotes tumor formation and cooperates with c-Myc in lymphomagenesis.* Nat Med, 2004. **10**(5): p. 484-6.
68. Truitt, M.L., et al., *Differential Requirements for eIF4E Dose in Normal Development and Cancer.* Cell, 2015. **162**(1): p. 59-71.
69. Flynn, A. and C.G. Proud, *Serine 209, not serine 53, is the major site of phosphorylation in initiation factor eIF-4E in serum-treated Chinese hamster ovary cells.* J Biol Chem, 1995. **270**(37): p. 21684-8.
70. Waskiewicz, A.J., et al., *Phosphorylation of the cap-binding protein eukaryotic translation initiation factor 4E by protein kinase Mnk1 in vivo.* Mol Cell Biol, 1999. **19**(3): p. 1871-80.
71. Ueda, T., et al., *Mnk2 and Mnk1 are essential for constitutive and inducible phosphorylation of eukaryotic initiation factor 4E but not for cell growth or development.* Mol Cell Biol, 2004. **24**(15): p. 6539-49.

72. Topisirovic, I., M. Ruiz-Gutierrez, and K.L. Borden, *Phosphorylation of the eukaryotic translation initiation factor eIF4E contributes to its transformation and mRNA transport activities.* Cancer Res, 2004. **64**(23): p. 8639-42.
73. Furic, L., et al., *eIF4E phosphorylation promotes tumorigenesis and is associated with prostate cancer progression.* Proc Natl Acad Sci U S A, 2010. **107**(32): p. 14134-9.
74. Konicek, B.W., et al., *Therapeutic inhibition of MAP kinase interacting kinase blocks eukaryotic initiation factor 4E phosphorylation and suppresses outgrowth of experimental lung metastases.* Cancer Res, 2011. **71**(5): p. 1849-57.
75. Robichaud, N., et al., *Phosphorylation of eIF4E promotes EMT and metastasis via translational control of SNAIL and MMP-3.* Oncogene, 2015. **34**(16): p. 2032-42.
76. Duffy, A.G., et al., *Modulation of tumor eIF4E by antisense inhibition: A phase I/II translational clinical trial of ISIS 183750-an antisense oligonucleotide against eIF4E-in combination with irinotecan in solid tumors and irinotecan-refractory colorectal cancer.* Int J Cancer, 2016. **139**(7): p. 1648-57.
77. Moerke, N.J., et al., *Small-molecule inhibition of the interaction between the translation initiation factors eIF4E and eIF4G.* Cell, 2007. **128**(2): p. 257-67.
78. Feng, Y., et al., *SBI-0640756 Attenuates the Growth of Clinically Unresponsive Melanomas by Disrupting the eIF4F Translation Initiation Complex.* Cancer Res, 2015. **75**(24): p. 5211-8.
79. Bordeleau, M.E., et al., *RNA-mediated sequestration of the RNA helicase eIF4A by Pateamine A inhibits translation initiation.* Chem Biol, 2006. **13**(12): p. 1287-95.
80. Bordeleau, M.E., et al., *Stimulation of mammalian translation initiation factor eIF4A activity by a small molecule inhibitor of eukaryotic translation.* Proc Natl Acad Sci U S A, 2005. **102**(30): p. 10460-5.
81. Low, W.K., et al., *Inhibition of eukaryotic translation initiation by the marine natural product pateamine A.* Mol Cell, 2005. **20**(5): p. 709-22.
82. Cencic, R., et al., *Antitumor activity and mechanism of action of the cyclopenta[b]benzofuran, silvestrol.* PLoS One, 2009. **4**(4): p. e5223.
83. Cerezo, M., et al., *Translational control of tumor immune escape via the eIF4F-STAT1-PD-L1 axis in melanoma.* Nat Med, 2018. **24**(12): p. 1877-1886.
84. Iwasaki, S., et al., *The Translation Inhibitor Rocaglamide Targets a Bimolecular Cavity between eIF4A and Polypurine RNA.* Mol Cell, 2019. **73**(4): p. 738-748 e9.
85. Roux, P.P. and I. Topisirovic, *Regulation of mRNA translation by signaling pathways.* Cold Spring Harb Perspect Biol, 2012. **4**(11).
86. Banko, J.L., et al., *The translation repressor 4E-BP2 is critical for eIF4F complex formation, synaptic plasticity, and memory in the hippocampus.* J Neurosci, 2005. **25**(42): p. 9581-90.
87. Peter, D., et al., *Molecular architecture of 4E-BP translational inhibitors bound to eIF4E.* Mol Cell, 2015. **57**(6): p. 1074-1087.
88. Poulin, F., et al., *4E-BP3, a new member of the eukaryotic initiation factor 4E-binding protein family.* J Biol Chem, 1998. **273**(22): p. 14002-7.
89. Tee, A.R. and C.G. Proud, *Caspase cleavage of initiation factor 4E-binding protein 1 yields a dominant inhibitor of cap-dependent translation and reveals a novel regulatory motif.* Mol Cell Biol, 2002. **22**(6): p. 1674-83.

90. Beugnet, A., X. Wang, and C.G. Proud, *Target of rapamycin (TOR)-signaling and RAIP motifs play distinct roles in the mammalian TOR-dependent phosphorylation of initiation factor 4E-binding protein 1.* J Biol Chem, 2003. **278**(42): p. 40717-22.
91. Gingras, A.C., et al., *Hierarchical phosphorylation of the translation inhibitor 4E-BP1.* Genes Dev, 2001. **15**(21): p. 2852-64.
92. Gingras, A.C., et al., *Regulation of 4E-BP1 phosphorylation: a novel two-step mechanism.* Genes Dev, 1999. **13**(11): p. 1422-37.
93. Le Bacquer, O., et al., *Elevated sensitivity to diet-induced obesity and insulin resistance in mice lacking 4E-BP1 and 4E-BP2.* J Clin Invest, 2007. **117**(2): p. 387-96.
94. Petroulakis, E., et al., *p53-dependent translational control of senescence and transformation via 4E-BPs.* Cancer Cell, 2009. **16**(5): p. 439-46.
95. Ding, M., et al., *The mTOR Targets 4E-BP1/2 Restrain Tumor Growth and Promote Hypoxia Tolerance in PTEN-driven Prostate Cancer.* Mol Cancer Res, 2018. **16**(4): p. 682-695.
96. Qin, X., B. Jiang, and Y. Zhang, *4E-BP1, a multifactor regulated multifunctional protein.* Cell Cycle, 2016. **15**(6): p. 781-6.
97. Braunstein, S., et al., *A hypoxia-controlled cap-dependent to cap-independent translation switch in breast cancer.* Mol Cell, 2007. **28**(3): p. 501-12.
98. Martin, M.E., et al., *4E binding protein 1 expression is inversely correlated to the progression of gastrointestinal cancers.* Int J Biochem Cell Biol, 2000. **32**(6): p. 633-42.
99. Coleman, L.J., et al., *Combined analysis of eIF4E and 4E-binding protein expression predicts breast cancer survival and estimates eIF4E activity.* Br J Cancer, 2009. **100**(9): p. 1393-9.
100. Alain, T., N. Sonenberg, and I. Topisirovic, *mTOR inhibitor efficacy is determined by the eIF4E/4E-BP ratio.* Oncotarget, 2012. **3**(12): p. 1491-2.
101. Yanagiya, A., et al., *Translational homeostasis via the mRNA cap-binding protein, eIF4E.* Mol Cell, 2012. **46**(6): p. 847-58.
102. Hulea, L., et al., *Translational and HIF-1alpha-Dependent Metabolic Reprogramming Underpin Metabolic Plasticity and Responses to Kinase Inhibitors and Biguanides.* Cell Metab, 2018. **28**(6): p. 817-832 e8.
103. Salehi, Z. and F. Mashayekhi, *Expression of the eukaryotic translation initiation factor 4E (eIF4E) and 4E-BP1 in esophageal cancer.* Clin Biochem, 2006. **39**(4): p. 404-9.
104. Saxton, R.A. and D.M. Sabatini, *mTOR Signaling in Growth, Metabolism, and Disease.* Cell, 2017. **169**(2): p. 361-371.
105. Eng, C.P., S.N. Sehgal, and C. Vezina, *Activity of rapamycin (AY-22,989) against transplanted tumors.* J Antibiot (Tokyo), 1984. **37**(10): p. 1231-7.
106. Martel, R.R., J. Klicius, and S. Galet, *Inhibition of the immune response by rapamycin, a new antifungal antibiotic.* Can J Physiol Pharmacol, 1977. **55**(1): p. 48-51.
107. Vezina, C., A. Kudelski, and S.N. Sehgal, *Rapamycin (AY-22,989), a new antifungal antibiotic. I. Taxonomy of the producing streptomycete and isolation of the active principle.* J Antibiot (Tokyo), 1975. **28**(10): p. 721-6.
108. Brown, E.J., et al., *A mammalian protein targeted by G1-arresting rapamycin-receptor complex.* Nature, 1994. **369**(6483): p. 756-8.

109. Cafferkey, R., et al., *Dominant missense mutations in a novel yeast protein related to mammalian phosphatidylinositol 3-kinase and VPS34 abrogate rapamycin cytotoxicity.* Mol Cell Biol, 1993. **13**(10): p. 6012-23.
110. Kunz, J., et al., *Target of rapamycin in yeast, TOR2, is an essential phosphatidylinositol kinase homolog required for G1 progression.* Cell, 1993. **73**(3): p. 585-96.
111. Sabatini, D.M., et al., *RAFT1: a mammalian protein that binds to FKBP12 in a rapamycin-dependent fashion and is homologous to yeast TORs.* Cell, 1994. **78**(1): p. 35-43.
112. Sabers, C.J., et al., *Isolation of a protein target of the FKBP12-rapamycin complex in mammalian cells.* J Biol Chem, 1995. **270**(2): p. 815-22.
113. Chung, J., et al., *Rapamycin-FKBP specifically blocks growth-dependent activation of and signaling by the 70 kd S6 protein kinases.* Cell, 1992. **69**(7): p. 1227-36.
114. Hagiwara, A., et al., *Hepatic mTORC2 activates glycolysis and lipogenesis through Akt, glucokinase, and SREBP1c.* Cell Metab, 2012. **15**(5): p. 725-38.
115. Brunn, G.J., et al., *Phosphorylation of the translational repressor PHAS-I by the mammalian target of rapamycin.* Science, 1997. **277**(5322): p. 99-101.
116. Meyuhas, O. and A. Dreazen, *Ribosomal protein S6 kinase from TOP mRNAs to cell size.* Prog Mol Biol Transl Sci, 2009. **90**: p. 109-53.
117. Hsieh, A.C., et al., *The translational landscape of mTOR signalling steers cancer initiation and metastasis.* Nature, 2012. **485**(7396): p. 55-61.
118. Thoreen, C.C., et al., *A unifying model for mTORC1-mediated regulation of mRNA translation.* Nature, 2012. **485**(7396): p. 109-13.
119. Miloslavski, R., et al., *Oxygen sufficiency controls TOP mRNA translation via the TSC-Rheb-mTOR pathway in a 4E-BP-independent manner.* J Mol Cell Biol, 2014. **6**(3): p. 255-66.
120. Hong, S., et al., *LARP1 functions as a molecular switch for mTORC1-mediated translation of an essential class of mRNAs.* Elife, 2017. **6**.
121. Philippe, L., et al., *La-related protein 1 (LARP1) repression of TOP mRNA translation is mediated through its cap-binding domain and controlled by an adjacent regulatory region.* Nucleic Acids Res, 2018. **46**(3): p. 1457-1469.
122. Tcherkezian, J., et al., *Proteomic analysis of cap-dependent translation identifies LARP1 as a key regulator of 5'TOP mRNA translation.* Genes Dev, 2014. **28**(4): p. 357-71.
123. Fonseca, B.D., et al., *La-related Protein 1 (LARP1) Represses Terminal Oligopyrimidine (TOP) mRNA Translation Downstream of mTOR Complex 1 (mTORC1).* J Biol Chem, 2015. **290**(26): p. 15996-6020.
124. Gandin, V., et al., *nanoCAGE reveals 5' UTR features that define specific modes of translation of functionally related MTOR-sensitive mRNAs.* Genome Res, 2016. **26**(5): p. 636-48.
125. Zaytseva, Y.Y., et al., *mTOR inhibitors in cancer therapy.* Cancer Lett, 2012. **319**(1): p. 1-7.
126. Janku, F., T.A. Yap, and F. Meric-Bernstam, *Targeting the PI3K pathway in cancer: are we making headway?* Nat Rev Clin Oncol, 2018. **15**(5): p. 273-291.
127. Feldman, M.E., et al., *Active-site inhibitors of mTOR target rapamycin-resistant outputs of mTORC1 and mTORC2.* PLoS Biol, 2009. **7**(2): p. e38.

128. Thoreen, C.C., et al., *An ATP-competitive mammalian target of rapamycin inhibitor reveals rapamycin-resistant functions of mTORC1.* J Biol Chem, 2009. **284**(12): p. 8023-32.
129. O'Reilly, K.E., et al., *mTOR inhibition induces upstream receptor tyrosine kinase signaling and activates Akt.* Cancer Res, 2006. **66**(3): p. 1500-8.
130. Engelman, J.A., J. Luo, and L.C. Cantley, *The evolution of phosphatidylinositol 3-kinases as regulators of growth and metabolism.* Nat Rev Genet, 2006. **7**(8): p. 606-19.
131. Katso, R., et al., *Cellular function of phosphoinositide 3-kinases: implications for development, homeostasis, and cancer.* Annu Rev Cell Dev Biol, 2001. **17**: p. 615-75.
132. Hiles, I.D., et al., *Phosphatidylinositol 3-kinase: structure and expression of the 110 kd catalytic subunit.* Cell, 1992. **70**(3): p. 419-29.
133. Castellano, E. and J. Downward, *RAS Interaction with PI3K: More Than Just Another Effector Pathway.* Genes Cancer, 2011. **2**(3): p. 261-74.
134. Porta, C., C. Paglino, and A. Mosca, *Targeting PI3K/Akt/mTOR Signaling in Cancer.* Front Oncol, 2014. **4**: p. 64.
135. Klippel, A., et al., *The C-terminal SH2 domain of p85 accounts for the high affinity and specificity of the binding of phosphatidylinositol 3-kinase to phosphorylated platelet-derived growth factor beta receptor.* Mol Cell Biol, 1992. **12**(4): p. 1451-9.
136. Ahmed, S.B.M. and S.A. Prigent, *Insights into the Shc Family of Adaptor Proteins.* J Mol Signal, 2017. **12**: p. 2.
137. Altomare, D.A. and J.R. Testa, *Perturbations of the AKT signaling pathway in human cancer.* Oncogene, 2005. **24**(50): p. 7455-64.
138. Sugimoto, Y., et al., *Evidence that the Rous sarcoma virus transforming gene product phosphorylates phosphatidylinositol and diacylglycerol.* Proc Natl Acad Sci U S A, 1984. **81**(7): p. 2117-21.
139. Kaplan, D.R., et al., *Phosphatidylinositol metabolism and polyoma-mediated transformation.* Proc Natl Acad Sci U S A, 1986. **83**(11): p. 3624-8.
140. Whitman, M., et al., *Association of phosphatidylinositol kinase activity with polyoma middle-T competent for transformation.* Nature, 1985. **315**(6016): p. 239-42.
141. Zhao, J.J., et al., *Human mammary epithelial cell transformation through the activation of phosphatidylinositol 3-kinase.* Cancer Cell, 2003. **3**(5): p. 483-95.
142. Samuels, Y., et al., *High frequency of mutations of the PIK3CA gene in human cancers.* Science, 2004. **304**(5670): p. 554.
143. Zhao, J.J. and T.M. Roberts, *PI3 kinases in cancer: from oncogene artifact to leading cancer target.* Sci STKE, 2006. **2006**(365): p. pe52.
144. Bachman, K.E., et al., *The PIK3CA gene is mutated with high frequency in human breast cancers.* Cancer Biol Ther, 2004. **3**(8): p. 772-5.
145. Crowder, R.J., et al., *PIK3CA and PIK3CB inhibition produce synthetic lethality when combined with estrogen deprivation in estrogen receptor-positive breast cancer.* Cancer Res, 2009. **69**(9): p. 3955-62.
146. Gonzalez, E. and T.E. McGraw, *The Akt kinases: isoform specificity in metabolism and cancer.* Cell Cycle, 2009. **8**(16): p. 2502-8.

147. Alessi, D.R., et al., *Characterization of a 3-phosphoinositide-dependent protein kinase which phosphorylates and activates protein kinase Balpha.* Curr Biol, 1997. **7**(4): p. 261-9.
148. Stokoe, D., et al., *Dual role of phosphatidylinositol-3,4,5-trisphosphate in the activation of protein kinase B.* Science, 1997. **277**(5325): p. 567-70.
149. Sarbassov, D.D., et al., *Phosphorylation and regulation of Akt/PKB by the rictor-mTOR complex.* Science, 2005. **307**(5712): p. 1098-101.
150. Downward, J., *PI 3-kinase, Akt and cell survival.* Semin Cell Dev Biol, 2004. **15**(2): p. 177-82.
151. Mayo, L.D. and D.B. Donner, *The PTEN, Mdm2, p53 tumor suppressor-oncoprotein network.* Trends Biochem Sci, 2002. **27**(9): p. 462-7.
152. Zhou, B.P. and M.C. Hung, *Novel targets of Akt, p21(Cipl/WAF1), and MDM2.* Semin Oncol, 2002. **29**(3 Suppl 11): p. 62-70.
153. Garami, A., et al., *Insulin activation of Rheb, a mediator of mTOR/S6K/4E-BP signaling, is inhibited by TSC1 and 2.* Mol Cell, 2003. **11**(6): p. 1457-66.
154. Inoki, K., et al., *Rheb GTPase is a direct target of TSC2 GAP activity and regulates mTOR signaling.* Genes Dev, 2003. **17**(15): p. 1829-34.
155. Dan, H.C., et al., *Phosphatidylinositol 3-kinase/Akt pathway regulates tuberous sclerosis tumor suppressor complex by phosphorylation of tuberin.* J Biol Chem, 2002. **277**(38): p. 35364-70.
156. Manning, B.D., et al., *Identification of the tuberous sclerosis complex-2 tumor suppressor gene product tuberin as a target of the phosphoinositide 3-kinase/akt pathway.* Mol Cell, 2002. **10**(1): p. 151-62.
157. Potter, C.J., L.G. Pedraza, and T. Xu, *Akt regulates growth by directly phosphorylating Tsc2.* Nat Cell Biol, 2002. **4**(9): p. 658-65.
158. LoPiccolo, J., et al., *Targeting Akt in cancer therapy.* Anticancer Drugs, 2007. **18**(8): p. 861-74.
159. Teng, D.H., et al., *MMAC1/PTEN mutations in primary tumor specimens and tumor cell lines.* Cancer Res, 1997. **57**(23): p. 5221-5.
160. Li, D.M. and H. Sun, *TEP1, encoded by a candidate tumor suppressor locus, is a novel protein tyrosine phosphatase regulated by transforming growth factor beta.* Cancer Res, 1997. **57**(11): p. 2124-9.
161. Li, J., et al., *PTEN, a putative protein tyrosine phosphatase gene mutated in human brain, breast, and prostate cancer.* Science, 1997. **275**(5308): p. 1943-7.
162. Maehama, T. and J.E. Dixon, *The tumor suppressor, PTEN/MMAC1, dephosphorylates the lipid second messenger, phosphatidylinositol 3,4,5-trisphosphate.* J Biol Chem, 1998. **273**(22): p. 13375-8.
163. Cairns, P., et al., *Frequent inactivation of PTEN/MMAC1 in primary prostate cancer.* Cancer Res, 1997. **57**(22): p. 4997-5000.
164. Chiariello, E., et al., *PTEN/MMAC1 mutations in primary glioblastomas and short-term cultures of malignant gliomas.* Oncogene, 1998. **16**(4): p. 541-5.
165. Feilotter, H.E., et al., *Analysis of the 10q23 chromosomal region and the PTEN gene in human sporadic breast carcinoma.* Br J Cancer, 1999. **79**(5-6): p. 718-23.

166. Gammon, A., K. Jasperson, and M. Champine, *Genetic basis of Cowden syndrome and its implications for clinical practice and risk management.* Appl Clin Genet, 2016. **9**: p. 83-92.
167. Pelicci, G., et al., *A novel transforming protein (SHC) with an SH2 domain is implicated in mitogenic signal transduction.* Cell, 1992. **70**(1): p. 93-104.
168. Ursini-Siegel, J. and W.J. Muller, *The ShcA adaptor protein is a critical regulator of breast cancer progression.* Cell Cycle, 2008. **7**(13): p. 1936-43.
169. Lai, K.M. and T. Pawson, *The ShcA phosphotyrosine docking protein sensitizes cardiovascular signaling in the mouse embryo.* Genes Dev, 2000. **14**(9): p. 1132-45.
170. Arany, I., et al., *p66shc inhibits pro-survival epidermal growth factor receptor/ERK signaling during severe oxidative stress in mouse renal proximal tubule cells.* J Biol Chem, 2008. **283**(10): p. 6110-7.
171. Ursini-Siegel, J., et al., *ShcA signalling is essential for tumour progression in mouse models of human breast cancer.* EMBO J, 2008. **27**(6): p. 910-20.
172. Davol, P.A., et al., *Shc proteins are strong, independent prognostic markers for both node-negative and node-positive primary breast cancer.* Cancer Res, 2003. **63**(20): p. 6772-83.
173. Frackelton, A.R., Jr., et al., *p66 Shc and tyrosine-phosphorylated Shc in primary breast tumors identify patients likely to relapse despite tamoxifen therapy.* Breast Cancer Res, 2006. **8**(6): p. R73.
174. Im, Y.K., et al., *The ShcA adaptor activates AKT signaling to potentiate breast tumor angiogenesis by stimulating VEGF mRNA translation in a 4E-BP-dependent manner.* Oncogene, 2015. **34**(13): p. 1729-35.
175. Lin, E.Y., et al., *Progression to malignancy in the polyoma middle T oncoprotein mouse breast cancer model provides a reliable model for human diseases.* Am J Pathol, 2003. **163**(5): p. 2113-26.
176. Ursini-Siegel, J., et al., *Insights from transgenic mouse models of ERBB2-induced breast cancer.* Nat Rev Cancer, 2007. **7**(5): p. 389-97.
177. Guy, C.T., R.D. Cardiff, and W.J. Muller, *Induction of mammary tumors by expression of polyomavirus middle T oncogene: a transgenic mouse model for metastatic disease.* Mol Cell Biol, 1992. **12**(3): p. 954-61.
178. Lin, E.Y., et al., *Colony-stimulating factor 1 promotes progression of mammary tumors to malignancy.* J Exp Med, 2001. **193**(6): p. 727-40.
179. Zhou, A.Y., et al., *Polyomavirus middle T-antigen is a transmembrane protein that binds signaling proteins in discrete subcellular membrane sites.* J Virol, 2011. **85**(7): p. 3046-54.
180. Campbell, K.S., et al., *Polyoma middle tumor antigen interacts with SHC protein via the NPTY (Asn-Pro-Thr-Tyr) motif in middle tumor antigen.* Proc Natl Acad Sci U S A, 1994. **91**(14): p. 6344-8.
181. Dilworth, S.M., et al., *Transformation by polyoma virus middle T-antigen involves the binding and tyrosine phosphorylation of Shc.* Nature, 1994. **367**(6458): p. 87-90.
182. Su, W., et al., *Association of Polyomavirus middle tumor antigen with phospholipase C-gamma 1.* J Biol Chem, 1995. **270**(21): p. 12331-4.
183. Talmage, D.A., et al., *Phosphorylation of middle T by pp60c-src: a switch for binding of phosphatidylinositol 3-kinase and optimal tumorigenesis.* Cell, 1989. **59**(1): p. 55-65.

184. Weidner, K.M., et al., *Interaction between Gab1 and the c-Met receptor tyrosine kinase is responsible for epithelial morphogenesis.* Nature, 1996. **384**(6605): p. 173-6.
185. Talmadge, J.E., *Immune cell infiltration of primary and metastatic lesions: mechanisms and clinical impact.* Semin Cancer Biol, 2011. **21**(2): p. 131-8.
186. Hanahan, D. and R.A. Weinberg, *Hallmarks of cancer: the next generation.* Cell, 2011. **144**(5): p. 646-74.
187. Tsukiyama-Kohara, K., et al., *Adipose tissue reduction in mice lacking the translational inhibitor 4E-BP1.* Nat Med, 2001. **7**(10): p. 1128-32.
188. Gotoh, N., M. Toyoda, and M. Shibuya, *Tyrosine phosphorylation sites at amino acids 239 and 240 of Shc are involved in epidermal growth factor-induced mitogenic signaling that is distinct from Ras/mitogen-activated protein kinase activation.* Mol Cell Biol, 1997. **17**(4): p. 1824-31.
189. Gotoh, N., A. Tojo, and M. Shibuya, *A novel pathway from phosphorylation of tyrosine residues 239/240 of Shc, contributing to suppress apoptosis by IL-3.* EMBO J, 1996. **15**(22): p. 6197-204.
190. Dowling, R.J., et al., *mTORC1-mediated cell proliferation, but not cell growth, controlled by the 4E-BPs.* Science, 2010. **328**(5982): p. 1172-6.
191. Seo, T.W., et al., *A novel function of cIAP1 as a mediator of CHIP-driven eIF4E regulation.* Sci Rep, 2017. **7**(1): p. 9816.
192. Karlsson, E., et al., *The mTOR effectors 4EBP1 and S6K2 are frequently coexpressed, and associated with a poor prognosis and endocrine resistance in breast cancer: a retrospective study including patients from the randomised Stockholm tamoxifen trials.* Breast Cancer Res, 2013. **15**(5): p. R96.
193. Topisirovic, I., et al., *Aberrant eukaryotic translation initiation factor 4E-dependent mRNA transport impedes hematopoietic differentiation and contributes to leukemogenesis.* Mol Cell Biol, 2003. **23**(24): p. 8992-9002.
194. Martinez, A., et al., *Phosphorylation of eIF4E Confers Resistance to Cellular Stress and DNA-Damaging Agents through an Interaction with 4E-T: A Rationale for Novel Therapeutic Approaches.* PLoS One, 2015. **10**(4): p. e0123352.
195. Robichaud, N., et al., *Translational control in the tumor microenvironment promotes lung metastasis: Phosphorylation of eIF4E in neutrophils.* Proc Natl Acad Sci U S A, 2018. **115**(10): p. E2202-E2209.
196. Topisirovic, I., et al., *Cap and cap-binding proteins in the control of gene expression.* Wiley Interdiscip Rev RNA, 2011. **2**(2): p. 277-98.
197. Teleman, A.A., Y.W. Chen, and S.M. Cohen, *4E-BP functions as a metabolic brake used under stress conditions but not during normal growth.* Genes Dev, 2005. **19**(16): p. 1844-8.